



8-2015

Synthesis of Phenothiazinium Derivatives

Selorm J. Fanah
East Tennessee State University

Follow this and additional works at: <https://dc.etsu.edu/etd>

 Part of the [Chemistry Commons](#)

Recommended Citation

Fanah, Selorm J., "Synthesis of Phenothiazinium Derivatives" (2015). *Electronic Theses and Dissertations*. Paper 2563. <https://dc.etsu.edu/etd/2563>

This Thesis - unrestricted is brought to you for free and open access by the Student Works at Digital Commons @ East Tennessee State University. It has been accepted for inclusion in Electronic Theses and Dissertations by an authorized administrator of Digital Commons @ East Tennessee State University. For more information, please contact digilib@etsu.edu.

Synthesis of Phenothiazinium Derivatives

A thesis

presented to

the faculty of the Department of Chemistry

East Tennessee State University

In partial fulfilment

of the requirements for the degree

Master of Science in Chemistry

by

Selorm J. Fanah

August 2015

Dr. Ismail O. Kady, Chair

Dr. Marina Roginskaya

Dr. Abbas G. Shilabin

Keywords: Photodynamic therapy (PDT), phenothiazinium (PTZN), dye sensitizing solar cell

(DSSC), metal organic frameworks (MOF)

ABSTRACT

Synthesis of Phenothiazinium Derivatives

by

Selorm J. Fanah

Photodynamic therapy (PDT) employs photosensitizing drugs for treating cancer. Once introduced into the body and localized in tumor cells, these photosensitizers are irradiated with light to produce active singlet oxygen radicals which kill cancer cells. The current drugs used in PDT have low quantum yield and always require a high energy radiation (normally laser). There is always a need for more effective drugs that have a high quantum yield and can be activated by visible light, in order to eliminate side effects caused by laser radiations.

In this work we synthesized derivatives of phenothiazine and phenothiazinium chromophores from the commercially available phenothiazine (**1**). These derivatives include: 3,7-dibromophenothiazinium perbromide (**2**), N-acetyl phenothiazine (**5**), N-acetyl-3,7-dibromophenothiazine (**6**), 3,7-dinitrophenothiazine (**10**), N-acetyl-3,7-dinitrophenothiazine (**11**), N-acetyl-3,7-diaminophenothiazine (**12**), thionine chloride (**15**) and 3,7-phenothiaziniumdinitrile (**14**). Synthesis of 3,7-phenothiazinium dicarboxylic acid was attempted using **1** and **15** as starting materials by exploring various synthetic routes for carboxylic acids.

DEDICATION

This work is dedicated to the Almighty God for His sustenance, protection and guidance, my parents; Mr. Solomon K. Seworh, Mrs. Theresah Seworh, Mrs. Ruth Adjei and the whole Fanah family.

ACKNOWLEDGEMENTS

My sincere thanks to God Almighty for His protection, sustenance, care, abundant grace and love throughout my study. I would also like to express my deepest gratitude to my advisor; Dr. Ismail O. Kady for his excellent guidance, patience, encouragement and providing me with an excellent atmosphere throughout this research work.

Thanks to Dr. Marina Roginskaya and Dr. Abbas G. Shilabin for serving as committee members and also Dr. Reza Mohseni for his assistance with instrumentation for this work.

I take this opportunity to express my profound gratitude to all faculty members of the Department of Chemistry, ETSU for their help and support. I also thank my parents and my family for their unceasing encouragement, support and attention.

Finally, I wish to express my gratitude to all graduate students of the Department of Chemistry, ETSU and my friends for their support throughout my study.

TABLE OF CONTENTS

	Page
ABSTRACT.....	2
DEDICATION.....	3
ACKNOWLEDGEMENTS.....	4
LIST OF FIGURES.....	10
LIST OF SCHEMES.....	11
LIST OF ABBREVIATIONS.....	12
Chapter	
1. INTRODUCTION.....	14
Photodynamic Therapy (PDT).....	14
Photosensitizers.....	16
Methylene Blue.....	18
Thionine.....	19
Basic Mechanism of Photosensitization.....	19
Metal Organic Frameworks (MOF).....	22
MOF's as Potential Drug Carriers.....	23
Dye-Sensitized Solar Cells (DSSC).....	25
Operating Principle of DSSC.....	25
Sensitizers (Dyes).....	27

Chapter	Page
Catalytic Hydrolysis: Role of Carboxylic Acids	28
General Acid-Base Ester Hydrolysis	29
General Acid Catalyzed Ester Hydrolysis	30
General Base Catalyzed Ester Hydrolysis	31
Phosphodiester Bonds.....	31
Research Objectives.....	33
2. RESULTS AND DISCUSSIONS.....	35
Synthesis of phenothiazin-5-ium tetra-iodide hydrate (PTZN).....	38
Synthesis of 3,7-dibromophenothiazinium perbromide (2).....	39
Synthesis of N-acetyl phenothiazine (5).....	40
Synthesis of N-acetyl-3,7-dibromophenothiazine (6).....	40
Synthesis of phenothiazin-3,7-dicarboxylic acid (4) and N-acetyl-3,7- phenothiazinedicarboxylic acid (8).....	42
Synthesis of 3,7-dinitrophenothiazine (10).....	42
Synthesis of N-acetyl-3,7-diaminophenothiazine (11).....	43
Synthesis of N-acetyl-3,7-diaminophenothiazine (12).....	44
Conversion of thionine acetate and N-acetyl-3,7-diaminophenothiazine (12) into thionine chloride (15).....	45
Synthesis of 3,7-phenothiaziniumdinitrile (14).....	47
3. EXPERIMENTAL.....	50
Materials and General methods	50

Chapter	Page
Experimental Procedures	50
Synthesis of phenothiazin-5-ium tetra iodide hydrate (PTZN)	50
Synthesis of 3, 7-dibromophenothiazin-5-ium perbromide (2)	51
Synthesis of 1-phenothiazin-10-ylethanone (5)	52
Synthesis of N-acetyl-3,7-dibromophenothiazine (6).....	52
Grignard synthesis of phenothiazin-3,7-dicarboxylic acid (4) and N-acetyl-3,7- phenothiazinedicarboxylic acid (8).....	53
Synthesis of 3,7-dinitrophenothiazine (10).....	54
Synthesis of N-acetyl-3,7-dinitrophenothiazine (11).....	55
Synthesis of N-acetyl-3,7-diaminophenothiazine (12)	56
Conversion of thionine acetate and N-acetyl-3,7-diaminophenothiazine (12) into thionine chloride (15).....	56
Synthesis of 3,7-phenothiaziniumdinitrile (14)	57
4. CONCLUSION.....	59
REFERENCES	61
APPENDICES	67
Appendix A: ¹ H NMR Spectrum for Compound 2 in DMSO-d ₆	67
Appendix B1: ¹ H NMR Spectrum for Compound 5 in DMSO-d ₆	68
Appendix B2: ¹ H NMR Spectrum for Compound 5 in DMSO-d ₆	69
Appendix B3: ¹³ C NMR Spectrum for Compound 5 in DMSO-d ₆	70
Appendix B4: ¹³ C NMR Spectrum for Compound 5 in DMSO-d ₆	71
Appendix B5: IR Spectrum for Compound 5	72

Chapter	Page
Appendix C1: ^1H NMR Spectrum for Compound 10 in DMSO-d ₆	73
Appendix C2: ^1H NMR Spectrum for Compound 10 in DMSO-d ₆	74
Appendix C3: ^{13}C NMR Spectrum for Compound 10 in DMSO-d ₆	75
Appendix C4: ^{13}C NMR Spectrum for Compound 10 in DMSO-d ₆	76
Appendix C5: IR Spectrum for Compound 10	77
Appendix D1: ^1H NMR Spectrum for Compound 11 in DMSO-d ₆	78
Appendix D2: ^1H NMR Spectrum for Compound 11 in DMSO-d ₆	79
Appendix D3: ^{13}C NMR Spectrum for Compound 11 in DMSO-d ₆	80
Appendix D4: ^{13}C NMR Spectrum for Compound 11 in DMSO-d ₆	81
Appendix D5: IR Spectrum for Compound 11	82
Appendix E1: ^1H NMR Spectrum for Compound 12 in DMSO-d ₆	83
Appendix E2: ^1H NMR Spectrum for Compound 12 in DMSO-d ₆	84
Appendix E3: IR Spectrum for Compound 12	85
Appendix F1: ^{13}C NMR Spectrum for Compound 15 in DMSO-d ₆	86
Appendix F2: ^{13}C NMR Spectrum for Compound 15 in DMSO-d ₆	87
Appendix F3: IR Spectrum for Compound 15	88
Appendix G1: ^1H NMR Spectrum for Compound 14 in DMSO-d ₆	89
Appendix G2: ^1H NMR Spectrum for Compound 14 in DMSO-d ₆	90
Appendix G3: ^{13}C NMR Spectrum for Compound 14 in DMSO-d ₆	91
Appendix G4: ^{13}C NMR Spectrum for Compound 14 in DMSO-d ₆	92
Appendix G5: IR Spectrum for Compound 14	93
Appendix H1: ^1H NMR Spectrum for Compound 6B in DMSO-d ₆	94

Chapter	Page
Appendix H2: ¹ H NMR Spectrum for Compound 6B in DMSO-d ₆	95
Appendix I1: ¹ H NMR Spectrum for PTZN in DMSO-d ₆	96
Appendix I2: ¹ H NMR Spectrum for PTZN in DMSO-d ₆	97
VITA.....	98

LIST OF FIGURES

Figure	Page
1. The mechanism of action for Photodynamic Therapy	16
2. Reactions for the Type I vs. Type II Photosensitization processes.....	20
3. Formation of a 1D MOF and the loading of a drug material by physical encapsulation into the pore aperture of the MOF	24
4. A typical structure of the DSSC.....	27
5. Tautomerism of aspartic acid at different pH	29
6. A section of the DNA showing phosphodiester bonds	32

LIST OF SCHEMES

Scheme	Page
1. Principal reactions that occur in a DSSC	26
2. Proposed mechanism for the hydrolysis of esters by aspartic acid under acidic conditions	30
3. Proposed mechanism for the hydrolysis of esters by aspartic acid under basic conditions.....	31
4. Proposed hydrolysis of the phosphodiester bond of RNA by aspartate.....	33
5. Proposed synthetic route for the PTZN dicarboxylic acid from unprotected phenothiazine using Grignard reaction.....	35
6. Proposed synthetic route for the PTZN dicarboxylic acid from protected phenothiazine using Grignard reaction	36
7. Proposed synthetic route of the PTZN dicarboxylic acid using Sandmeyer reaction.....	37
8a. Proposed mechanism for the conversion of thionine acetate into thionine chloride	46
8b. Proposed mechanism for the conversion of thionine amide into thionine chloride	47
9a. Conversion of thionine amide into the phenothiazine dinitrile derivative	49
9b. Conversion of thionine chloride into the phenothiazine dinitrile derivative	49

LIST OF ABBREVIATIONS

CdTe	Cadmium telluride
CIGS	Copper Indium Gallium Selenides solar cells
DMF	Dimethylformamide
DMSO	Dimethyl sulfoxide
DNA	Deoxyribonucleic acid
DSSC	Dye sensitizing solar cells
FT-IR	Fourier Transform Infra Red
HOMO	Highest Occupied Molecular Orbitals
hrs	Hours
I_{sc}	Short Circuit Current
IR	Infra-Red
LUMO	Lowest unoccupied molecular orbital
MB	Methylene Blue
MOF	Metal organic frameworks
Min	Minutes
mmol	Millimoles
mL	Milliliter
NMR	Nuclear Magnetic Resonance
PDT	Photodynamic Therapy
PTPases	Protein Tyrosine Phosphatases
RNA	Ribonucleic acid
R_f	Retention factor

THF	Tetrahydrofuran
TLC	Thin Layer Chromatography
V_{oc}	Open Circuit Voltage
μs	Microsecond
1D	1 Dimensional

CHAPTER 1

INTRODUCTION

Developing alternative therapeutic ways of treating cancer and tumor cells have become an important field of study and much interest for scientists. Although chemotherapy has been widely used, its associated side effects and cost have paved way for photodynamic therapy.³

The key component of photodynamic therapy (PDT) is the use of a suitable drug (photosensitizer) that can absorb radiation at a specific wavelength. However, there are limitations for the use of photosensitizers in PDT, such as poor absorptivity, contamination by other compounds, low photostability of the drug, toxicity, and the ability of the drug to be localized in neoplastic tissues.^{4,5} A good number of compounds and their analogues have been synthesized for this method over the last few decades. Among them are some phenothiazine derivatives which have shown distinctive characteristics in photo antimicrobial activities.⁵

The primary purpose of this work is to synthesize derivatives of phenothiazine that satisfy most of the requirements mentioned above. For example, a potential advantage of attaching a carboxylate group to phenothiazine is to convert the aromatic chromophore into one which would have a high singlet oxygen quantum yield when exposed to light.^{11,17} Such derivatives can have further application in dye sensitized solar cells (DSSC), and syntheses of new generations of metal-organic frameworks (MOF's).

Photodynamic Therapy (PDT)

Photodynamic therapy (PDT) employs drugs which are sensitive to light (photosensitizers) in the treatment of cancer cells. This treatment uses light rays of a specific wavelength in the treatment of the cells. The wavelength of the light used determines which parts

of the body with tumor cells can be treated. Also, the type of photosensitizers used at a time determines which wavelength of light to be used since each of the light sensitive drugs can only absorb photons produced at specific wavelengths of light. When photosensitizers absorb photons, they are excited. These excited photosensitizers transfer energy to tissue oxygen which generates singlet oxygen to kill cancer cells.¹⁻³ The light source for irradiating the cells can be from lasers which is directed through fiber optics to the affected areas during treatments.²

Photosensitive agents which are introduced into the body by injection are absorbed into the blood streams by all body cells and tumor or cancer cells, but their life span in the cancer cells are much longer than the normal body cell due to their strong selective binding to cancer cells. This selective binding of photosensitizers to cancer cells is made possible by such features as a larger volume, larger fraction of macrophages, leaky microvasculature, poor lymphatic drainage, lower extracellular pH, larger amount of newly formed collagens, and numerous receptors for lipoprotein.⁶

Approximately one or two days after they are introduced into the body, most of the drugs would leave the normal host cells but remain in higher concentrations in tumor cells. These cells are then exposed to red light of a specific wavelength (600 nm) which activates the photosensitizing drugs to produce reactive singlet oxygen radicals that kill the cancer cells as shown in **Figure 1**.^{1,5}

In addition to killing cancer cells, this therapy appears to destroy and reduce the diameter of tumor cells through some other routes. The photosensitive drugs damage blood vessels of tumor cells cutting the supply of blood nutrients to them and also activate the body immune system to attack tumor cells.¹⁻⁴

This breakthrough of treating cancer cells can be traced to the work of Rabb Oscar, a medical student of Prof. Herman Von Trappeiner in 1900.⁵ In his work, he noticed an elevated harmfulness of acridine orange towards paramicium in the presence of light. Von Trappeiner reported his first test for the treatment of skin carcinoma using eosin solution. He later named this method the photodynamic therapy (PDT) in 1943.⁵

Despite the advantage of this method of treating cancer over chemotherapy, it has a few limitations. Undoubtedly, one of these limitations is the small number of photosensitizing drugs available in the market.³

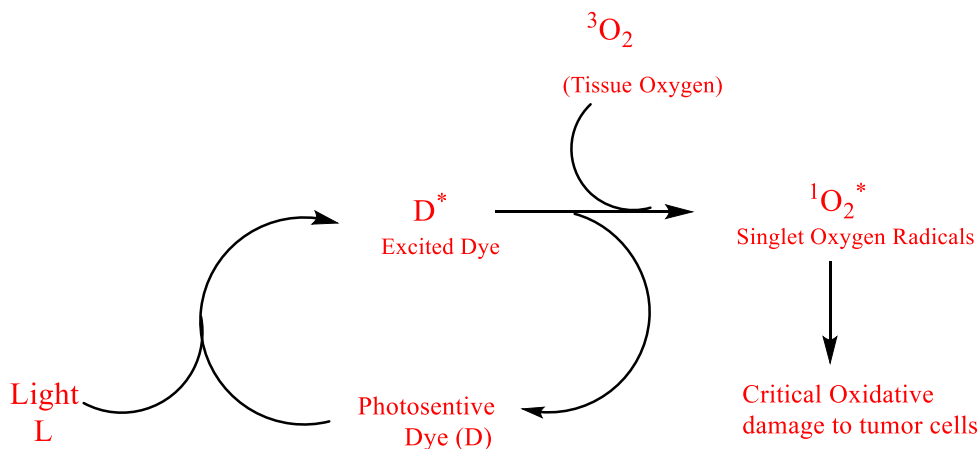


Figure 1: The mechanism of action for Photodynamic Therapy.⁵

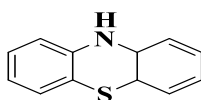
Photosensitizers

Photosensitizing agents are compounds that can activate singlet oxygen upon exposure to light of a specific wavelength at which the compound can absorb. The wavelength of operating light for PDT ranges between 600 nm to 900 nm.⁶ Light of wavelength below 600 nm tends to be absorbed by endogenous molecules such as hemoglobin; light of wavelength above 900 nm

does not produce enough reactive singlet oxygen radicals. Moreover, a light source with higher wavelength can penetrate body tissues more easily leading to severe side effects.⁶

Although there are a number of photosensitive agents, only a few can be employed in PDT based on specific criteria which they need to meet. A photosensitizer needs to be nontoxic, highly soluble in lipids, produce a high amount of active singlet oxygen radicals when exposed to radiations (*i.e.*, of a high quantum yield),⁸ selective towards hyper-proliferating tissues,⁷ and needs to be photostable.⁹ All these requirements need to be met for a photosensitizer to be used clinically.⁷⁻⁹

Some porphyrin derivatives have over the years been the most used photosensitizers for clinical PDT.¹⁰ Garbo, Keck and Selman reported in their work that dihematoporphyrin derivatives, which are widely used as photosensitizers for clinical photodynamic therapy, have poor absorption in the visible region; therefore there is a need for new photosensitizers.¹⁰ Other groups of photosensitizers include purpurins, porphycenes, pheophorbids, and most recently phenothiazine.¹¹



Phenothiazine

Over the years, photosensitizers with phenothiazinium chromophore have found considerable use in PDT and photodynamic antimicrobial therapy (PACT). Phenothiazinium dyes, under the influence of light, are known to inhibit viral growth.¹⁸ The major compound of this group is methylene blue which is still used in most cancer treatments, photo disinfection of oral cavity, and blood plasma photo decontamination.¹²

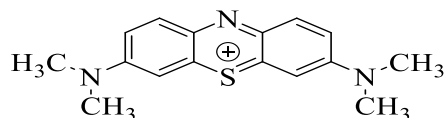
Despite the useful effects of these lead compounds, developing other analogues with different side groups are slowly emerging.¹² Work by Tiana *et. Al.*, showed that the tissue absorption rate of some phenothiazine-based compounds is very high, and that some of these compounds can be used in dye-sensitized solar cells (DSSC).^{11, 17} Other useful derivatives of phenothiazine that are used in DSSC technology are thionine, azure C, and toluidine blue.^{11,12}

Methylene Blue

Methylene Blue (MB) is a phenothiazine derivative that contains two dimethyl amino groups. The dimethyl amino auxochromes and the phenothiazine chromophore make up the body of this dye. This lead compound and its derivatives have been used in drug research for treating various viral and bacterial infections.¹⁷

Methylene blue was part of the first group of drugs ever synthesized as an antiseptic for clinical therapy.¹⁷ This dye's λ max values of 608 and 668 nm are within the suitable range of wavelength for PDT photosensitizers.¹⁶ Clinically, methylene blue (MB) is available as an aqueous solution (1% w/v; 10 g/ L or 26.7 mM), and the recommended dose is between 1 and 4 mg per kg of body weight.¹⁵

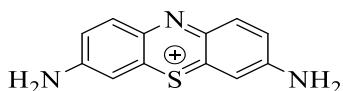
Although this derivative of phenothiazine meets most of the requirements for application in PDT, its poor lipophilicity decreases its uptake by damaged and cancer cells. Therefore, any work leading to improving lipophilicity of methylene blue and increasing its ability to photo cleave DNA is considered attractive.¹⁹



Methylene blue

Thionine

Another name for thionine is Lauth's violet. This metachromatic dye is mostly used in biological staining.¹³ It is sometimes used to mediate electron transfer in microbial fuel cells.^{13,14} Thionine is used in place of Schiff's reagent in the quantitative staining of the DNA.¹⁴ When both amines on the phenothiazine rings are methylated, the product is the widely known phenothiazinium compound methylene blue, and the intermediate compound is azure C (monomethyl thionine).¹⁴



Thionine

Basic Mechanism of Photosensitization

Photosensitization is a reaction that is initiated by a light-absorbing molecule (photosensitizer) which is capable of transferring energy to other species.³⁰ Molecules used in this reaction must absorb photons before they can have an effect in their environment. In some instances, the light-absorbing molecules are chemically altered after the absorption of photons, but they do not react with other molecules in the system.³⁰

On the other hand, in some cases, there are alterations of other molecules (substrate or acceptor) in the system after photons or light have been absorbed by the photosensitizers. This reaction can occur in living cells or tissues, or can take place in pure chemical systems.³⁰ PDT is much concerned with the reaction of light-absorbing species in the living cells and tissues.

The process is initiated by excitation of photosensitizers (D^*) to energy rich states when photons are absorbed. These excited photosensitizers have a half-life between 10^{-6} to 10^{-9} seconds during which the excited molecules undergo internal reactions that ultimately lead to the alteration of the chemical nature of substrates.³⁰ The molecules then either relax to the ground state via fluorescence or via intersystem crossing to other excited energy states, usually the triplet states where the excited molecule tend to have a much longer half-life of 10^{-3} seconds.^{11,30} It is the prolonged interaction of photosensitizers with tissue oxygen in the triplet excited state that generates high amounts of singlet oxygen species; for destroying tumor cells. This occurs in one of two types of reactions as seen in **Figure 2**.¹¹

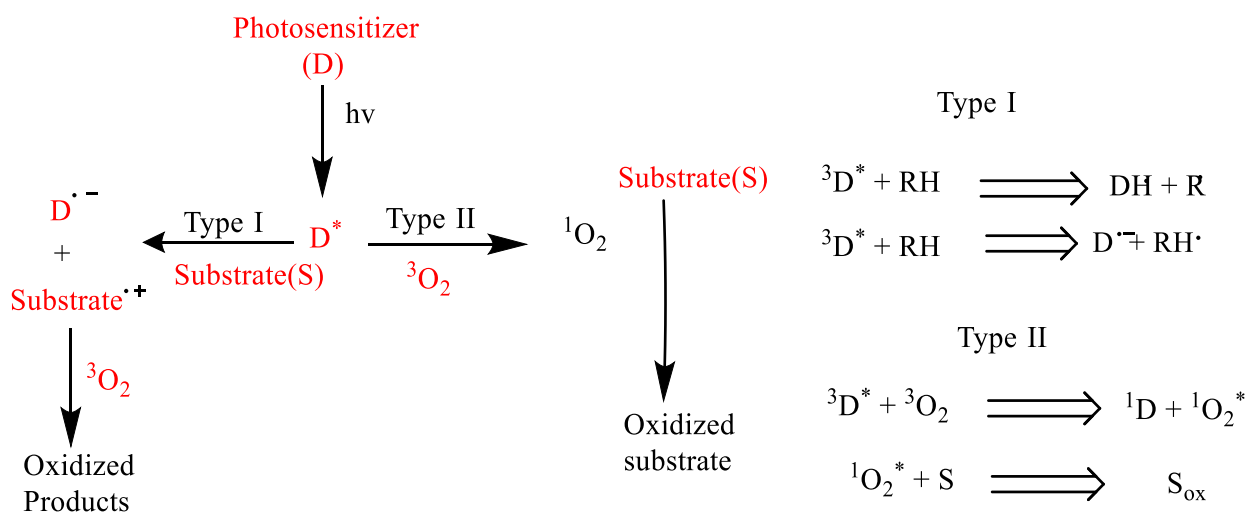


Figure 2: Reactions for the Type I vs Type II Photosensitization processes.^{11, 30-32}

Photosensitizer in the type I path reacts directly with the substrate to produce a radical or a radical ion in the substrate as well as the photosensitizer as a result of an electron transfer that takes place during the reaction process. The electron transfer can proceed from any of the reactants. Photosensitizer usually accepts an electron from the substrate which results in the formation of a photosensitizer radical anion ($D^{\cdot-}$) and a substrate radical cation ($\text{Substrate}^{\cdot+}$).^{30,32} When oxygen is present, these radicals further react to produce oxygenated molecules leading to the loss of the photosensitizer due to its conversion to the oxidized product. Regeneration of the original photosensitizer is also possible from the type I pathway, when there is a direct transfer of an extra electron from the photosensitive radical anion to oxygen to produce superoxide form of the radical anion ($O_2^{\cdot-}$).^{30,31}

In pathway II, excess energy is transferred from the photosensitizer to a ground-state molecular oxygen (3O_2) which is naturally in the triplet state to produce singlet oxygen species (1O_2). The original form of photosensitizers in the ground-states are generated in this pathway as the excited singlet oxygen reacts with substrates to form oxidized products.³⁰

These singlet oxygen species have a life span shorter than 0.01- 0.04 μs and diffusion distance between 0.01-0.02 μm per second.^{6,11} Quantum yields for lipophilic photosensitizers are much higher compared to hydrophilic ones due to the high diffusion rate of singlet oxygen in lipophilic photosensitizers.¹¹ This high diffusion rate also makes them more selective in localization in cell and tissue parts with high lipid concentrations.¹¹

Nuclear membranes, mitochondria, and reticulum lysosomes are typical examples of parts in living cells with higher concentrations of lipids where the photosensitizers can selectively accumulate to enhance apoptosis (cell death) when irradiated with red light.¹¹ Photooxidation

further enhances apoptosis by activating phospholipase enzymes in cell membranes which ultimately results in dynamism in the permeability of cell membrane and inhibition other enzymes such as mitochondrial enzymes. This inhibition of cell enzyme action is believed to be the major cause of cell death in photodynamic therapy.¹¹

Metal Organic Frameworks (MOF)

Metal Organic Frameworks (MOF's) are porous crystalline compounds in 1, 2, or 3 dimensional robust structures.²⁴ These materials are formed from joining metal ions with organic linkers (dicarboxylic acids), using strong bonds to create a crystalline metal cluster with permanent porosity.²⁴ Materials and crystals of high porosity and stability are of high importance because they allow other molecules to be trapped in these pores.²⁵ These pore apertures control the size of molecules that may pass through by providing the surface and pore gaps to perform the desired functions.^{24,25} The challenge over the years has been the making of materials and crystals with pores suitable for trapping large organic, inorganic, and biological molecules.²⁹ The largest reported aperture for a pore is 32 by 24 Å, and the largest internal pore diameter reported is 47 Å, both of which were present MOFs.^{28, 29}

This exceptional porosity of MOF's makes them potential materials for many industrial applications such as gas storage, separation, and catalysis.²⁵ They have become an extensive subject of study, specifically in the energy industries due to their high thermal stability and for their potential application in energy technologies such as fuel cells, super capacitors, and catalytic convertors.²⁶ To maximize the storage capacity of gases in these highly porous crystalline materials, it is important to increase the number of absorptive sites within the MOF

structure.^{25,26} This can be achieved by modification of the organic linkers to give ultra-high porosity.

However, large linkers lead to fragile frameworks and to lattice interpenetrations which reduces the porosity.^{25, 26} The use of expanded linkers mixed with second linkers has resulted in stable frameworks with the highest known porosity and surface area. MOFs have limitless future applications due to the porosity, larger surface area, adjustable compositions and tunable pore size.²⁷ The surface area to volume makes them perfect to replace zeolites at every level when produced on a large scale.²⁷ As solid structures produced from coupling of mechanical and chemical properties on molecular scale, MOF's have very unique electrical properties which can be explored for production of energy on a large scale or even used as good electric conductors.²⁵ The pores on their surfaces also make them good and effective materials for drug loading.²⁷

MOF's as Potential Drug Carriers

MOF's have over the years been developed as capable materials for drug delivery, owing to their high porosity which enables high drug loading, versatile functionality, larger surface area, biodegradability, and chemical stability.²⁷ Large amount of drug materials that are absorbed into pore apertures of MOFs including procainamide, ibuprofen, and nitric oxide can be released once they are introduced into the body (see **Figure 3**).²⁷

Recent developments have seen MOF materials scaled down to nanosizes to serve as carriers for selective delivery in cisplatin prodrugs.²⁷ Despite the remarkable improvement made in the use of MOF's for delivery of drugs, many other feature developments must occur in order for them to become viable nano-therapeutic agents.²⁷ Limitations of current therapeutics such as

poor pharmacokinetics, rapid clearance, high doses, and high side effects must see some advancement in disease treatment.²⁷ Most of these limitations associated with small molecular drugs can be relieved by making use of novel systems from MOF's which has improved characteristics such as biocompatibility, kinetics of drug release, high loading ability, size, and surface properties.²⁷

Moreover, these nanoparticles can specifically be designed to target tissues of certain disease (*e.g.* tumor and cancer cells) by conjugation present in targeting ligands.²⁷ They can be engineered to contain agents which provide both imaging and therapy, which is much difficult to achieve in conventional therapeutic methods.²⁷ Abraxane and Doxil demonstrate the clinical success of the nanoparticle therapeutic approach.²⁷

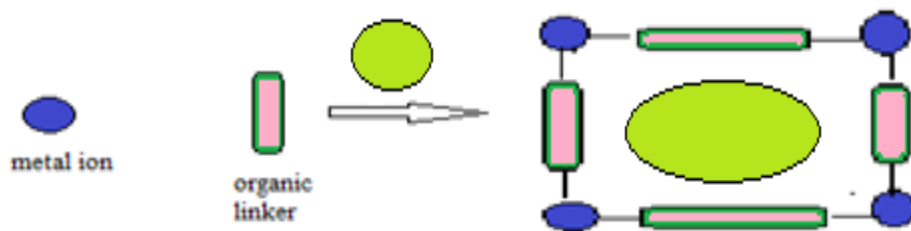


Figure 3: Formation of a 1D MOF and the loading of a drug material by physical encapsulation into the pore aperture of the MOF (modified from Huxford *et. Al.*).²⁷

Dye-Sensitized Solar Cells (DSSC)

DSSC (shown in **Figure 4**) are third generation solar cells based on a photo electrochemical system with a semiconductor formed between an electrolyte and a photo-sensitized anode.³⁴ They include Cadmium telluride (CdTe), Copper Indium Gallium Selenides solar cells (CIS or CIGS) and other amorphous solar cells.³⁵

The production cost of this solar cell concept compared to the traditional silicon and cells is predicted to be about five times lower, with a conversion efficiency of about 6-10% depending on the size and thickness of dye used.³⁶ Although their construction is simple and less expensive, DSSC suffer some major challenges such as low efficiency, low scalability and low stability.³⁷

Factors such as internal resistance, open circuit voltage (V_{oc}), short circuit current (I_{sc}), and fill factor of dyes affect the efficiency of DSSC greatly.³⁷ The current output of DSSC can be improved through the reduction of the internal resistance by modifying the roughness factor, adjusting the thickness of conducting layer and making the gaps between electrodes much smaller.^{36,37} The employment of chemically aggressive liquid electrolytes makes the use of silver fingers very difficult for current collection and also affect the upscale of the cell.³⁷

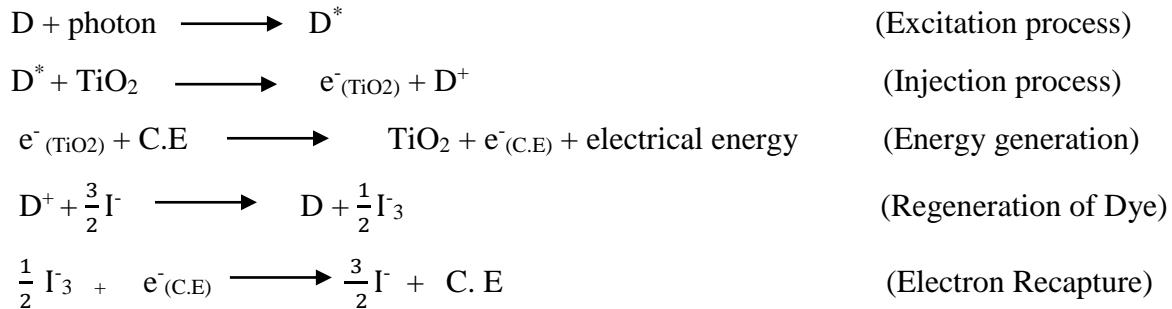
Operating Principle of DSSC

The photo-electrode is coated with nanocrystalline TiO_2 (Titanium Oxide) which is porous to provide a large surface area for adsorption of the photosensitive dye. This porous TiO_2 layer allows for charge transfer upon excitation. The quality of the TiO_2 electrode significantly affects the efficiency of photo conversion in DSSC. When photons are absorbed, the molecules of the dye are excited from the ground state highest occupied molecular orbitals (HOMO) to the

excited states lowest unoccupied molecular orbital (LUMO) as shown in **Figure 4**. Once excited, electrons are injected into the conduction band of the nanostructured semiconductor TiO₂ film, and transported between the oxide nanoparticles (refer to **Figure 4**).^{38, 39}

The transported electron is then extracted to a load where it delivers electrical energy as its work done.³⁸ Once the injection of the electron occurs, the dye becomes oxidized.³⁸ Injected electrons are replenished from the dye in the excited states from the electrolyte ($3\text{I}^- \rightarrow \text{I}_3^- + 2\text{e}^-$) such as the iodide/triiodide couple (electrolyte). The couple receives electrons from an external circuit and is regenerated by reduction ($\text{I}_3^- + 2\text{e}^- \rightarrow 3\text{I}^-$) of the triiodide at the cathode³⁸. In other words, the iodide-triiodide (I^-/I_3^-) couple electrolyte serves as an electron mediator between the TiO₂ electrode and the counter electrode coated with carbon (see **Scheme 1** and **Figure 4**).^{38,39}

Moreover, the dye molecules are regenerated from their oxidized form by accepting electrons from the redox I^-/I_3^- electron mediator.^{38,39} The internally donated electron which is injected to the oxide layer is substituted by electron from I_3^- which gets reduced to I^- ion (**Scheme 1**).³⁹ Electric power generation in DSSC cause no permanent transformation in chemical composition. This is as a result of electron movements through the wider band gap present in the conduction band of the nanostructured semiconductor. This is accompanied by charge-compensating diffusion of cations in the electrolytic layer of the nanoparticle surface.³⁹



Scheme 1: Principal reactions that occur in DSSC.³⁹

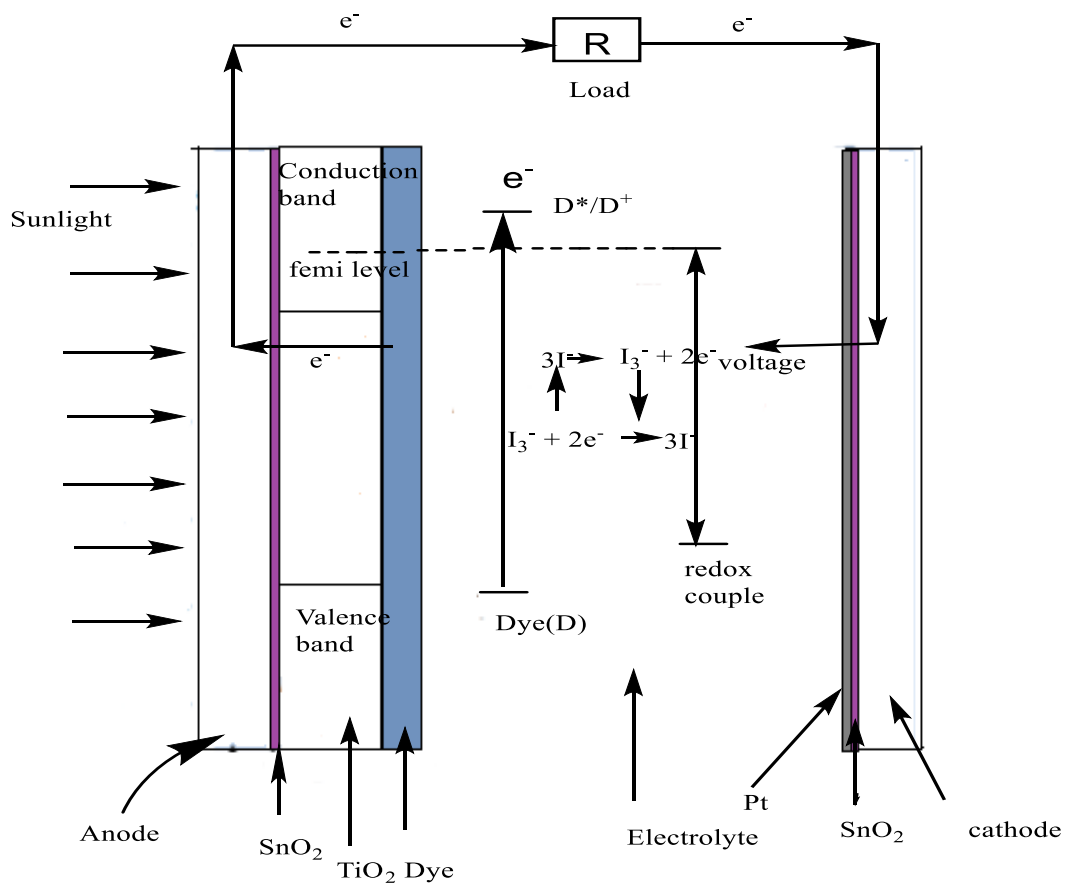


Figure 4: A typical structure of the DSSC (modified from Khalil *et. Al.*).³⁹

Sensitizers (Dyes)

The most prominent and promising group of dyes used in DSSC are ruthenium (II) complexes and metal-free organic dyes.³⁹ These Ru (II) complexes show high rates of charge transfer to ligand in the visible region of the electromagnetic spectrum; a pre-requisite for injecting electrons efficiently into the wide conduction band of the TiO₂ semiconductor.³⁹

However, due to the scarcity of ruthenium, Ru dyes used in DSSC are very expensive.⁴⁰ Metal-free organic dyes, on the other hand, have high molar extinction coefficients, are less expensive, are flexible in molecular tailoring, and are environmentally compatible.⁴⁰ Some of the metal-free organic dyes used extensively in studies for construction of dye moieties in DSSC include triphenylamine (TPA), carbazole, coumarins, indole-dye, porphyrin, and phenothiazine (PTZ).^{39,40}

Recent studies on phenothiazine-based sensitizers show promising improvement on the efficiency due to their electronic and structural properties.^{39,40} Anchor dyes of phenothiazine with strong electron withdrawing groups such as cyanides (CN) and carboxylic acids (-COOH) effectively inject electrons into the conduction band of the TiO₂ due to the extension of their π -system.⁴⁰ This effective electron injection is further confirmed with calculations on the adsorption energies on the TiO₂ surfaces after preferred anchoring configurations were established.⁴⁰

Catalytic Hydrolysis: Role of Carboxylic Acids

Carboxylic acid hydrolysis is depicted in all amino acids which play essential roles as building units of proteins and as intermediates in metabolism. For instance, certain conserved amino acid residues of protein tyrosine phosphatases (PTPases) are strongly involved in catalytic activities at the enzyme active site.⁴² Investigations of the role of aspartic acids confirmed its essential role in the enzyme's catalytic activity.⁴²

Kinetic analysis by Lohse *et. Al.* on aspartic acid reactions with mammalian phosphatases at different pH suggests a phosphoryl group transfer, which leads to the hydrolysis

of dipeptide bonds.⁴² Other findings by Denu *et. Al.*, in an efforts to understand the structure, function and biological properties of PTPases through kinetic analysis, showed that the aspartic acid residues were conserved and involved in a general acid catalytic mechanism.⁴²

General Acid-Base Ester Hydrolysis

The partial transfer of a proton by a Bronsted acid to a reactant in the transition state denotes general acid catalysis, while the acceptance of the proton by a Bronsted base leads to an increase in the reaction rate which results in the basic catalysis.⁴⁴ Side chains of aspartic and glutamic acids have considerable acidic and basic properties and would likely behave as catalysts in general acid-base reactions in cells. Hydrolysis of carboxylic acids and phosphate esters, carbonyl additions and amino lysis of esters are typical acid-base reactions of aspartic acids⁴⁴.

Also, due to the amphoteric nature of amino acids, aspartic acid readily undergoes nucleophilic and electrophilic reactions at different pH as shown in **Figure 5** below. These properties make aspartic acid catalyze both acidic and basic reactions.⁴⁴

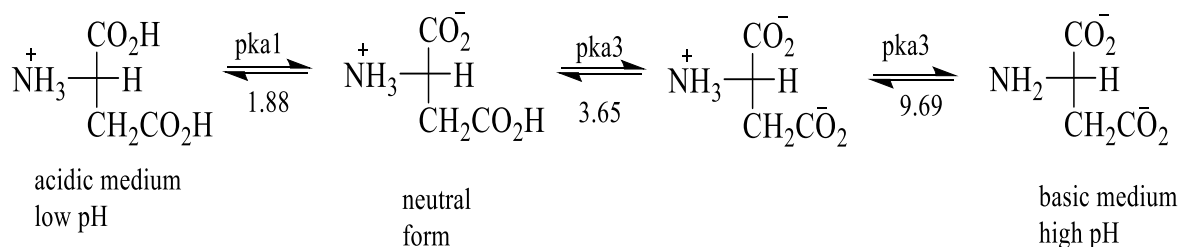
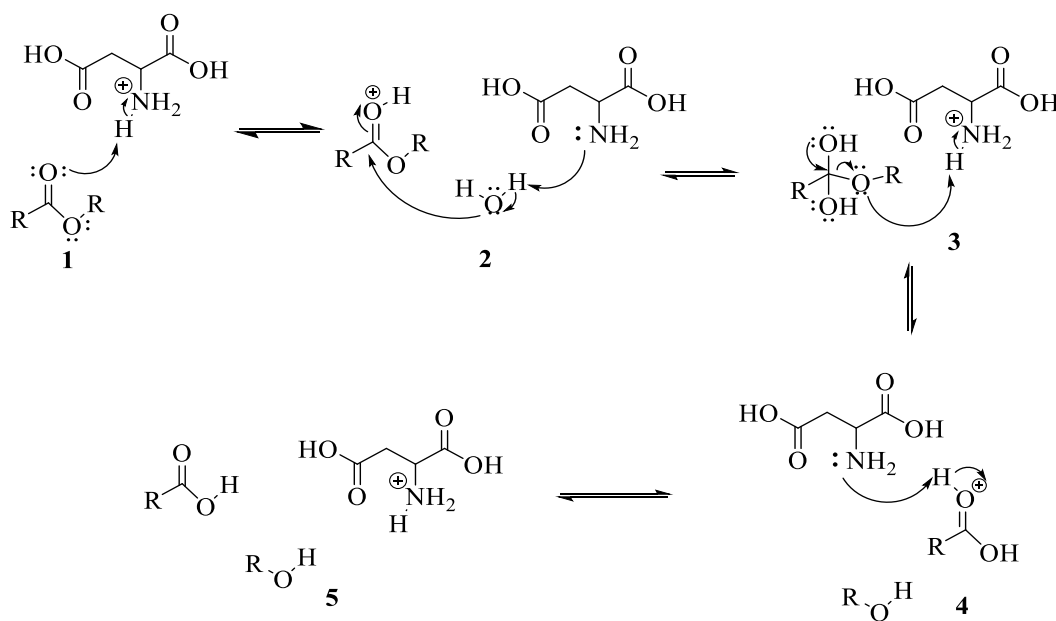


Figure 5: Tautomerism of aspartic acid at different pH.

General Acid Catalyzed Ester Hydrolysis

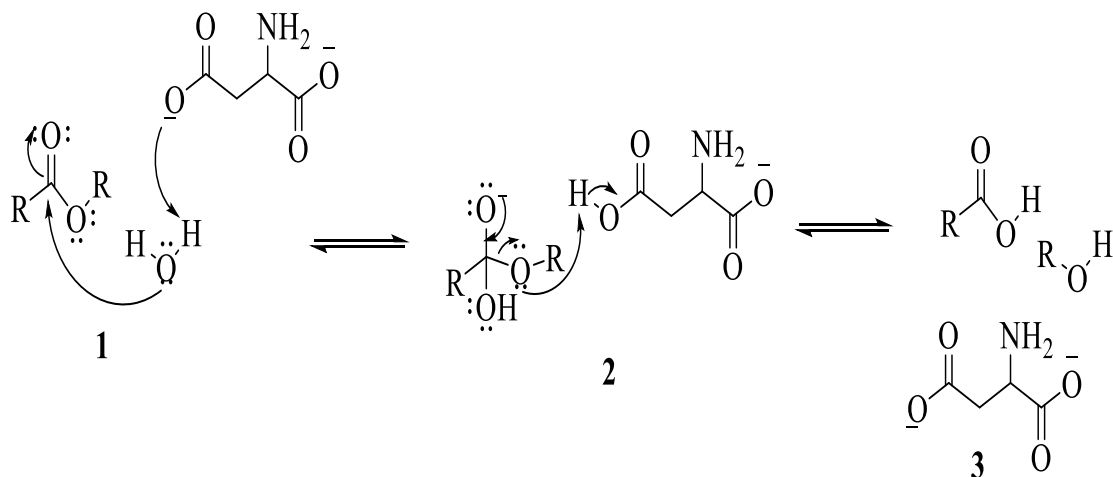
The initial step in the proposed mechanism under acidic condition as shown in **Scheme 2** involves the abstraction of a proton from the protonated amino group ($-\text{NH}_2^+$) in the aspartic acid (amino acid). This facilitates the nucleophilic attack of water on the carbonyl carbon with a corresponding proton transfer of proton between the water molecule and aspartic acid.⁴³ This proton transfer step stabilizes the intermediate formed.⁴³ Tautomerism between the alcohol group and carbonyl group easily releases the alkoxy group by proton abstraction from the protonated amino group of aspartic acid. Finally in step 4, aspartic acid abstracts a proton which is transferred to water, leaving the carboxylic acid and alcohol formed as the final product.⁴³



Scheme 2: Proposed mechanism for the hydrolysis of esters by aspartic acid under acidic conditions.⁴³

General Base Catalyzed Ester Hydrolysis

The base catalyzed mechanism (**Scheme 3**) involves the addition of a nucleophile which is followed by the abstraction of a proton by the amino group from water while the water molecule in turn attack the carbonyl group of the ester.⁴³

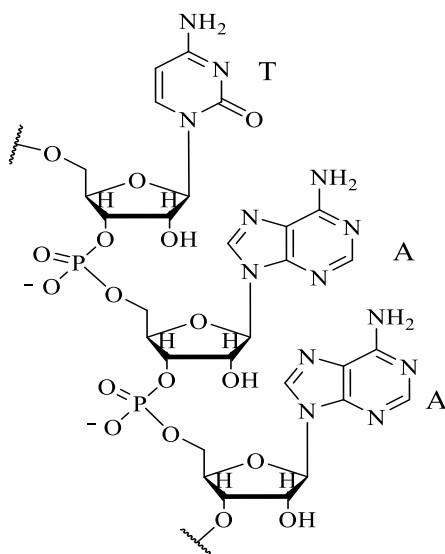


Scheme 3: Proposed mechanism for the hydrolysis of esters by aspartic acid under basic conditions.⁴³

Phosphodiester Bonds

Amino acids such as aspartic acid and glutamic acids have shown an ability to increase the rate of hydrolysis of many molecules because of their amphoteric nature.²⁰ Phosphodiester bonds are found in every part of the biological systems. They are essential to all life since they constitute the backbone of deoxyribonucleic acids (DNA), ribonucleic acids (RNA), and also exist in various parts of cell membranes (**Figure 6**).²⁰

In cellular membranes, phosphodiester bonds function as linkages in phospholipids. These linkages are strong covalent bonds existing in between phosphate groups and two ring pentoses over two ester bonds.²¹ The phosphodiester covalent bonds holding the pentose groups of DNA and RNA can be broken through alkaline hydrolysis through hydrophobic or hydrophilic interactions of the tail ends of polar groups present in their bonds.^{20,21}

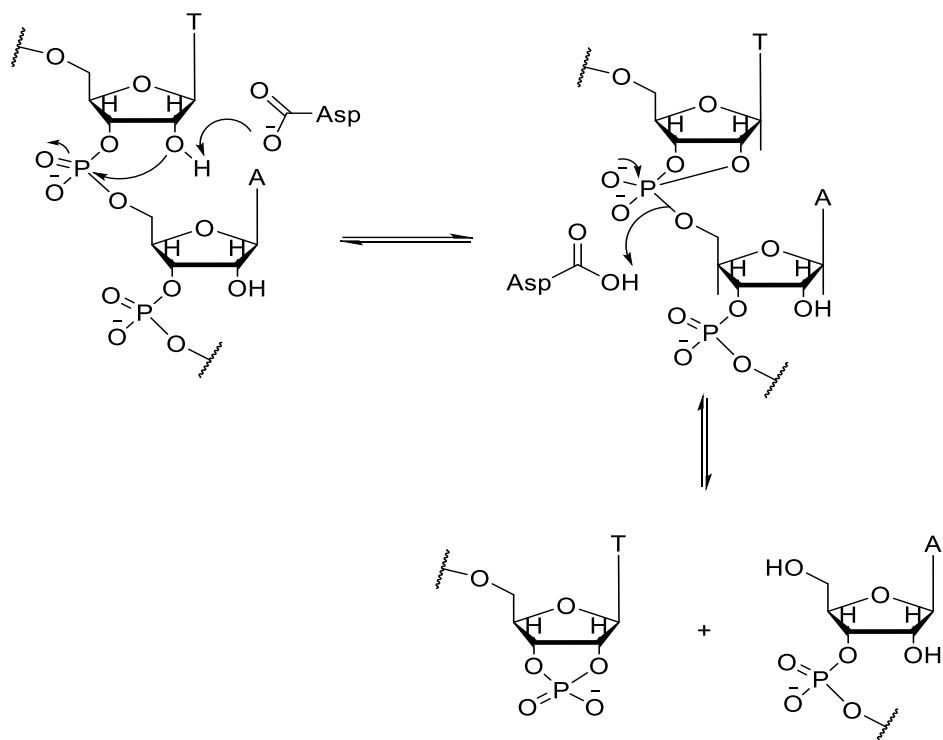


T: Thymine

A: Adenine

Figure 6: A section of the DNA showing phosphodiester bonds.^{20,21}

Phosphodiester bonds of RNA have received a lot of scientific interest over the years; further studies on the mechanism of their hydrolysis by enzymes are needed to provide more insight and to develop artificial enzyme models.⁴⁴ The function of a base in hydrogen abstraction depicted by aspartate plays an essential role in the cleavage of the phosphodiester bonds of RNA (**Scheme 4**).⁴⁴ A similar mechanism is the hydrolytic cleavage of the phosphodiester bonds of RNA and DNA.⁴⁵



Scheme 4: Proposed hydrolysis of the phosphodiester bond of RNA by aspartate.⁴⁵

Research Objectives

The major aim of this research is to synthesize selected phenothiazinium derivatives for potential applications in photodynamic therapy, DSSC, and MOFs technologies. Synthesis of phenothiazinium derivatives with two carboxylic acid side groups are of special interest for their relevance to hydrolytic enzymes that utilize carboxylic groups in their catalytic activities. Carboxylic groups are encountered in amino acids, proteins, enzymes, and fatty acids. This functional group has important biological activities; it can be easily masked into alkyl or aryl esters and can be regenerated in the body during metabolism. This feature enhances the

lipophilicity of phenothiazine derivatives to selectively concentrate more in malignant tissues, while leaving the chromophore intact for irradiation in PDT. The excess alkyl esters in the body can be readily cleaved by esterase in blood, liver, and other body tissues to ensure their decomposition in the body at a faster rate than those present in malignant tissues. Moreover, photosensitizers bearing carboxylic groups and hydroxy groups have been reported in literature to be non-toxic (Asmiyenti *et Al.* 2012),⁴¹ therefore we expect the new derivatives to be nontoxic.

The specific positions of certain side groups on the phenothiazinium ring make them attractive as organic linkers for metal organic frameworks (MOF's). Binding of the metal ions to organic linkers which are not too large and too small such as the three core aromatic rings of phenothiazine will increase the robustness and right pore aperture for metal organic frameworks synthesized from our derivative for potential application in the energy industry. MOF's with the right size of their surface pores can be used gas capture and storage for hydrogen gas alongside drug delivery by storing drug materials in their pores and discharging them to targeted sites in the human body.

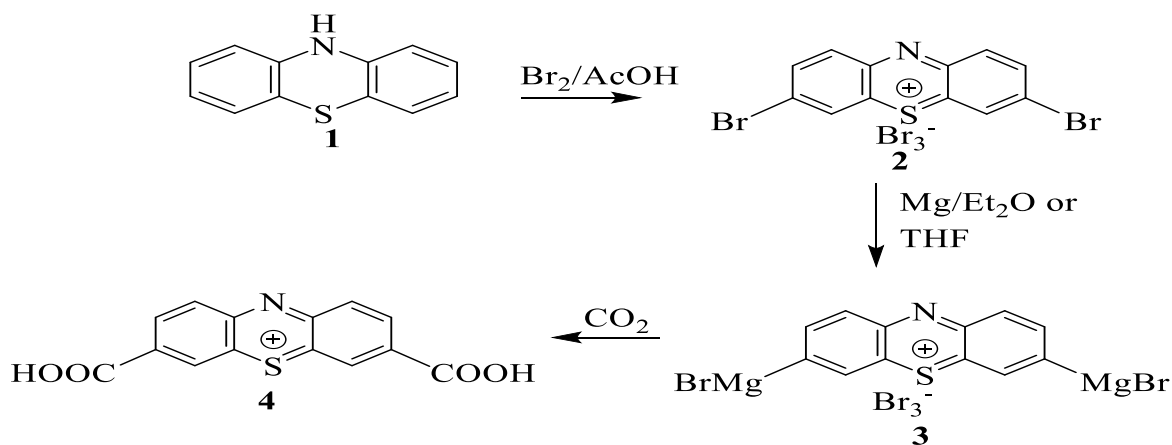
We further anticipate these derivatives to effectively inject electrons into conduction bands in DSSC when excited by sunlight light. This feature is a key characteristic of the dyes employed in DSSC. These derivatives with two carboxylic acid groups directly attached to the phenothiazinium ring are expected to counter the electron withdrawing effect of the electron-deficient sulfur cation. These derivatives are expected to effectively bind to the surface of titanium oxide (TiO₂) through the carboxylic groups. This binding can improve the efficiency of DSSC.

CHAPTER 2

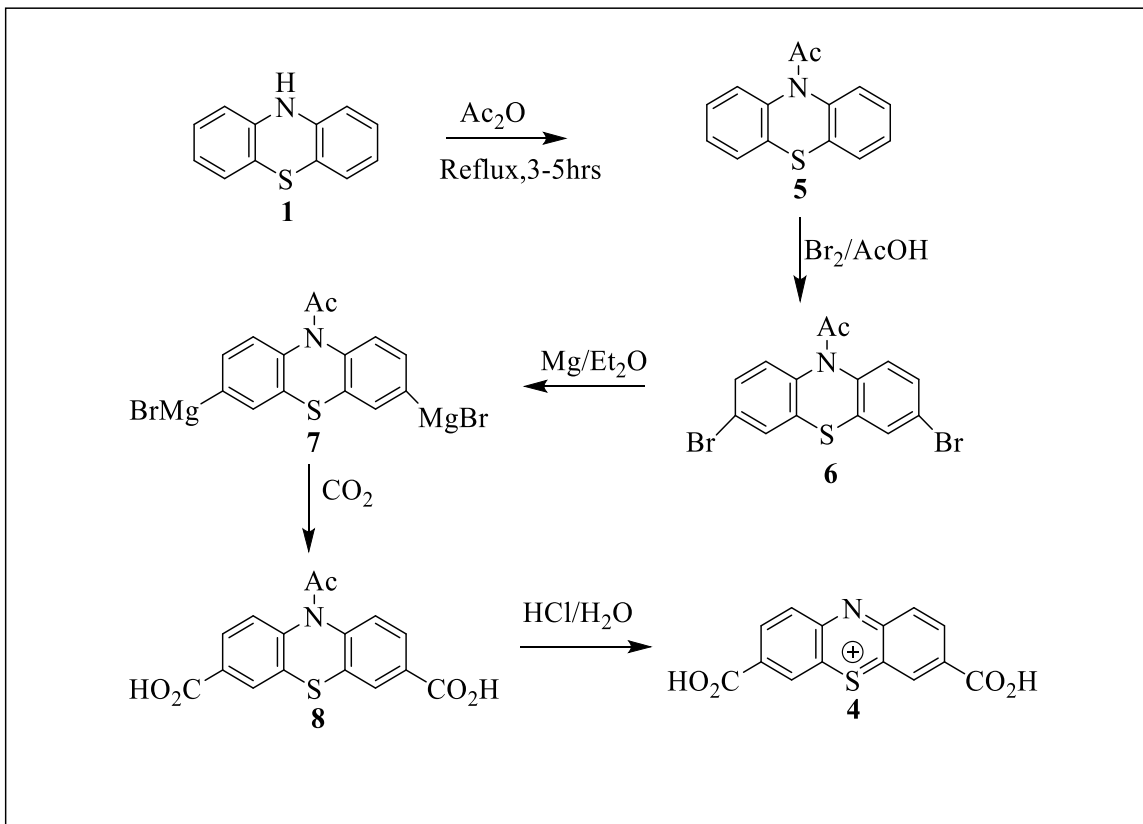
RESULTS AND DISCUSSIONS

Various simple monosubstituted carboxylic acid derivatives of phenothiazine have been reported in literature, which have shown remarkable antimicrobial activities. A number of these derivatives have also been tested in PDT and DSSC and have proved to be efficient photosensitizing agents in these fields.^{11, 16, 17, 33, 40} In all these reports, mono-substituted carboxylic acid derivatives were more successfully synthesized and found to be of low toxicity in PDT applications.^{41, 48}

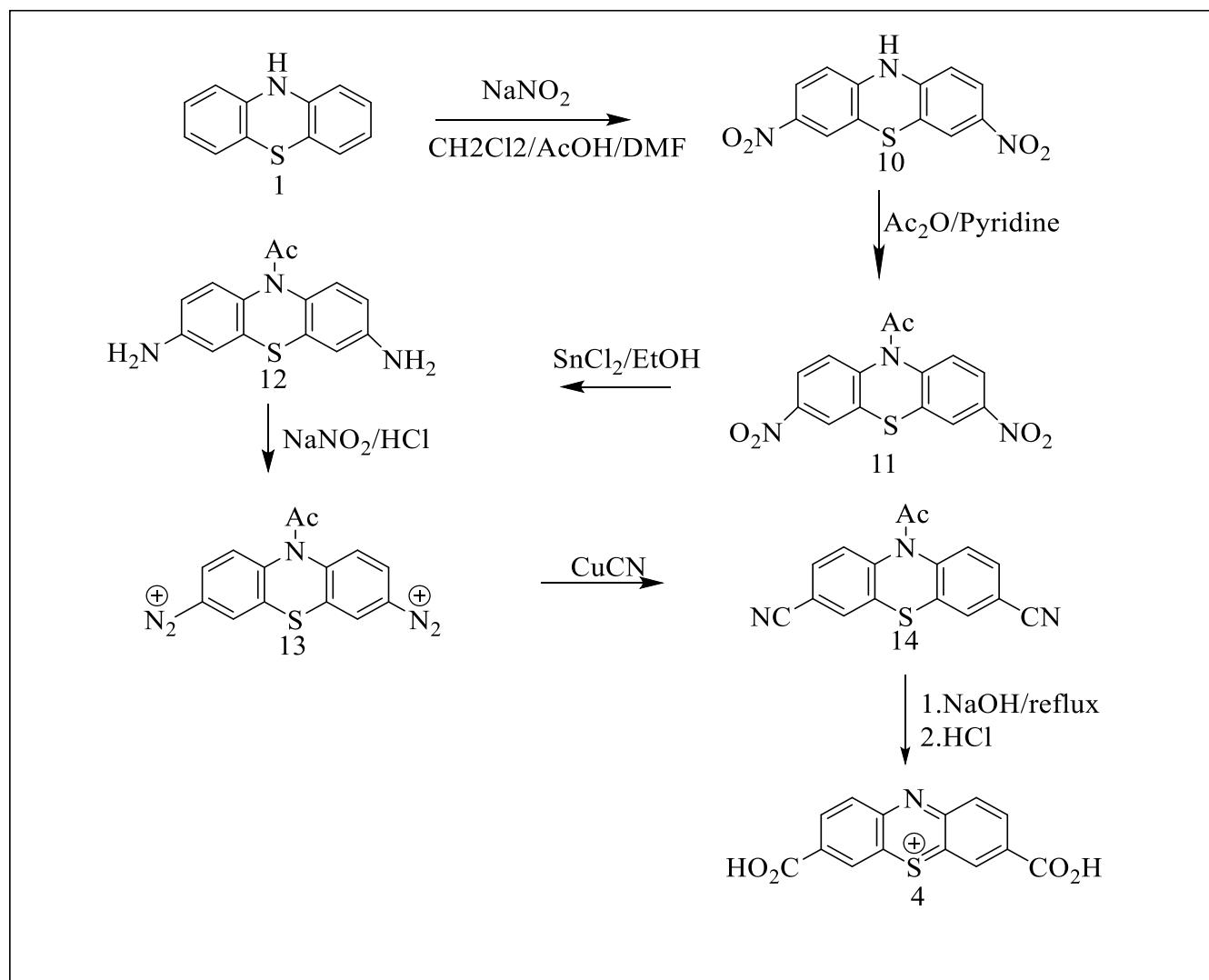
However, these mono substituted derivatives were difficult to purify and were of low percentage yields.⁴⁸ We observed similar drawbacks in our attempts to synthesize 3,7-phenothiazinium dicarboxylic acid (PTZ dicarboxylic acid), **Schemes 5-7**. All compounds that were synthesized in this work were characterized by NMR and IR spectroscopy. TLC was used for monitoring the progress of reactions and checking the purity of products.



Scheme 5: Proposed synthetic route for the PTZN dicarboxylic acid from unprotected phenothiazine using Grignard reaction.



Scheme 6: Proposed synthetic route for the PTZN dicarboxylic acid from protected phenothiazine using Grignard reaction.



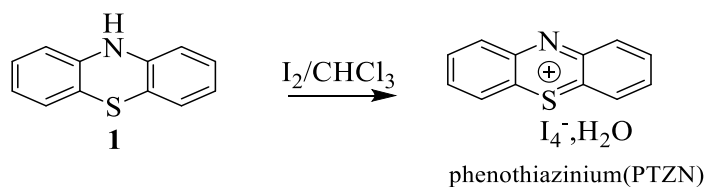
Scheme 7: Proposed synthetic route of the PTZN dicarboxylic acid using Sandmeyer reaction.

Synthesis of phenothiazine-5-ium tetra iodide hydrate (PTZN)

This compound was synthesized using a modified procedure from the one reported by Wainwright (**Reaction 1**) upon addition of a solution of iodine to phenothiazine over a period of 1 hour (**Reaction 1**).^{12, 17} A dark blue product was obtained in 72 % yield, with physical data consistent with that reported in literature.

Initial TLC analysis of the product in chloroform/ methanol mixture (3:1, v/v) showed three spots of different R_f values and colors. One of the spots was colorless with $R_f = 0.550$ comparable to that of phenothiazine starting material (this spot was oxidized to a blue compound upon exposure of the TLC plate to air). The TLC indicated that the reaction was incomplete.

A second TLC analysis of the product, after washing of the crude product thoroughly with chloroform (CHCl_3), showed only two spots. The spot which disappeared after washing with excess chloroform is believed to be from excess iodine used as an oxidizing agent in the reaction. The remaining two spots were separated by column chromatography to give 0.157 g (72%) as dark blue to green product. The product (PTZN) had a higher R_f (0.702) compared to phenothiazine (0.553). ^1H NMR analysis of this compound showed two doublets and two triplets. There was no singlet peak for N-H as seen in phenothiazine; indicating the oxidation of the aromatic ring (ref. to spectra in **Appendix I 1** and **I 2**).



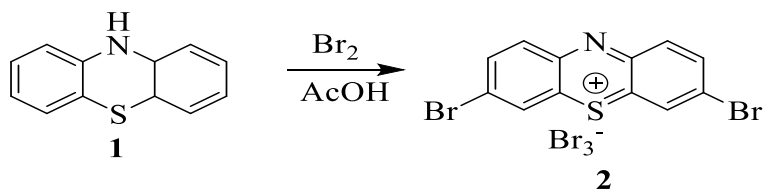
(Reaction 1)

Synthesis of 3,7-dibromophenothiazinium perbromide (2)

This compound was prepared by suspending phenothiazine in an excess amount of bromine in glacial acetic acid (**Reaction 2**). The dark red solution was stirred for 16 hours at room temperature, and then treated with an adequate amount of sodium sulfite to reduce the excess bromine.

A green solid that precipitated out was obtained by filtration, and further recrystallized from a mixture of ethyl acetate/hexane (8:1, v/v), to give (2) in 75 % yield. TLC analysis of the product (mp = 263-265 °C) showed one spot which has a relatively lower R_f (0.535) value compared to phenothiazine.

The physical appearance of the product was consistent with literature reports.⁴⁶ Proton NMR analysis of the product showed two doublets and a singlet at 7.360 (d, $J = 8.4$ Hz), 7.778 (d, $J = 8.0$ Hz), and 8.199 (s) respectively (refer to the spectrum in **Appendix A**). The absence of a second singlet peak (N-H) in this product comparable to phenothiazine indicates the product is in the oxidized as seen in **Reaction 1**. The counter ion reported for this oxidized product is the tribromide.⁴⁶

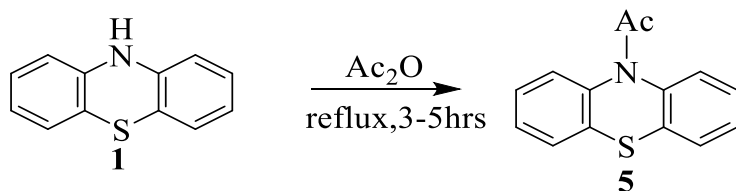


(Reaction 2)

Synthesis of N-acetyl phenothiazine (5)

Compound **5** was prepared by refluxing phenothiazine in acetic anhydride for 3-5 hours (**Reaction 3**). After washing with acetone, the product was obtained in 95% yield as a yellow solid, (mp 197-198 °C, lit. 196-197 °C) .²²

TLC analysis of the product after recrystallization from acetone gave a single spot which is a little higher in R_f value compared to the starting phenothiazine compound. ^1H NMR spectrum of the product was consistent with that reported in literature,²³ which showed two triplets and two doublets in the aromatic region, and one singlet in the aliphatic region (refer to the spectra in **Appendix B1** and **B2**). ^{13}C NMR of the product showed 6 peaks, in the aromatic region, 1 in the alkane region and 1 peak in the amide region confirming the protection of the aromatic ring.



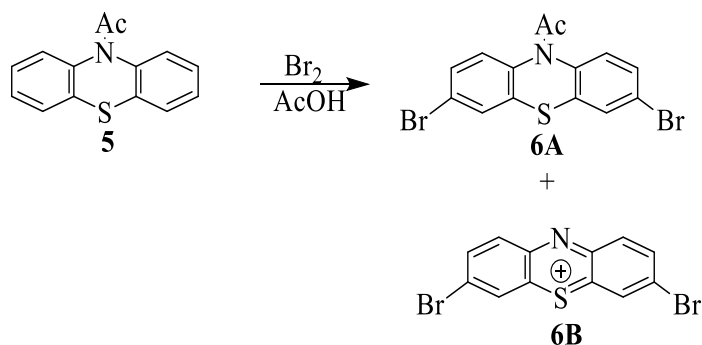
(Reaction 3)

Synthesis of N-acetyl-3,7-dibromophenothiazine (6)

Synthesis of this compound was carried out under two different conditions (**Reaction 4**). First, the amide derivative (N-acetylphenothiazine, **5**) was stirred for 16 hrs, at room temperature in glacial acetic acid, with excess bromine. A green product (**6**) was obtained, but of ~ 10% yield. The second reaction which involved refluxing (110-120 °C) compound **5** with bromine in glacial

acetic acid gave 62% yield of the product (pale green in appearance). The product obtained by this approach was found to be the unprotected 3,7-dibromophenothiazinium, **6B** (mp 206-208 °C). The melting point of **6B** is different from compound **2**. This may be due to the difference in counter ion of this product (**6B**) compared to compound **2**. Reported work by Plater and co-workers indicates that the counter ion in this product is either a mono bromide (Br^-) or a tribromide (Br_3^-) ion.⁴⁶

TLC analysis of the product showed one spot indicating the compound is pure. ^1H NMR of this product showed only three signals, with all of them in the aromatic region: a doublet of doublet, a doublet, and a singlet (refer to the spectrum of **Appendix H1** and **H2**). Lack of CH_3 signal in the aliphatic region of the spectrum indicates that de-protection and oxidation of phenothiazine to phenothiazinium took place. When the reaction is conducted at 70-80 °C (instead of refluxing) a dark-purple product is isolated alongside **6B**. ^1H NMR of this side product shows two doublets in the aromatic region and a singlet in the aliphatic region (for the protecting acetyl group). The melting point value of the purple product is 227-229 °C. This product could be the tetra bromophenothiazine amide (**6A**) resulting from poly bromination of the compound **5** as the reaction progressed.



(Reaction 4)

Synthesis of phenothiazin-3,7-dicarboxylic acid (4) and

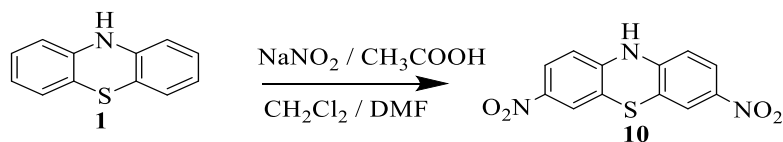
N-acetyl-3,7-phenothiazinedicarboxylic acid (8)

We attempted to synthesize compound **4** and **8** starting with **2** (**Reaction 2**) and **6B** (**Reaction 4**). A series of trials failed to yield the expected products (**4** and **8**). One major challenge was the insolubility of starting materials in diethyl ether (the solvent that is commonly used in the Grignard reaction). One starting material (**6B**) was quite soluble in THF when heated, but failed to react with Mg to form the Grignard intermediate. Other trials using t-butyl methyl ether and 1,4-dioxane as solvents experienced the same challenges mentioned above.

Synthesis of 3,7-dinitrophenothiazine (10)

In this procedure, the nitration of phenothiazine was done using sodium nitrite in a mixture of chloroform and acetic acid to give 70% yield of **10** as a brown solid (**Reaction 5**). TLC analysis of the brown product (chloroform-methanol, 3:1, v/v as eluent) gave only one spot ($R_f = 0.667$). ^1H NMR of the product showed three signals in the aromatic region; a doublet of doublet, two doublets, and a singlet in the alkane region. ^{13}C NMR of the product showed the expected 6 peaks in the aromatic region and two additional peaks in the alkane region and amide region. These peaks may be from DMF contamination of the product or acetate counter ions from acetic acid used in the reaction (ref. to spectra in **Appendix C1, C2, C3** and **C4**). IR analysis showed a medium sharp peak around 3400 cm^{-1} (N-H) indicating a secondary nitrogen. The melting point (220-222 °C) value of the product indicates that the product is pure.

Several other attempts were made in synthesizing this derivative via other routes. The first attempt involved nitrating phenothiazine amide (**5**) using sulfuric acid and nitric acid in 1:1(v/v) and 1:3(v/v) ratios, respectively, as nitrating reagents. The reaction yielded an orange solid, which is reported as 3,7-dinitrophenothiazin-5-oxide in literature.⁴⁸ This formation of this product is a result of the high oxidative nature of the concentrated nitric acid and the high affinity of oxygen by sulfur. Another attempt using sodium nitrite in the presence of hydrochloric acid *in situ* yielded an intractable reddish brown precipitate; no further attempts were made to characterize this product.



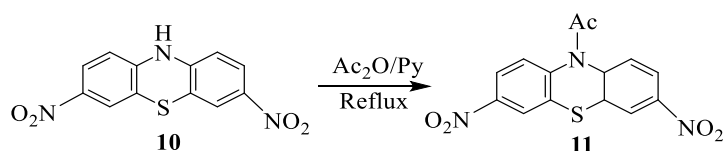
(Reaction 5)

Synthesis of N-acetyl-3,7-dinitrophenothiazine (**11**)

This synthesis involved the protection of the phenothiazine ring through amide bond formation which is carried out at reflux temperatures between 120-130 °C. The product obtained was a yellow solid in 71 % yield (mp 213-214 °C), after purification by column chromatography and recrystallization from acetone (**Reaction 6**). TLC analysis of the yellow product (chloroform-methanol, 3:1, v/v as eluent) gave only one spot of R_f (0.645) which was lower than compound **10**. ¹H NMR of **11** showed four signals; a doublet of doublet and two doublets (all corresponding to the aromatic protons between 7-8.5 ppm) and a singlet for the acetyl group in

the alkane region (ref. to spectra in **Appendix D1** and **D2**). Integrations of these individual peaks showed a 1:1:1 ratio for protons in the aromatic region and 1.5 for the singlet in the alkane region; corresponding to 2H for each of the aromatic signals and 3H for the acetyl group. ^{13}C NMR gave 8 peaks as expected with the characteristic amide carbon and alkane carbon at 168.696 (C=O) and 23.397 (CH₃) ppm respectively (ref to spectra in appendix **D3** and **D5**). IR spectrum (ref. to spectrum at **Appendix D5**) showed a peak at 1710 cm⁻¹ for C=O stretching in the acetyl group.

Other attempts which involved nitrating the amide derivative (**5**) with nitric acid (HNO₃) in the presence of sulfuric acid were not successful. This could be due to the protonation of the carbonyl bond (C=O) or the de-protection of the ring via amide hydrolysis which readily occurs in acidic medium. Another reason could be due to the mono nitration product which is formed in low yield that may affect the overall yield of the product.



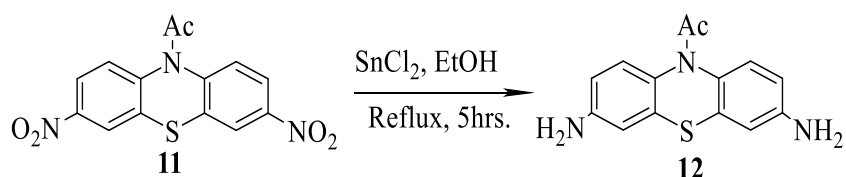
(Reaction 6)

Synthesis of N-acetyl-3,7-diaminophenothiazine (**12**)

This product was isolated as a blue solid from **Reaction 7** below. TLC analysis of the product gave one spot with a higher R_f(0.688) value compared to compound **11**. The melting point value of the product was 172-174 °C; indicating the isolated product is pure. ^1H NMR

showed four peaks; a doublet-doublet and two other doublets, all corresponding to the aromatic protons in the regions of 7-8.5 and two characteristic singlet peaks for the acetyl group in the alkane region and the amino group (-NH₂) at 5-6 ppm, respectively (ref. to spectra at **Appendix E1** and **E2**). The singlet peak for the NH₂ was broad. Integrations of these individual peaks showed a 1:1:1 ratio for protons in the aromatic region and 1.5 and 2 for the singlet at 2 ppm and 5.6 ppm for the -CH₃ and -NH₂ respectively. IR analysis also showed a stretching frequency around 1710 cm⁻¹ for C=O and 3350 cm⁻¹ for the two peaks of the primary amine resulting from the reduction of the nitro groups (ref. to spectrum at **Appendix E3**).

Other attempts using tin (II) chloride in hydrochloric acid yielded less than 13% of the product, mixed with unreacted amounts of compound **11**. This could be a result of the protonation of the carbonyl group by HCl which may undergo further hydrolysis of the amide.



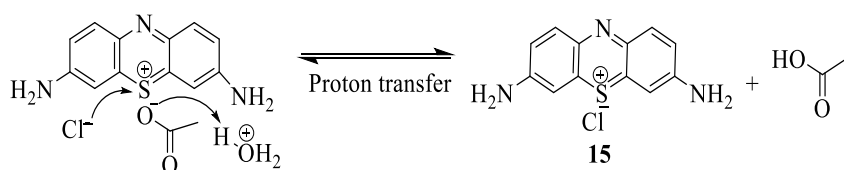
(Reaction 7)

Conversion of thionine acetate and N-acetyldiaminophenothiazine (**12**) into thionine chloride (**15**)

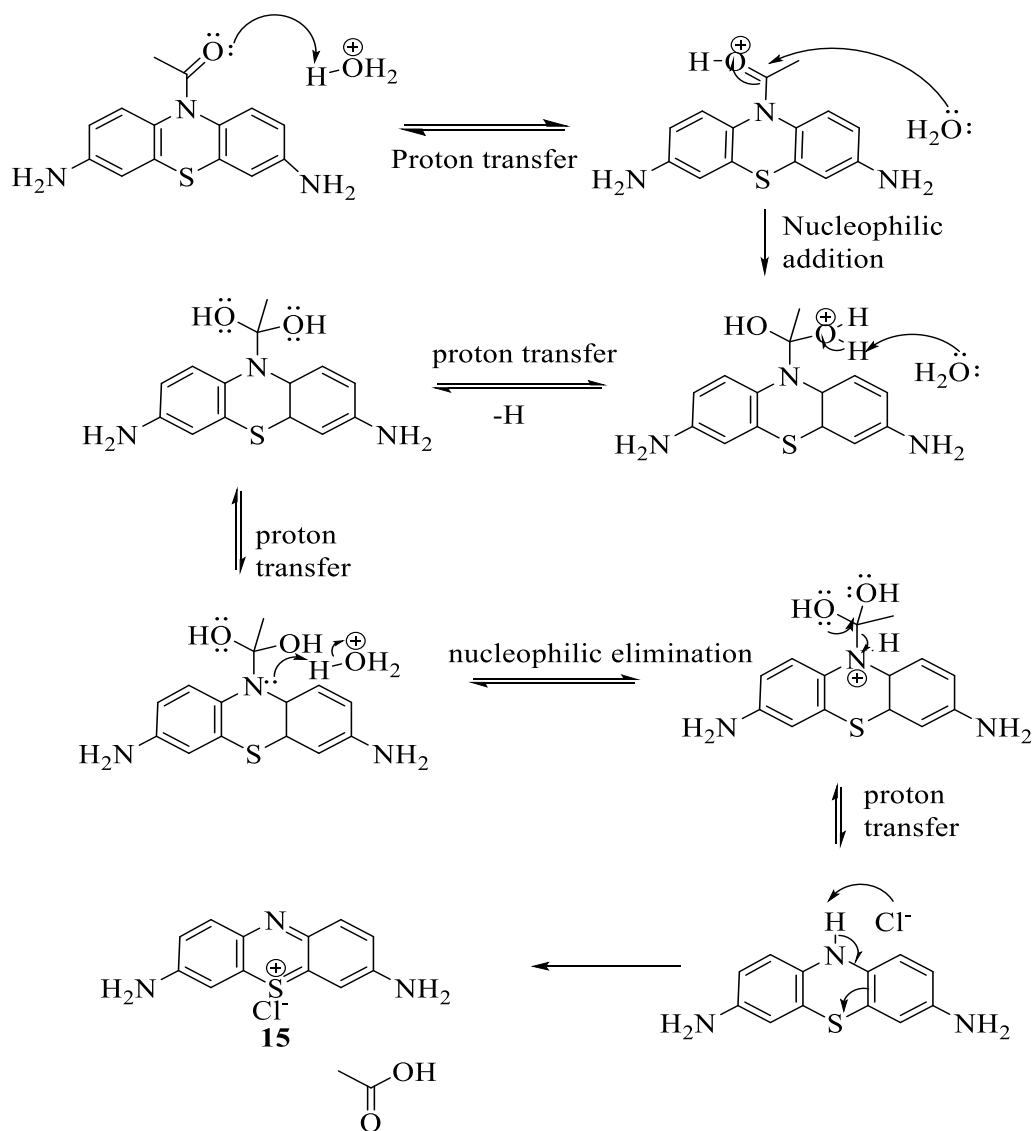
This derivative was synthesized using two different starting materials (thionine acetate or thionine amide) under different conditions as shown in **Scheme 8**. The first approach which involves the use of thionine amide (**12**) was refluxed in hydrochloric acid at temperatures

between 110-120 °C for 2-3 hrs (**Scheme 8b**). The product precipitated as a blue solid upon cooling.

The second approach using thionine acetate as the starting material was carried out at room temperature. This reaction proceeded readily at room temperature (**Scheme 8a**).⁴³ TLC analysis of the product using chloroform/ methanol mixture (3:1, as eluent) showed a single spot of R_f (0.698). ¹³C NMR spectrum showed six peaks corresponding to carbons in the aromatic region (ref. to spectra at **Appendix F1** and **F2**).



Scheme 8a: Proposed mechanism for the conversion of thionine acetate into thionine chloride.⁴³



Scheme 8b: Proposed mechanism for the conversion of thionine amide into thionine chloride.⁴³

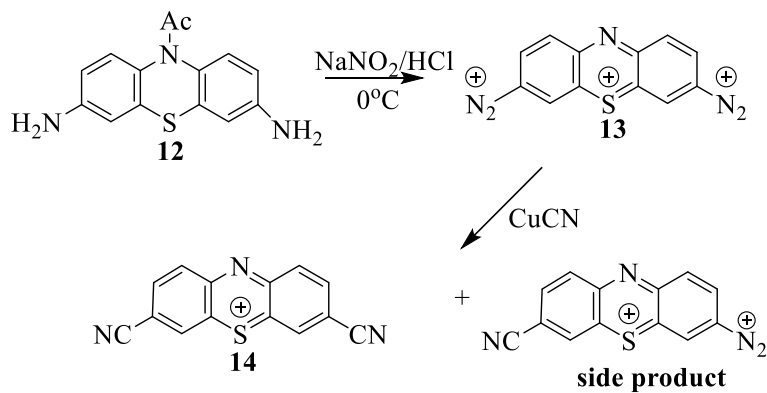
Synthesis of 3,7-phenothiaziniumdinitrile (**14**)

The synthesis of this derivative follows a two-step synthetic pathway. The first step involved the formation of diazonium salts from thionine chloride or thionine amide and converting it to the nitrile derivative. The diazonium salt is prepared *in-situ* by dissolving the

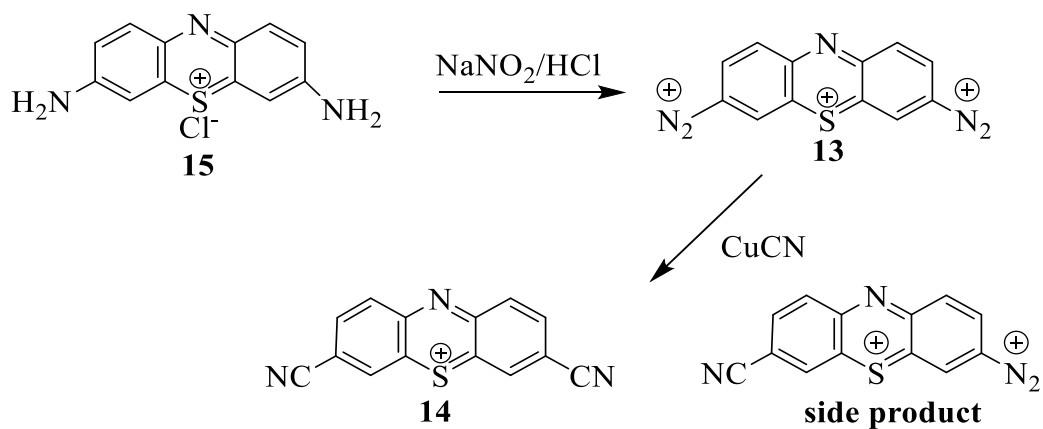
amino derivatives (**12** or **15**) in dilute hydrochloric and stirring in ice. The reaction was carried out at a constant temperature between 0-4 °C in order to prevent the decomposition of the diazonium salt through coupling.

The second step involved the conversion of the intermediate diazonium salt into the nitrile upon reaction with cuprous cyanide, to give a dark solid as shown in **Scheme 9**. IR analysis of the solid shows a medium sharp peak for the CN stretching between 2200-2400 cm^{-1} and medium sharp peak for C=C around 1600 cm^{-1} (ref spectrum at **Appendix G5**). ^1H NMR showed a doublet of doublets, a doublet, and two singlets in the aromatic region. There was no singlet peak in the alkane region even when thionine amide is used in this reaction. This may be due to the simultaneous de-protection of the ring through hydrolysis as the diazotation reaction proceeds (ref. to spectra at **Appendix G1** and **G2**). ^{13}C NMR analysis showed more than 7 peaks as expected in the product (ref. to spectra at **Appendix G3** and **G4**). The extra peaks could be resulting from coupling products that are common in Sandmeyer's reaction. Another reason could be due to the formation of monocyanide side product resulting from the reaction.

Other attempts using potassium cyanide in the second step of the reaction also yield low amounts of the dark product.



Scheme 9a: Conversion of N-acetyl diaminophenothiazine into the phenothiaziniumdinitrile derivative.



Scheme 9b: Conversion of thionine chloride into the phenothiaziniumdinitrile derivative.

CHAPTER 3

EXPERIMENTAL

Materials and General Method

All reactions proceed from phenothiazine which was commercially obtained from Sigma Aldrich. Every chemical reagent and solvent listed were also obtained from commercial sources and used without further purification unless stated.

The compounds synthesized were characterized by ^1H NMR and IR spectroscopy. All NMR spectra were recorded on a JEOL-NMR Eclipse-400 MHz spectrophotometer. The different chemical shifts of all peaks are quoted in parts per million (ppm) using the high-frequency position conversion, and the coupling constants value (J) are reported in Hz. The splitting patterns of resonance were described as follows: singlet (s), doublet (d), doublet of doublet (dd), triplet (t), quartet (q), and multiplet (m). All IR spectra were recorded from Shimadzu 1R Prestige-21 FT-IR spectrometers. Melting points of synthesized compounds were measured without correction from a Cambridge Melt-Temp device. Chromatographic techniques (thin layer chromatography and column chromatography) were also carried out in order to obtain the pure form of synthesized compounds.

Experimental Procedures

Synthesis of phenothiazin-5-ium tetra iodide hydrate (PTZN)

A solution of iodine (0.83 g, 3.3 mmol) in 19 mL of chloroform was added drop wise to a solution of phenothiazine (0.21 g, 1.1 mmol) in 7.5 mL of chloroform. After the addition was

complete, the solution was stirred for half an hour in an ice bath, the resulting mixture was filtered and the precipitate was washed with 20 mL of chloroform until filtrate was colorless and dried under reduced pressure to give 0.157 g (72% yield) of the desired product.¹⁷

NMR (DMSO- d_6): $\delta_H = 6.231$ (d, 2H, $J = 8.4$ Hz), $\delta_H = 6.843$ (t, 2H), $\delta_H = 6.949$ (t, 2H), $\delta_H = 7.029$ (d, 2H, $J = 7.6$ Hz)

Synthesis of 3, 7-dibromophenothiazin-5-ium perbromide (2)

Phenothiazine (0.20 g, 0.20 mmol) was suspended in 7.2 mL of glacial acetic acid. Br_2 (1.5 mL, 0.063 mol) in 20 mL of glacial acetic acid was added all at once to the reaction mixture with vigorous stirring, stirring continued for 24 more hours at room temperature. The reaction was then cooled with an ice bath and 0.25 g (0.50 mmol) of sodium sulfite (Na_2SO_3) was added to the reaction mixture.⁴⁶ About 1-2 mL of water was added to the reaction mixture to form a deep-violet color within three hours of stirring. A 1 M sodium hydroxide (NaOH) aqueous solution was added to the solution with stirring for 30 minutes. A dark-purple solid precipitated out of solution which was filtered off and stirred in excess hot ethyl acetate/hexane mixture (1:8, v/v).⁴⁹ 0.23 g (88% yield, mp 263-265 °C) of the product was obtained as a green powder which was filtered off and dried under vacuum.

NMR (DMSO- d_6): $\delta_H = 7.360$ (d, 2H, $J = 8$ Hz), $\delta_H = 7.778$ (d, 2H, $J = 8.4$ Hz), $\delta_H = 8.199$ (s, 2H) ppm.

Synthesis of 1-phenothiazin-10-ylethanone (5)

Phenothiazine (1 g, 5 mmol) was suspended in 10 mL of acetic anhydride. The mixture was refluxed for 3-5 hrs and monitored with TLC. The warm solution was allowed to cool to room temperature and further cooled in an ice bath. A pale yellow solid precipitated, which was filtered and recrystallized from acetone to produce 1.220 g (92.5% yield, mp 197-198 °C) of the product.

NMR (DMSO- d_6): $\delta_H = 7.550$ (d, 2H, $J = 6.4$ Hz), $\delta_H = 7.641$ (d, 2H, $J = 8$ Hz), $\delta_H = 7.403$ (t, 2H, $J = 6.8$ Hz), $\delta_H = 7.308$ (t, 2H, $J = 6.4$ Hz), $\delta_H = 2.150$ (s, 3H); $\delta_C = 168.982$ (C=O), $\delta_C = 139.228$ (ArC), $\delta_C = 132.527$ (ArC), $\delta_C = 128.416$ (ArC), $\delta_C = 128.018$ (ArC), $\delta_C = 127.827$ (ArC), $\delta_C = 127.544$ (ArC), 23.271 (CH₃) ppm.

IR (ν_{max}/cm^{-1}): 1700 (s, C=O), 1600 (w, C=C), 1470 (m, C=C)

Synthesis of N-acetyl-3,7-dibromophenothiazine (6)

Approach 1:

Compound **5** (0.9637 g, 3.9 mmol) was suspended in 38 mL of glacial acetic acid and stirred for 10 minutes. To the stirring mixture, 0.64 mL (12 mmol) Br₂ in 38 mL of glacial acetic acid was slowly added to the reaction mixture and stirred for 16 h at room temperature. The reaction was cooled with an ice bath and 1.25 g (9.9 mmol) of Na₂SO₃ was added to the reaction mixture. By adding a little water (1.0 mL), a deep-violet color formed within three hours. After the addition of a solution of 1% of KOH aqueous solution, a pale green solid formed which was

filtered. The solid was washed with cold isopropanol to give 0.410 g (29 % yield) of the titled product.

Approach 2:

Compound **5** (0.3 g, 1.24 mmol) of was suspended in 12 mL of glacial acetic acid and stirred for 10 minutes. To the stirring mixture, 0.2 mL (3.95 mmol) Br₂ in 38 mL of glacial acetic acid was slowly added to the reaction mixture and maintained at reflux for 16 hrs at temperatures between 70-80 °C and 120 °C respectively, while monitoring with TLC. A purple precipitate was obtained from reaction conditions of 70-80 °C temperature and a pale green solid was obtained from reaction conditions at 120 °C. After cooling the solution to room temperature and further on ice, the precipitates were filtered and washed with cold isopropanol and dried to give 0.450 g (65 % yield) of the purple (**6A**) product and 0.320 g (72.5 % yield, mp 206-208 °C) of the pale green (**6B**) product.

Grignard synthesis of phenothiazin-3,7-dicarboxylic acid (**4**) and

N-acetyl-3,7-phenothiazinedicarboxylic acid (**8**)

Anhydrous diethyl ether (0.5 mL) was added to 50 mg (2 mmol) of magnesium powder in a dry test tube sealed with a septum. In a second dry test tube, 1 mL of anhydrous diethyl ether was added to 100 mg of 3,7-dibromophenothiazine (**2**) using the same syringe. About 0.1 mL of the dibromophenothiazine-ether mixture was added dropwise to the magnesium-ether mixture with a syringe and mixed by shaking the test tube. The septum was pierced with a clean syringe for pressure relief while the reaction progressed vigorously. The remaining dibromophenothiazine-ether mixture was added dropwise when the reaction is less vigorous until

all the mixture was exhausted. A magnetic stirrer was added to the reaction tube and stirred until only a small amount of the metal was left. While the reaction progressed, the volume of the ether was checked periodically to make sure the volume has not decreased and a little more ether was added when the volume was low. Since the Grignard reagent deteriorates on standing, the next step was done immediately; the solution was separated from the magnesium metal left.

Carbon dioxide gas was bubbled through the Grignard solution for about 20 to 30 minutes in a dry test tube sealed with a septum. The septum was pierced with a syringe to relieve the pressure built up in the tube. To the pale yellow viscous solution formed, 3 ml of 3 M hydrochloric acid was added. The aqueous layer was removed and discarded. The ether layer is then shaken with 1mL of water and left to stand for a few minutes. The aqueous layer was once again removed and discarded. The product was extracted from the ether layer with 3 x 1 mL of 3 M aqueous sodium hydroxide solution. The ether layer was discarded and the clear solution was heated briefly to drive off the excess dissolved ether. 3 M hydrochloric acid was added to the mixture until the solution tested acidic. The mixture was cooled on ice and the product collected by vacuum filtration. The solid was recrystallized from water. These steps in Grignard synthesis were also carried out on the 10-acetyl-3,7-dibromophenothiazine.

Synthesis of 3,7-dinitrophenothiazine (10)

Sodium nitrite (0.2 g, 3 mmol) was added to a mixture of phenothiazine (0.2 g, 1 mmol), 0.4 mL of acetic acid and 1mL of dichloromethane (CH_2Cl_2) and stirred for 10 minutes. An additional 0.4 mL of acetic acid, 1 mL of dichloromethane, and sodium nitrite (0.2 g, 3 mmol) were added to the mixture. 1.2 mL of acetic acid was further added to break the thick reaction

mixture and stirred for 3 to 5 hours.⁴⁷ The solid suspension was filtered out and washed with 1 mL of ethanol, followed by 1 mL of water and finally 1 ml of ethanol to give a purple-brown solid. The residue was stirred in a minimum volume (5 mL) of hot DMF (Dimethylformamide),⁴⁷ and allowed to cool before filtering out to give 0.1744 of the product (70 % yield, mp 220-222 °C) which was washed with another 3 mL of ethanol and dried under vacuum.

NMR (DMSO- d_6): $\delta_H=6.835$ (d, 2H, $J = 8.8$ Hz), $\delta_H= 7.729$ (d, 2H, $J = 2.4$ Hz), $\delta_H= 7.845$ (dd, 2H, $J = 6.4$ Hz), $\delta_H = 1.830$ (s, 3H); $\delta_C = 173.693$ (C=O), $\delta_C =146.134$ (ArC), $\delta_C = 142.868$ (ArC), $\delta_C = 125.304$ (ArC), $\delta_C = 122.168$ (ArC), $\delta_C = 117.194$ (ArC), $\delta_C = 115.516$ (ArC), $\delta_C = 26.750$ (CH₃) ppm.

IR ($\nu_{\max}/\text{cm}^{-1}$): 3400(s, N-H), 1510 and 1575 (m, N-O), 1600 (m, C=C)

Synthesis of N-acetyl-3,7-dinitrophenothiazine (11)

A mixture of 3,7-dinitrophenothiazine (1 g, 3.45 mmol) and acetic anhydride (6 mL, 63.4 mmol) were stirred in pyridine (10 mL) at reflux for 24 hrs. The warm solution was carefully poured over crushed ice and allowed to stand for a few minutes to form a precipitate. The precipitate formed was then filtered, dissolved in dichloromethane and dried over anhydrous sodium sulfate. The solution was filtered and concentrated to give a brown-orange solid which was purified by column chromatography (silica gel, 2:3 ethyl acetate and petroleum ether, loaded as dichloromethane solution) to give 0.8128 g (71 % yield, mp 213-214 °C) of the product.⁴⁷

NMR (DMSO- d_6): $\delta_H= 7.962$ (d, 2H, $J = 9.2$ Hz), $\delta_H= 8.290$ (dd, 2H, $J =6.8$ Hz), $\delta_H= 8.482$ (d, 2H, $J = 2.4$ Hz), $\delta_H= 2.250$ (s, 3H); $\delta_C = 168.696$ (C=O), $\delta_C = 146.317$ (ArC), $\delta_C = 143.683$

(ArC), $\delta_c = 133.520$ (ArC), $\delta_c = 128.825$ (ArC), $\delta_c = 123.904$ (ArC), $\delta_c = 123.568$ (ArC), $\delta_c = 23.397$ (CH₃) ppm. IR (vmax/cm⁻¹): 1700 (s, C=O), 1510 (s, NO), 1550 (w, NO)

Synthesis of N-acetyl-3,7-diaminophenothiazine (12)

A mixture of 10-acetyl-3,7-dinitro-phenothiazine (0.3 g, 0.9 mmol), tin (II) chloride dihydrate (2.1195 g, 3 mmol), and ethanol (3 mL) was heated to reflux and stirred at this temperature for 5 hours.⁴⁷ The mixture was then cooled to room temperature and poured over ice water. The pH was adjusted to 7 with 5% sodium hydrogen carbonate before the product was extracted with ethyl acetate (3 x 3 mL).⁴⁷ The extracts were washed with brine and dried over anhydrous sodium sulfate, filtered, and concentrated to give 0.1890 g (77.4 % yield, mp 172-174 °C) of the product.

NMR (DMSO-d₆): $\delta_H = 5.234$ (s, 4H), $\delta_H = 6.484$ (dd, 2H, $J = 6$ Hz), $\delta_H = 6.618$ (s, 2H), $\delta = 7.147$ (d, 2H, $J = 8.4$ Hz), $\delta_H = 2.010$ (s, 3H) ppm.

IR (vmax/cm⁻¹): 3300 (m, NH), 1675 (s, C=O), 1600 (s, C=C), 2850 (w, CH)

Conversion of thionine acetate and N-acetyl-3,7-diaminophenothiazine (12) into thionine chloride (15)

Two approaches were used in the synthesis of this phenothiazinium derivative using two different starting materials. In the first approach, 0.1 g (0.37 mmol) thionine amide (12) which is the starting material was hydrolyzed with a few mL of concentrated hydrochloric acid (HCl) for

2-3 hours by refluxing at 110 °C. The hot solution was cooled to room temperature and further in ice to obtain 0.0882 g (90 % yield) of the product.

In the second approach, commercial thionine acetate (0.5 g, 1.74 mmol) was hydrolyzed by first dissolving in water, followed by the addition of a few mL of concentrated hydrochloric acid (HCl). This approach gave 0.4363 g (95 % yield) of the product which was blue in color.

NMR (DMSO- d_6); δ_C 157.122 (ArC), δ_C = 138.840 (ArC), δ_C = 135.206 (ArC), δ_C = 134.816 (ArC), δ_C = 121.862 (ArC), δ_C = 107.792 (ArC) ppm

IR (ν_{max}/cm^{-1}): 3307 (m, NH), 3000 (s, CH), 1602 (s, C=C), 1490 (s, C=C)

Synthesis of 3,7-phenothiaziniumdinitrile (14)

Hydrochloric acid (5 mL, 6 M) was added to 0.1 g (0.35 mmol) of thionine chloride and stirred until all solids dissolved. The solution was left to cool in ice to 0 °C. 0.2 g (2.89 mmol) of sodium nitrite in 5 ml of cold water was added dropwise until the reaction was complete. After 2-3 hours of stirring with monitoring by TLC, a solution of 0.3 g (3.35 mmol) copper cyanide in 3mL of hydrochloric acid (12 M) was added with continuous stirring for 2 hours. A dark-brown solid complex precipitated. The mixture was taken off the ice and left to stand for 10 minutes. It was then warmed to 40 °C at which point a vigorous reaction ensued (nitrogen gas evolution; separation of a solid and foaming). After reacting for half an hour, the mixture was heated on an oil bath for 10 minutes at 70 °C and allowed to cool to room temperature and further in ice. The solid product was collected by filtration, washed with a few ml of cold water (2-3 mL) and stirred in cold ethanol. The solid was filtered off and dried to give 0.0719 g (66 % yield) of the titled product which was purple-brown.

NMR (DMSO-d₆): $\delta_{\text{H}} = 8.825$ (s), 7.905 (dd, 2H, $J = 9.6$ Hz), 7.273 (d, 2H, $J = 9.2$ Hz), 7.202 (s, 2H); $\delta_{\text{C}} = 136.464$ (ArC), $\delta_{\text{C}} = 135.730$ (ArC), $\delta_{\text{C}} = 135.164$ (ArC), $\delta_{\text{C}} = 133.799$ (ArC), $\delta_{\text{C}} = 133.057$ (ArC), $\delta_{\text{C}} = 130.710$ (ArC), $\delta_{\text{C}} = 125.571$ (ArC), $\delta_{\text{C}} = 125.059$ (ArC), $\delta_{\text{C}} = 123.216$ (ArC), $\delta_{\text{C}} = 119.821$ (ArC), $\delta_{\text{C}} = 118.850$ (ArC)

IR ($\nu_{\text{max}}/\text{cm}^{-1}$): 3040 (w, CH), 2171 (m, CN), 1600 (s, C=C)

CHAPTER 4

CONCLUSION

In this project, various derivatives of phenothiazine and phenothiazinium were synthesized, using commercially available phenothiazine (**1**). These derivatives include: 3,7-dibromophenothiazinium perbromide (**2**), N-acetyl phenothiazine (**5**), N-acetyl-3,7-dibromophenothiazine (**6**), 3,7-dinitrophenothiazinium acetate (**10**), N-acetyl-3,7-dinitrophenothiazine (**11**), N-acetyl-3,7-diaminophenothiazine (**12**), thionine chloride (**15**), and 3,7-phenothiaziniumdinitrile (**14**). Synthesis of 3,7-phenothiazinium dicarboxylic acid was attempted using **1** and **15** as starting materials, as shown in **schemes 4-6**.

Synthesis of the dicarboxylic acid derivative via Grignard synthesis was not successful after several attempts. This method faced challenges of solubility of phenothiazinium dibromide in diethyl ether and t-butyl methyl ether. On the other hand, although solvents such as THF and 1,4-dioxane could dissolve the phenothiazinium dibromide, the Grignard reaction failed to yield the dicarboxylic acid.

Synthesis of the dicarboxylic acid from thionine chloride (**15**), via the Sandmeyer reaction, gave a number of intractable products; with none being the desired phenothiazinium dicarboxylic acid. The phenothiazinium dinitrile intermediate was difficult to purify; its ¹H NMR showed aromatic impurities, resulting from unreacted starting material and some coupling products of the diazonium salt.

Future work would involve further purification of the dinitrile product. After purification the dinitrile could be hydrolyzed to the dicarboxylic acid derivatives. Synthesis of

phenothiazinium dicarboxylic acid can also be explored by other methods such as the Rosenmund Von Braun reaction.

After the synthesis and purification of phenothiazinium dicarboxylic acid it will be tested in photodynamic therapy (PDT). We will seek collaboration with scientists in the medical field for completing this part of this work. The new derivative will also be tested for applications in the dye sensitizing solar cells (DSSC), and in the synthesis of metal organic frameworks (MOF's).

REFERENCES

1. Dolmans D.E, Fukumura D, Jain R.K., Photodynamic therapy for cancer. *Nature Reviews Cancer* **2003**; 3(5):380–387.
2. Wilson B.C. Photodynamic therapy for cancer: principles. *Canadian Journal of Gastroenterology*, **2002**; 16(6):393–396.
3. Vrouenraets M.B, Visser G.W, Snow G.B, Van Dongen G.A., Basic principles, applications in oncology and improved selectivity of photodynamic therapy. *Anticancer Research*, **2003**; 23(1B):505–522.
4. Dougherty T.J, Gomer C.J, Henderson B.W, *et al.* Photodynamic therapy. *Journal of the National Cancer Institute*, **1998**; 90(12):889–905.
5. 4. Celli J. P.; Spring B. Q.; Rizvi, I.; Conor L. E.; Kimberley S. S.; Sarika, V.; Pogue, B. W.; Hasan T., Imaging and Photodynamic Therapy: Mechanisms, Monitoring, and Optimization. *Chem. Rev.*, **2010**, 110, 2795–2838.
6. Patrice T., Comprehensive series in photochemistry and photobiology; Photodynamic therapy, Royal Society of Chemistry, UK, **2003** (2).
7. Lukšienė Ž., Photodynamic therapy: mechanism of action and ways to improve the efficiency of treatment, *Medicina*, **2003**, 39, Tomas, Nr. 12.
8. Ron R.A.; Downie G. H.; Cuenca, R.; Hu, X.; Carter, J. C.; Sibata, C. H., Photosensitizers in clinical PDT; Photodiagnosis and Photodynamic Therapy, **2004**, 1, 27-42.
9. Dolphin D.; New O. M. Design and Synthesis of Novel Phenothiazinium Photosensitizer Derivatives, *Eur. J. Org. Chem.* **2009**, 2675-2686.

10. Morgan, A. R., Garbo, G. M., Kreimer-Birnbaum, M., Keck, R. W., Chau dhuri, K., and Selman, S. H., A morphologic study of the combined effect of purpurin derivatives and light on transplantable rat bladder tumors, *Cancer Res.*, **1987**, 47:496-498..
11. Calin, M. A.; Parasca, S. V., Photodynamic therapy in oncology. *Journal of Optoelectronics and Advanced Materals*, **2006**, 8(3), 1173 – 1179
12. Wainwright, M.; Meegan, K.; Loughran, C.; Giddens, R. M., Phenothiazinium photosensitisers, part VI: photobactericidal asymmetric derivatives. *Dyes and pigments*, **2009**, 82, 387-391.
13. Edward G., Synthetic dyes in biology, medicine and chemistry Academic Press, London, England, **1971**
14. Eugenio K.; Andrew N. S., Willner I, In; Wolf Vielstich, *Handbook of fuel cells Fundamentals, Technology, Applications*, 4-Volume Set, **2003**, Wiley. p. 5. ISBN 978-0-471-49926-8
15. Clifton I.I. J, Leikin J.B, Methylene blue., *Am J. Ther.*,**2003**; 10:289-91
16. Wagner S. J, Skripchenku .A, Robinette D; Foley J .W, Cincotta I. Factors affecting virus photoinactivation by a series of phenothiazine dyes, *Photochem Photobiol* **1998**; 67:243-9
17. Wainwright. M, Crossley K.B., Methylene blue- a therapeutic dye for all seasons?, *J Chemother*, **2002**; 14:431-43
18. Wagner S.J., Skripchenko A., Robinette D., Mallory D.A., Hirayama J., Cincotta L., Foley J. , "The use of dimethylmethylene blue for virus photoinactivation of red cell suspensions". *Dev. Biol. (Basel)*, **2000**,102: 125–9. PMID 10794099
19. Wainwright, M. Photosensitisers in Biomedicine; Wiley-Blackwell: UK, **2009**.

20. "Nomenclature of Lipids - Phospholipids". *IUPAC-IUB Commission on Biochemical Nomenclature (CBN)*, Retrieved , **2011**
21. Bruce A., Bray D., Lopkin K., Johnson A., Lewis J., Raff M., Roberts K., Walter P., – *Essential Cell biology*, edition 3, New York-Garland science, **2010**, p. 235
22. Suad M. A., Mohammad R. A., Luma S. A., Synthesis of New C-Substituted Phenothiazine Derivatives, *Al-Mustansirya J. Sci*; **2009**, 20 (3).
23. Gal E., Gaina L., Lovasz T., Synthesis and fluorescence properties of new Schiff bases containing phenothiazine units. *Studia UBB Chemia* **2009**, 54:17-24
24. Yaghi O. M. *et al.*, Reticular synthesis and the design of new materials. *Nature* 423, **2003**, 705 -714.
25. Mueller U. *et al.*, Metal-organic frameworks—prospective industrial applications. *J. Mater. Chem.*, **2006**, 16, 626-636.
26. Jacoby M., Heading to market with MOFs. *Chem. Eng. News*, **2008**, 86, 13.
27. Huxford R.C., Rocca J.D., Lin W., Metal-organic frameworks as potential drug carrier, *Current Opinion in Chemical Biology*, **2010**, 14 (2), 262 - 268.
28. Ma L., Falkowski J. M., Abney C., Lin, W., A series of isorecticular chiral metal-organic frameworks as a tunable platform for asymmetric catalysis. *Nat. Chem.* 2, **2010**, 838–846.
29. Deng H., Grunder S., Cordova K. E., Valente C., *Large-Pore Apertures in a Series of Metal-Organic Frameworks* , **2012**, 10.
30. Oleinick N.L, Basic Photosensitization, [Available online; Photo biological sciences]; <www.photobiology.info/Oleinick.html>

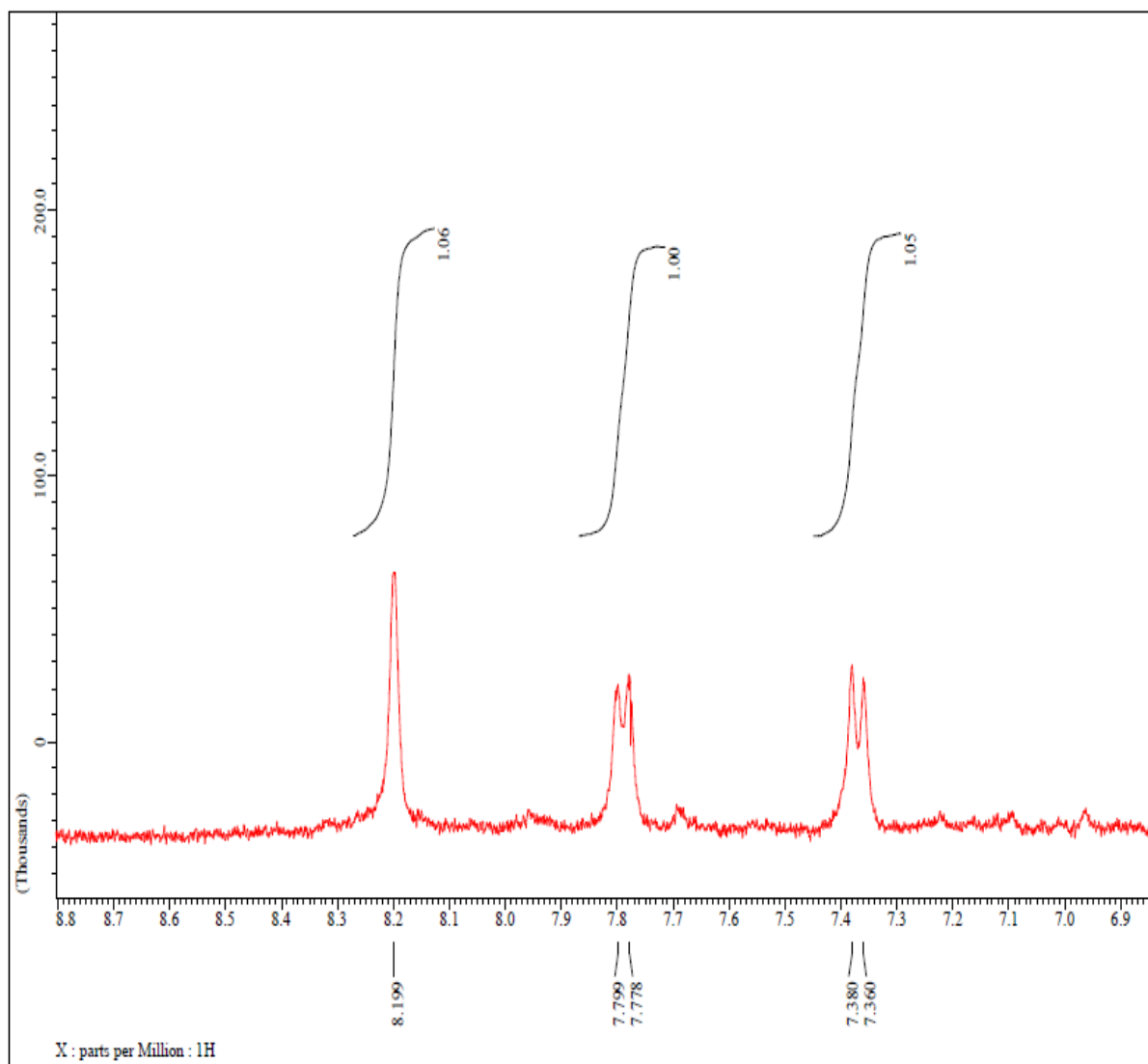
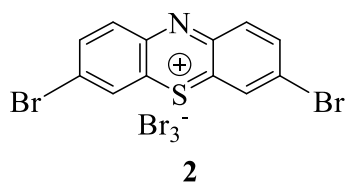
31. Valenzeno D. P., Membrane Photomodification. In: *Photobiological Techniques*, Valenzeno D.P., Pottier R.H., Mathis P. and Douglas R.H., eds. Plenum Press, New York and London, **1991**, 99-115.
32. Spikes J. D., Photosensitization. In: *The Science of Photobiology*, Kendric C. S., ed. Plenum Press, New York and London, **1989**, p 79-110.
33. Gibson, S. L.; Murant, R. S.; Chazen, M. D.; Kelly, M. E.; Hilf, R. In vitro photosensitization of tumour cell enzymes by photofrin II administered in vivo. *Br. J Cancer*. **1989**, 59(1), 47–53.
34. Wenham S.R., Green M.A., Watt M.E. and Corkish R., “Chapter 2: *Semiconductors and P-N Junctions*,” *Applied Photovoltaics*, Earth scan, **2007**, pp 31-38.
35. Lin S.Y., Chou W.Y., *Investigation of Pentacene/Perylene Derivative Based Organic Solar Cells*, National Cheng Kung University, Tainan Taiwan, **2007**.
36. Gerischer H., Electrochemical behavior of semiconductors under illumination, *J. Electrochem. Soc.*, 113, **1966**, 1174-1182
37. Lee W.J., E. Ramasamy, D.Y. Lee, Song J.S., *Glass frit overcoated silver gridlines for nano-crystalline dye sensitized solar cells*, *Journal of Photochemistry and Photobiology A: Chemistry* ,183, **2006**, 113-137.
38. Gratzel M., *Review Dye-Sensitized Solar Cells*, *Journal of Photochemistry and Photobiology C, Photochemistry Reviews*, 4, **2003**, 145-153
39. Khalil E.J, *Dye Sensitized Solar Cells - Working Principles, Challenges and Opportunities*, *Solar Cells - Dye-Sensitized Devices*, Prof. Leonid A. Kosyachenko , **2011**, ISBN: 978-953-307-735-2.

40. Jing-Jing F., Yu-Ai D., Jian-Zhao Z., Mei-Song G., Yi L., Theoretical investigation of novel phenothiazine-based D-p-A conjugated organic dyes as dye-sensitizer in dye-sensitized solar cells, *Journal of Computational and Theoretical Chemistry*, p 1045 , **2014**, 145–153
41. Asmiyenti D. D, Kartasmita R.E., Ibrahim S. and Tjahjono D. H., Toxicity Prediction of Photosensitizers Bearing Carboxylic Acid Groups by ECOSAR and Toxtree, *Journal of Pharmacology and Toxicology*, 7: **2012**, 219-230.
42. Lohse D. L.; Denu J. M.; Dixon J. E.; Santoro N., Roles of aspartic acid-181 and serine-222 in intermediate formation and hydrolysis of the mammalian protein-tyrosine-phosphatase (PTP1), In: *Biochemistry*, **1997**, 36(15), p4568, 8.
43. Karty J., Melzer M.; *Organic Chemistry, Principles and Mechanisms*, 1st Ed, w.w.norton and company, New York-London, **2014**, 861 and 1011-1014.
44. Herman R.H., “*Principles of metabolic control in mammalian system*”,**2013**,107
45. Lonnberg H., Cleavage of RNA phosphodiester bonds by small molecular entities: a mechanistic insight, *Organic and Biomolecular chemistry*, **2011**, Issue 6.
46. Plater J.M, Harrison W.T.A, “Characterization of 3,7-dibromophenothiazin-5-ium perbromide and its use for enhancing latent fingerprints”, *Journal for chemical research*, **2009**, no. 6, 384-387.
47. Wischik, C.M., Rickard, J.E., Harrington, C.R., Horsley, D., Storey, J.M.D., Marshall, C., Sinclair, J.P., Baddeley T. “3,7-diamino-10H-phenothiazine salts and their use”: WO2007110627, **2011**, Patent No. US7888350 B2.
48. Massie S.P., “The chemistry of Phenothiazine”, *Chemical Review*, **1954**, 797-833

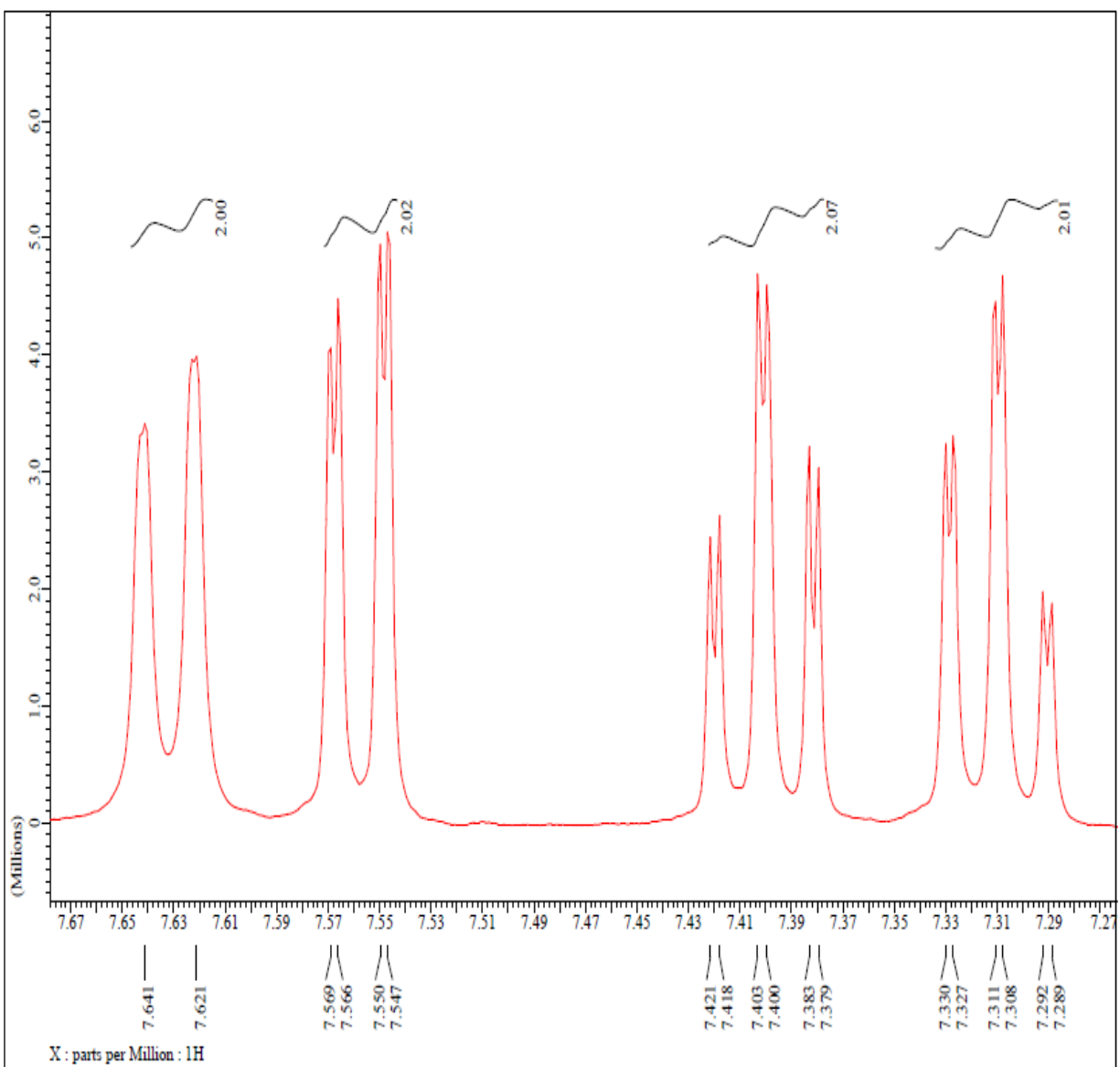
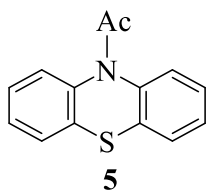
49. Hsin-hung L., Cheng-chun C., Spectroscopic investigations of vinyl-substituted 10H-phenothiazine, *dyes and pigments*,**2009**

APPENDICES

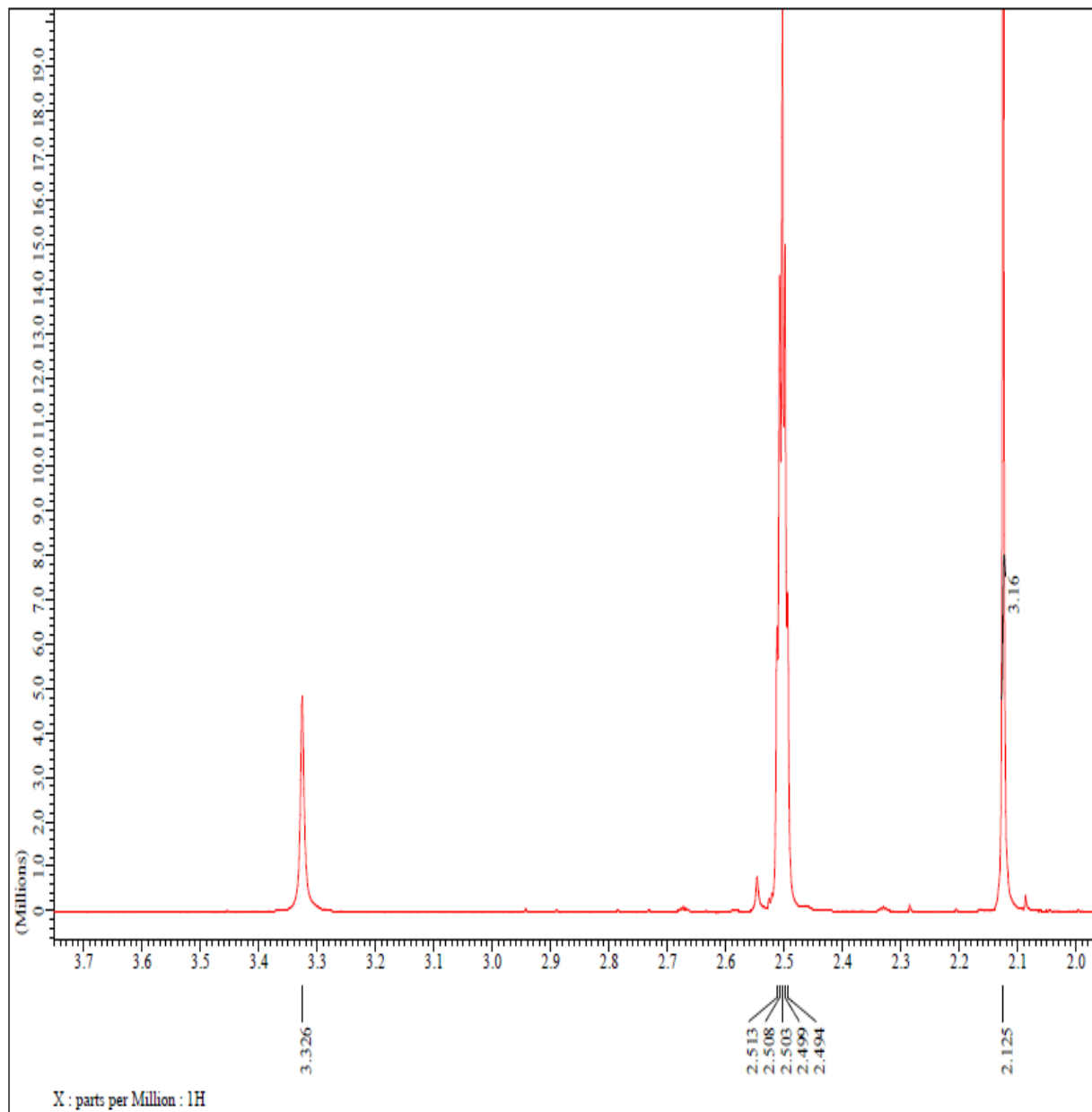
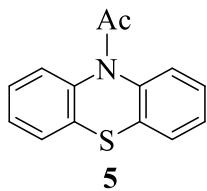
Appendix A: ^1H NMR Spectrum for Compound **2** in DMSO- d_6



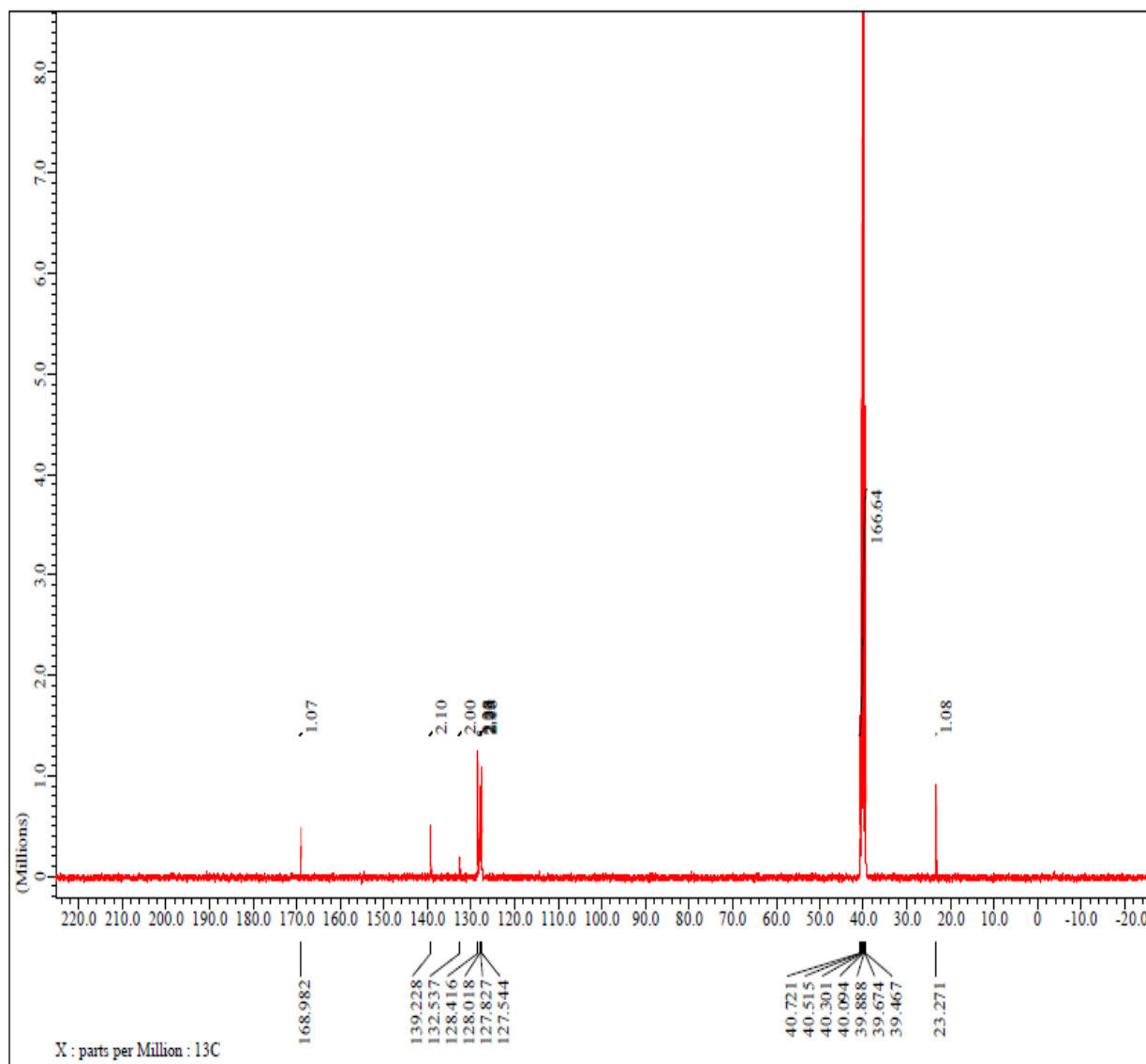
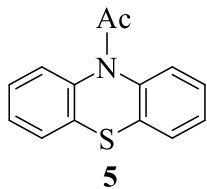
Appendix B1: ^1H NMR Spectrum for Compound **5** in DMSO-d₆



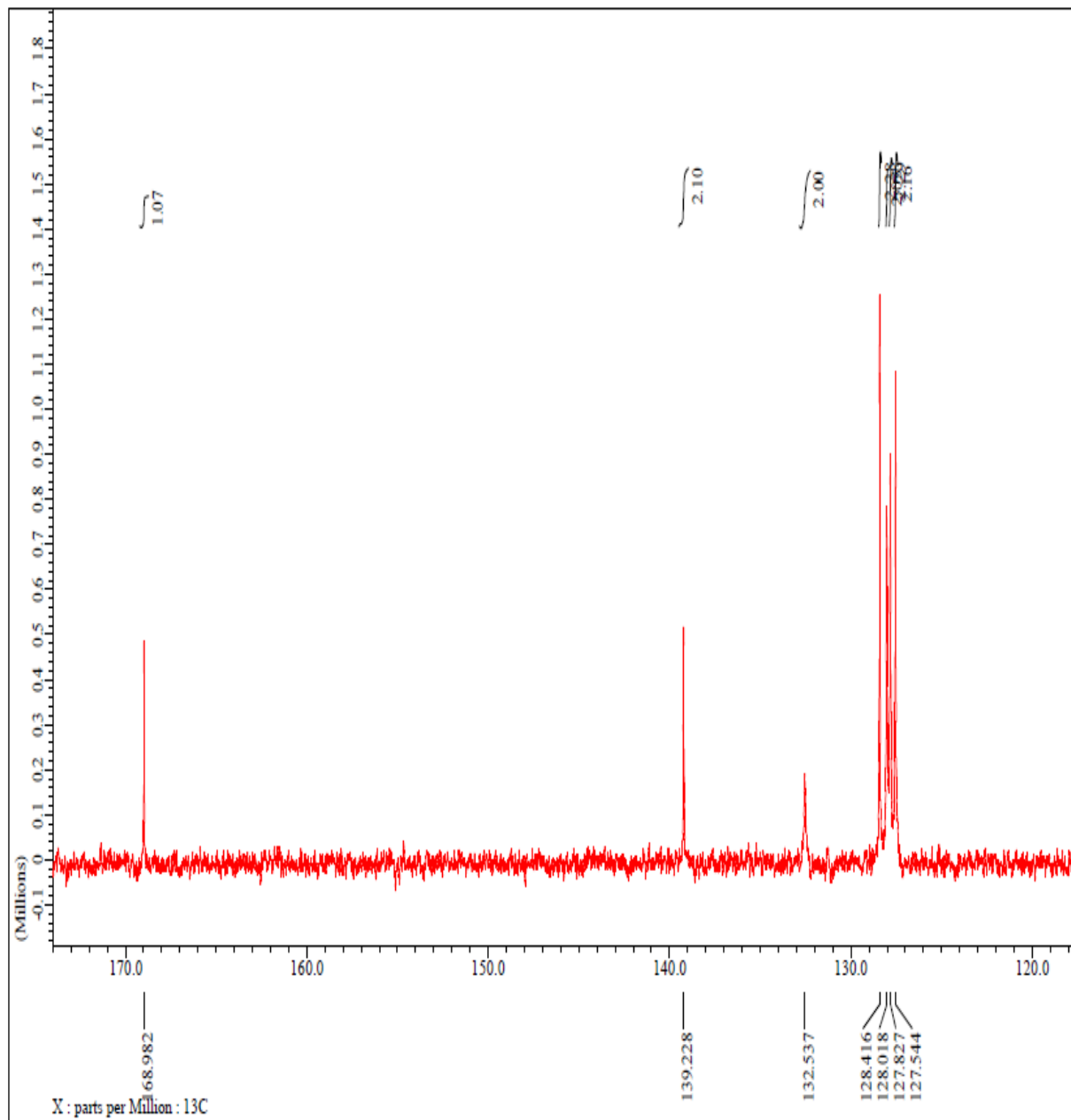
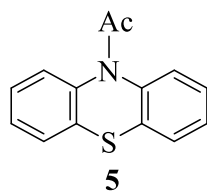
Appendix B2: ^1H NMR Spectrum for Compound **5** in DMSO-d₆



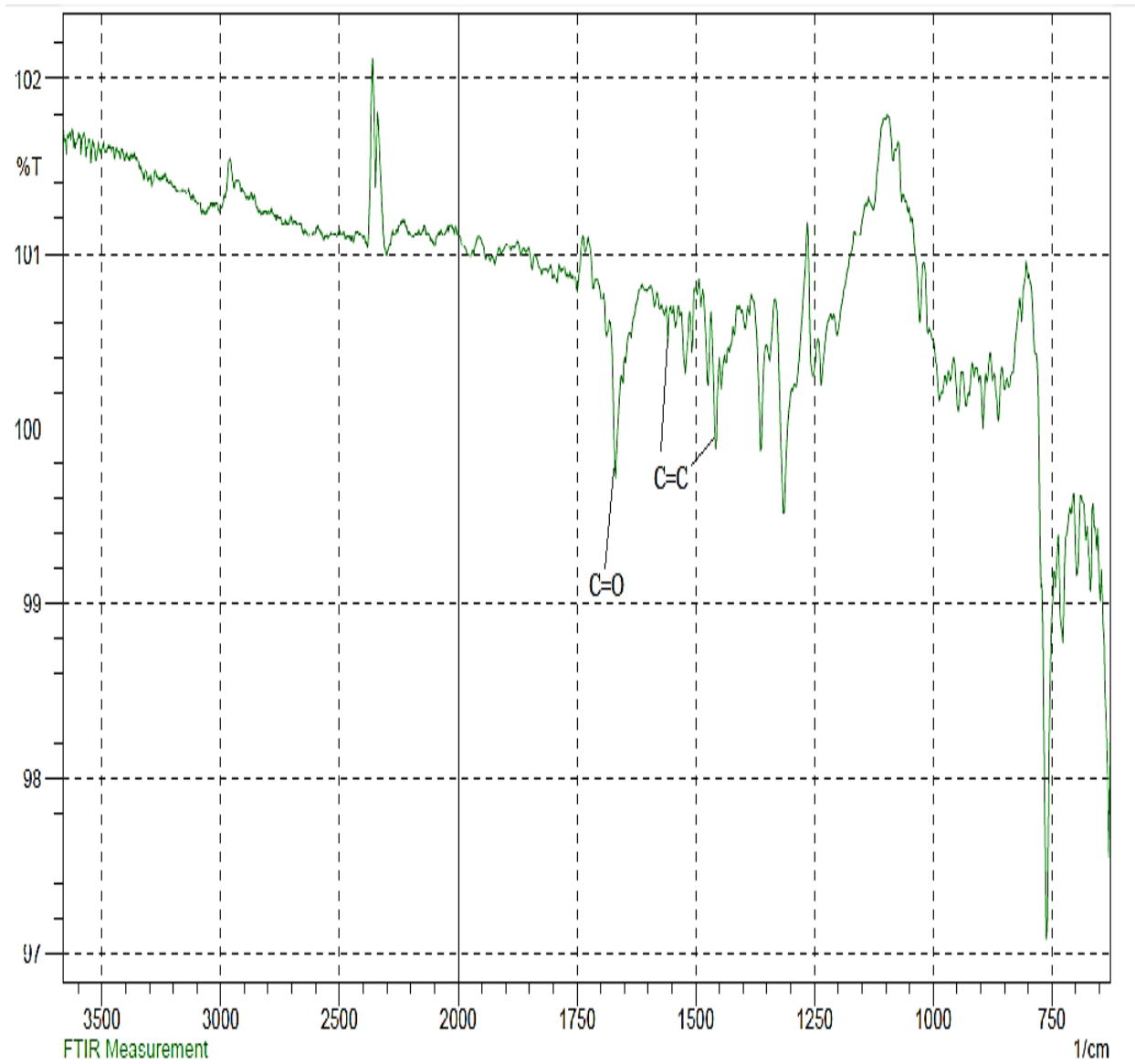
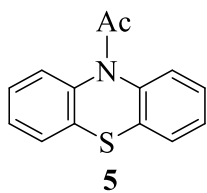
Appendix B3: ^{13}C NMR Spectrum for Compound **5** in DMSO- d_6



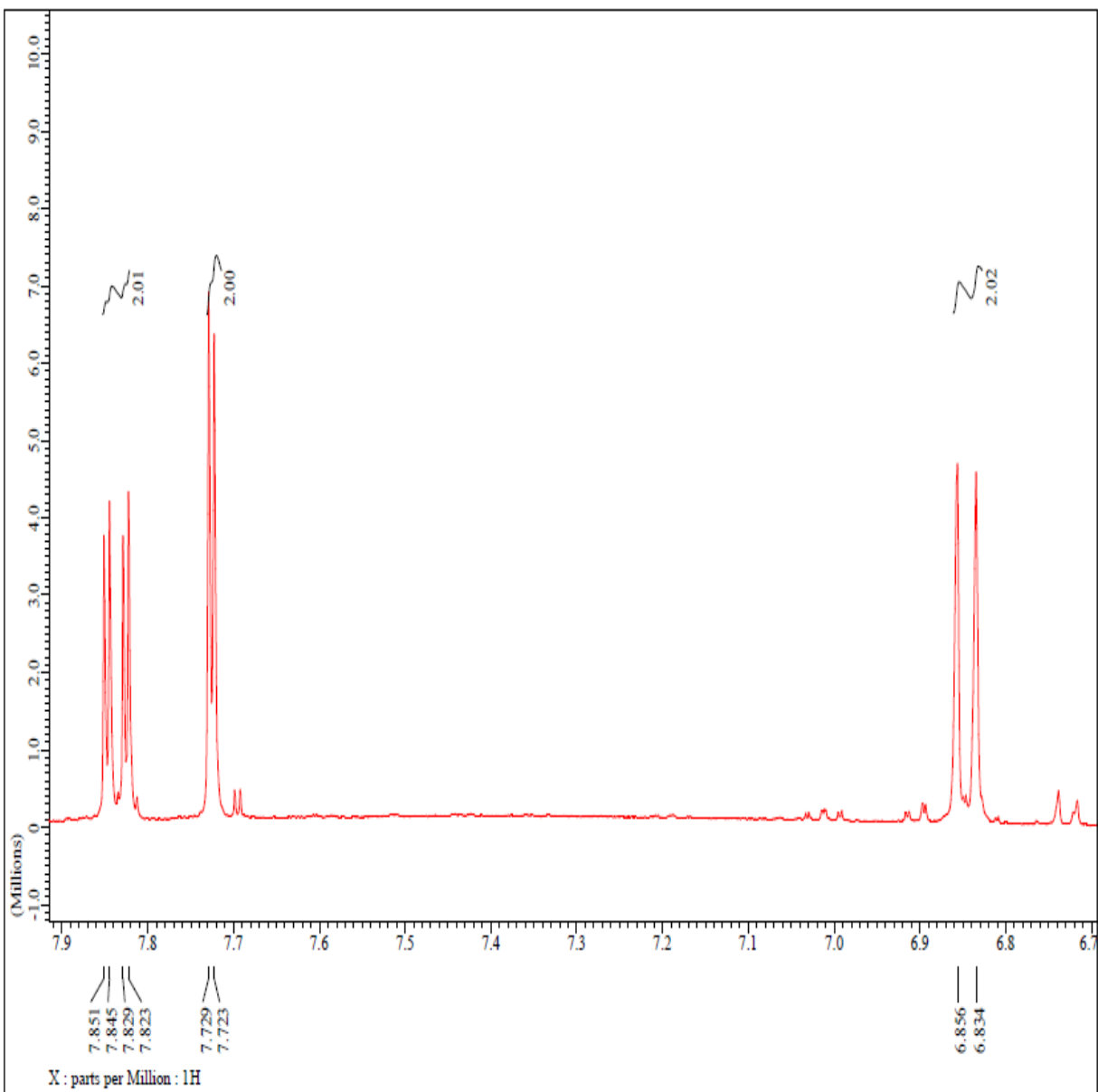
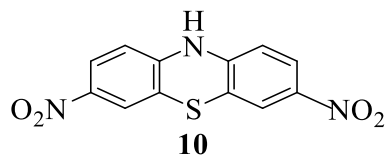
Appendix B4: ^{13}C NMR Spectrum for Compound **5** in DMSO- d_6



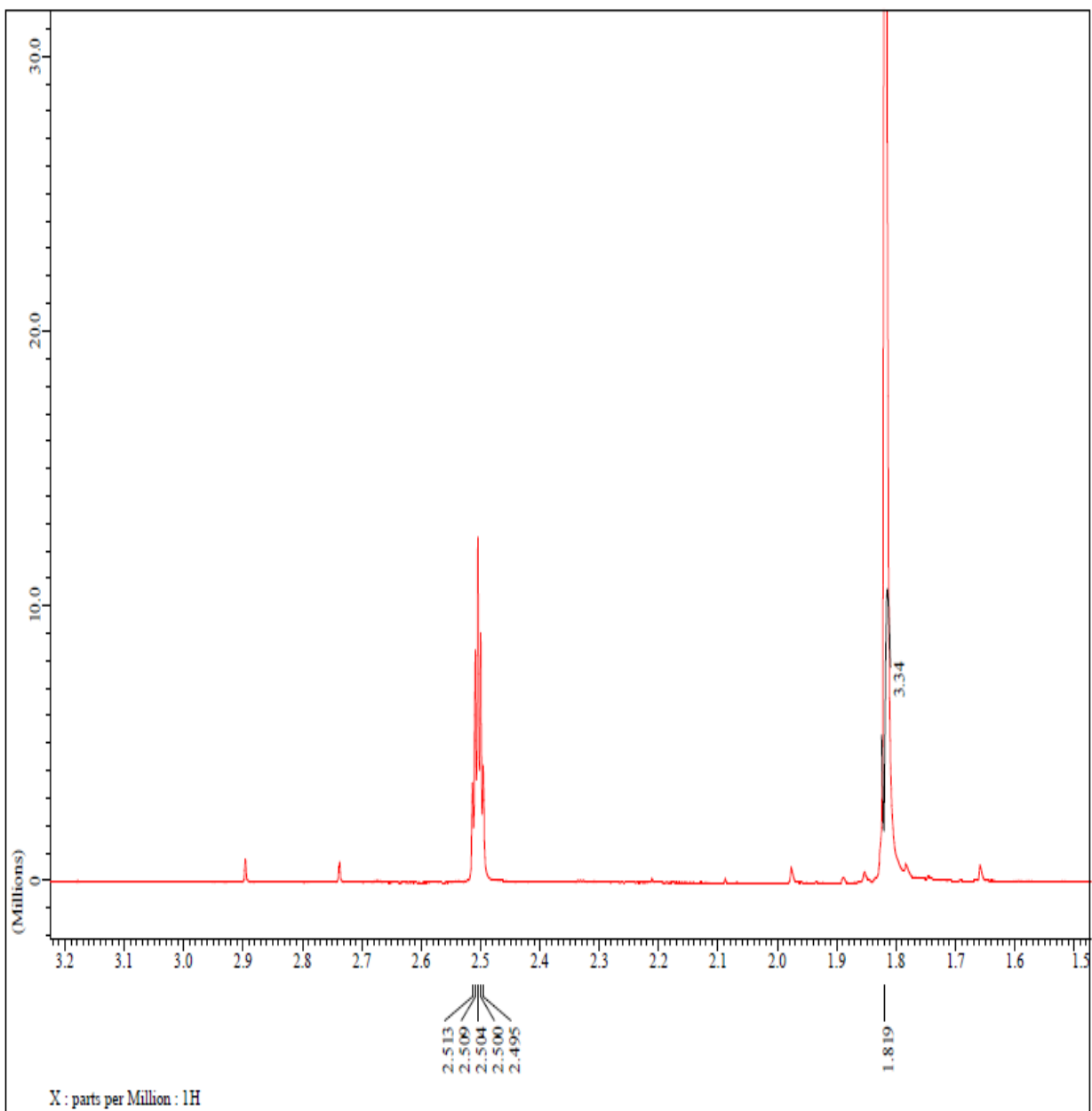
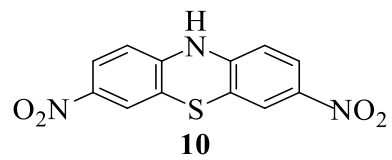
Appendix B5: IR Spectrum for Compound 5



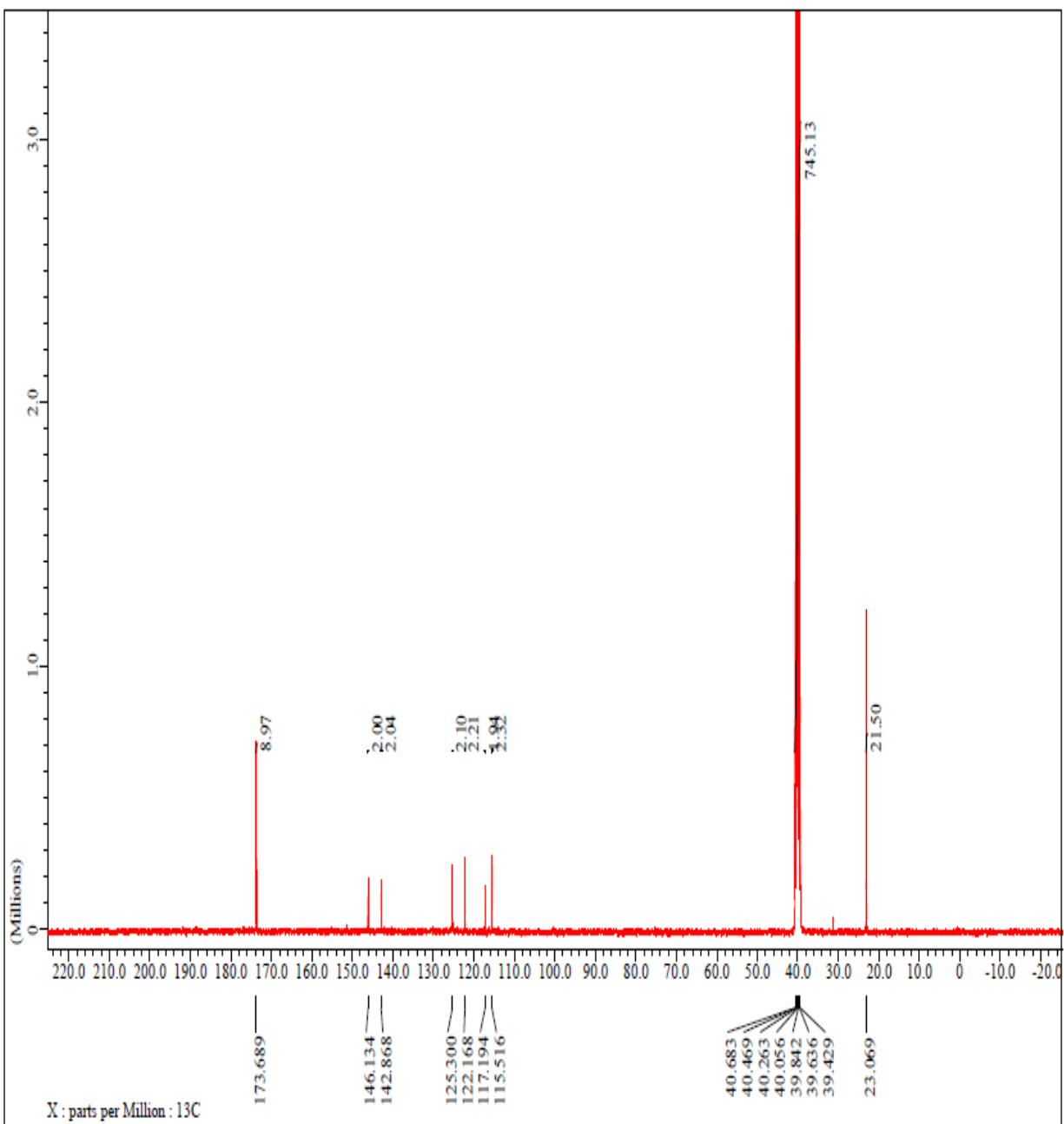
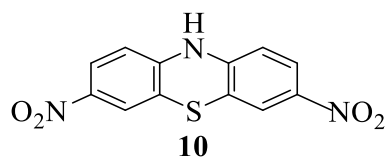
Appendix C1: ^1H NMR Spectrum for Compound **10** in DMSO- d_6



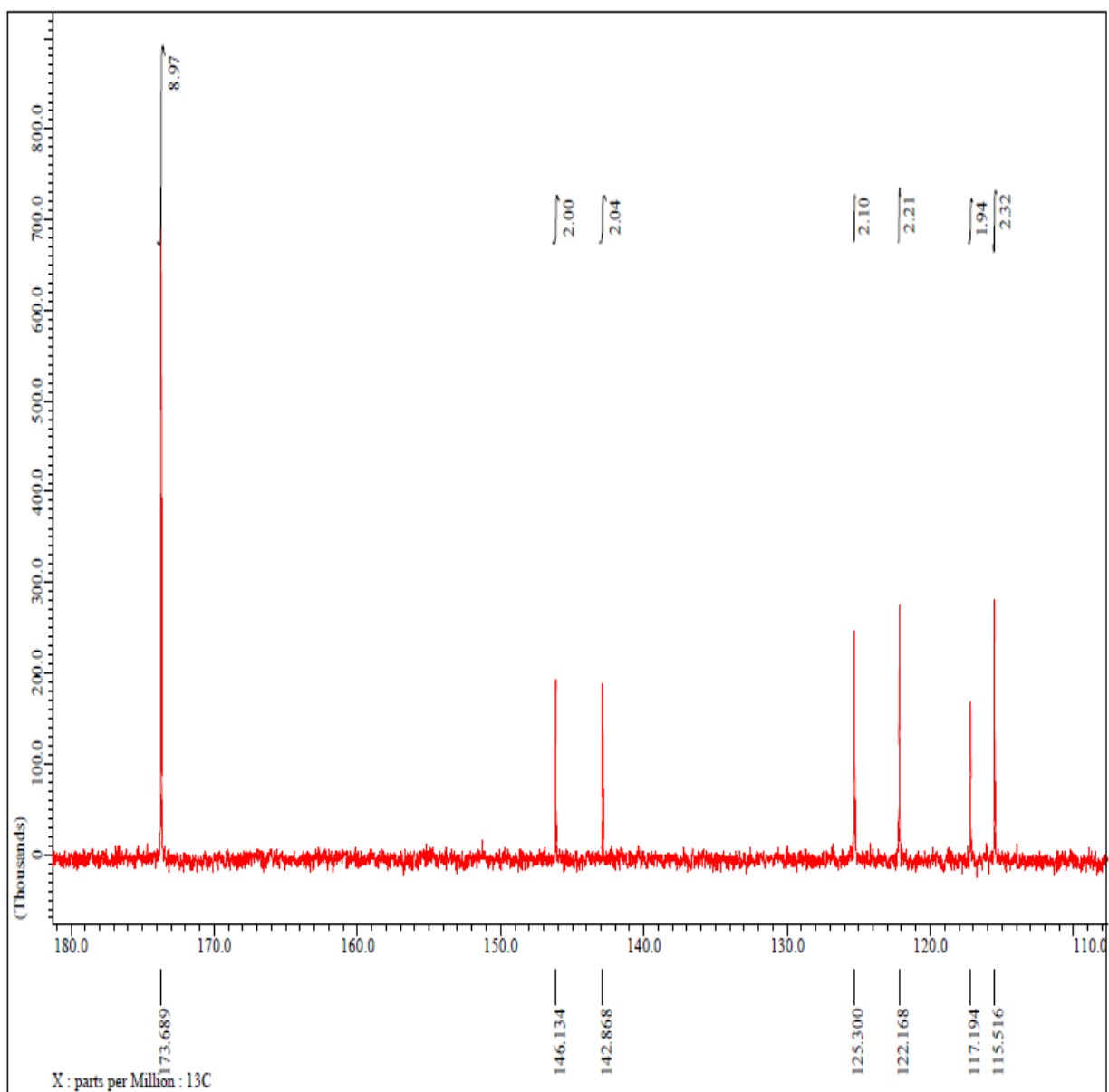
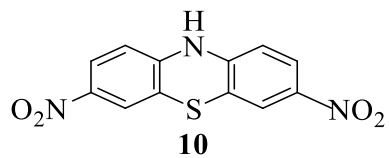
Appendix C2: ^1H NMR Spectrum for Compound **10** in DMSO- d_6



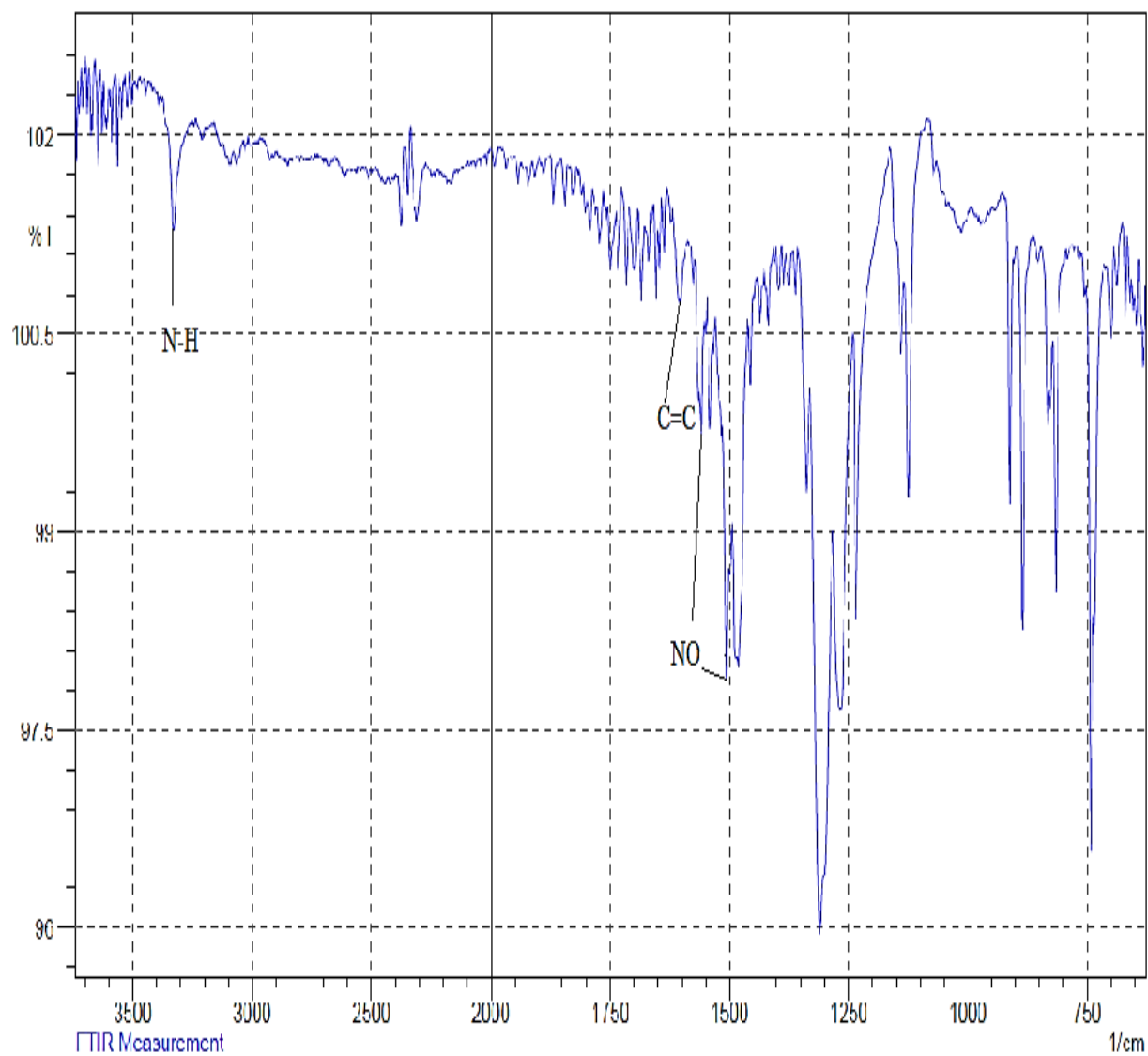
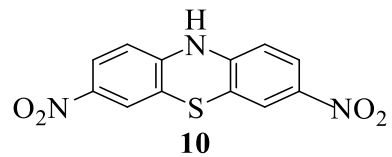
Appendix C3: ^{13}C NMR Spectrum for Compound **10** in DMSO- d_6



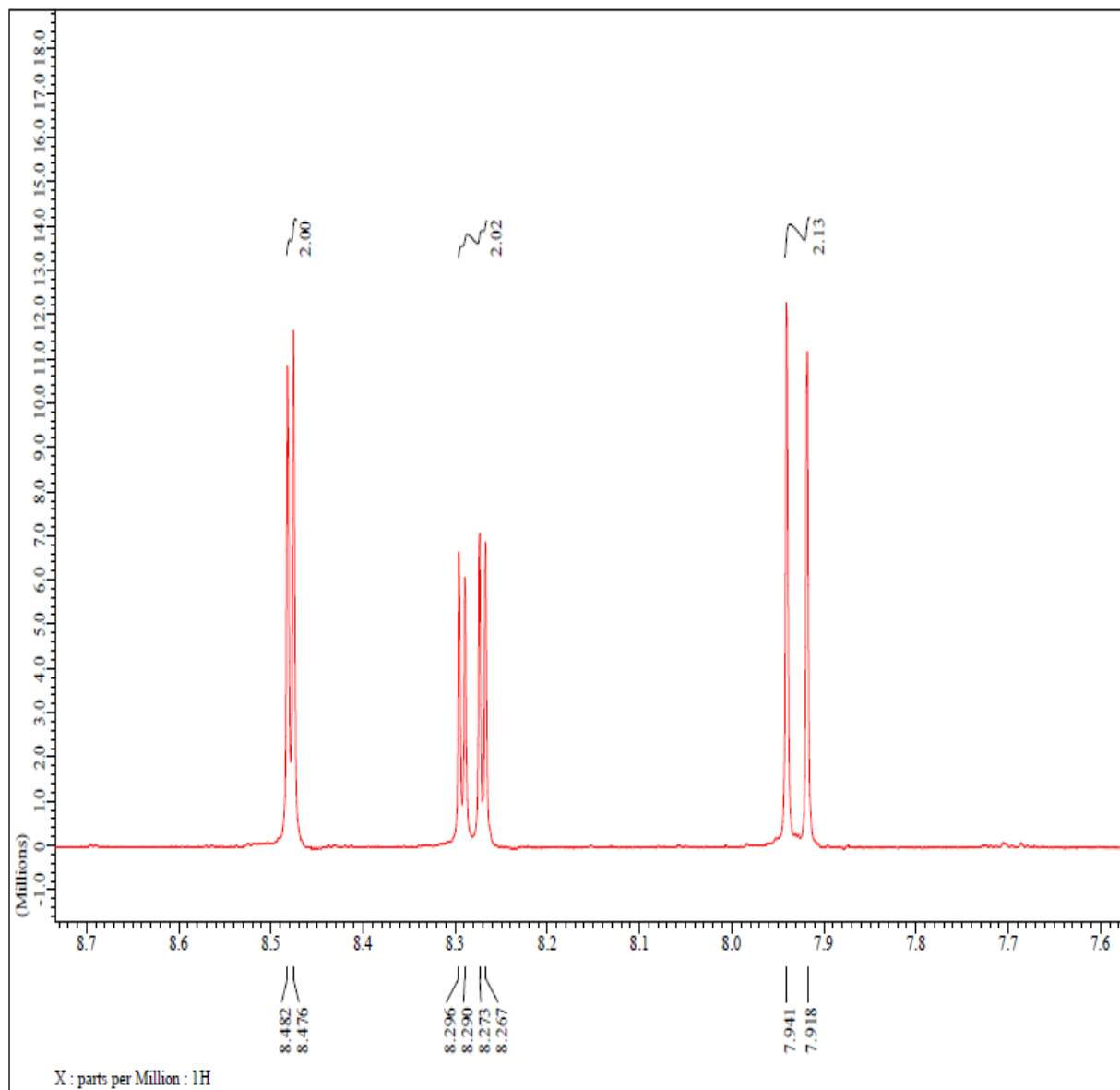
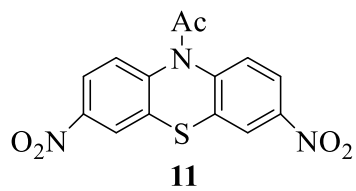
Appendix C4: ^{13}C NMR Spectrum for Compound **10** in DMSO-d₆



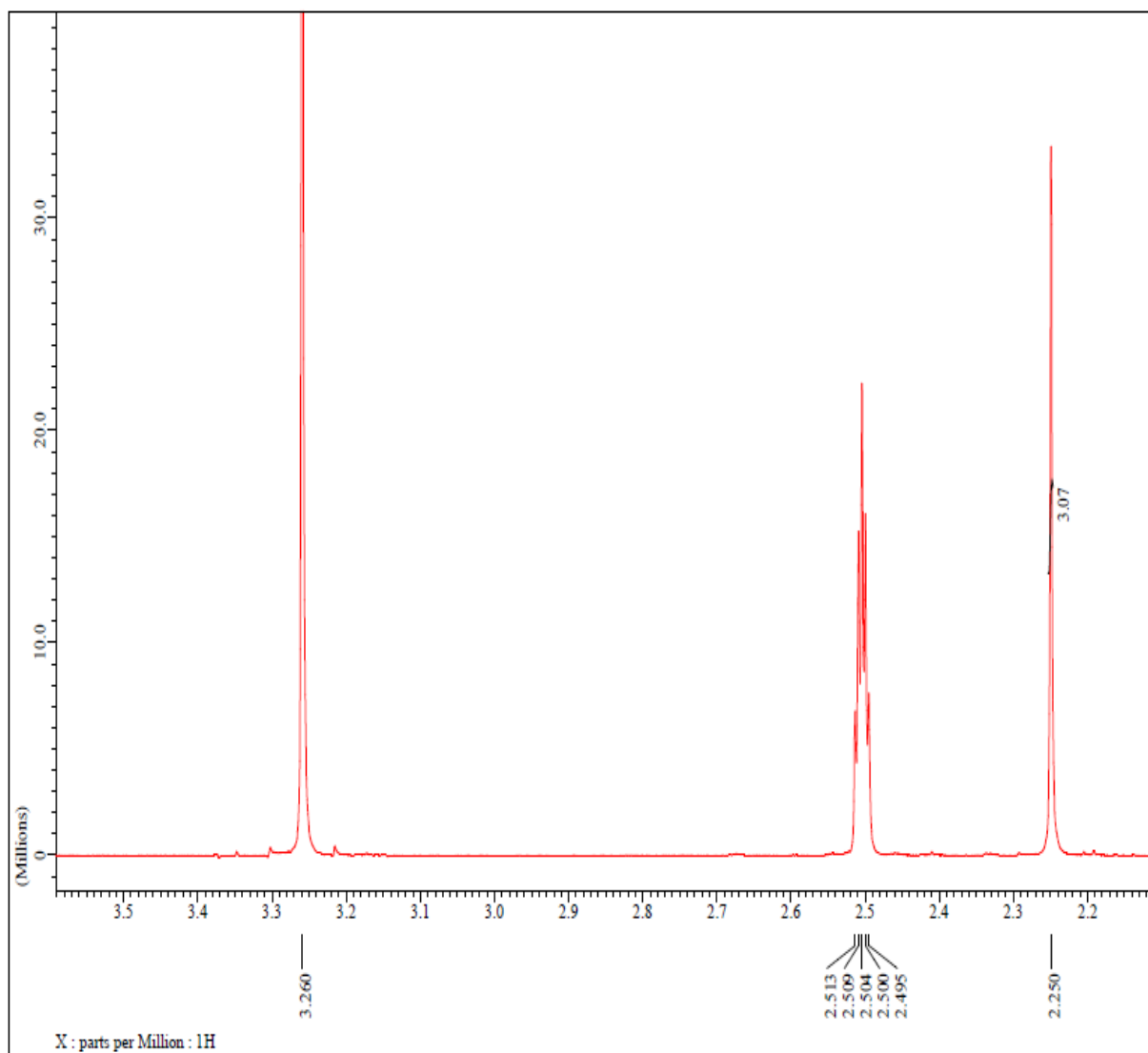
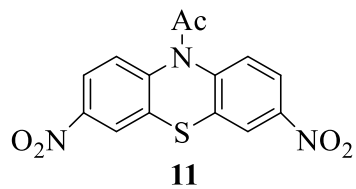
Appendix C5: IR Spectrum for Compound **10**



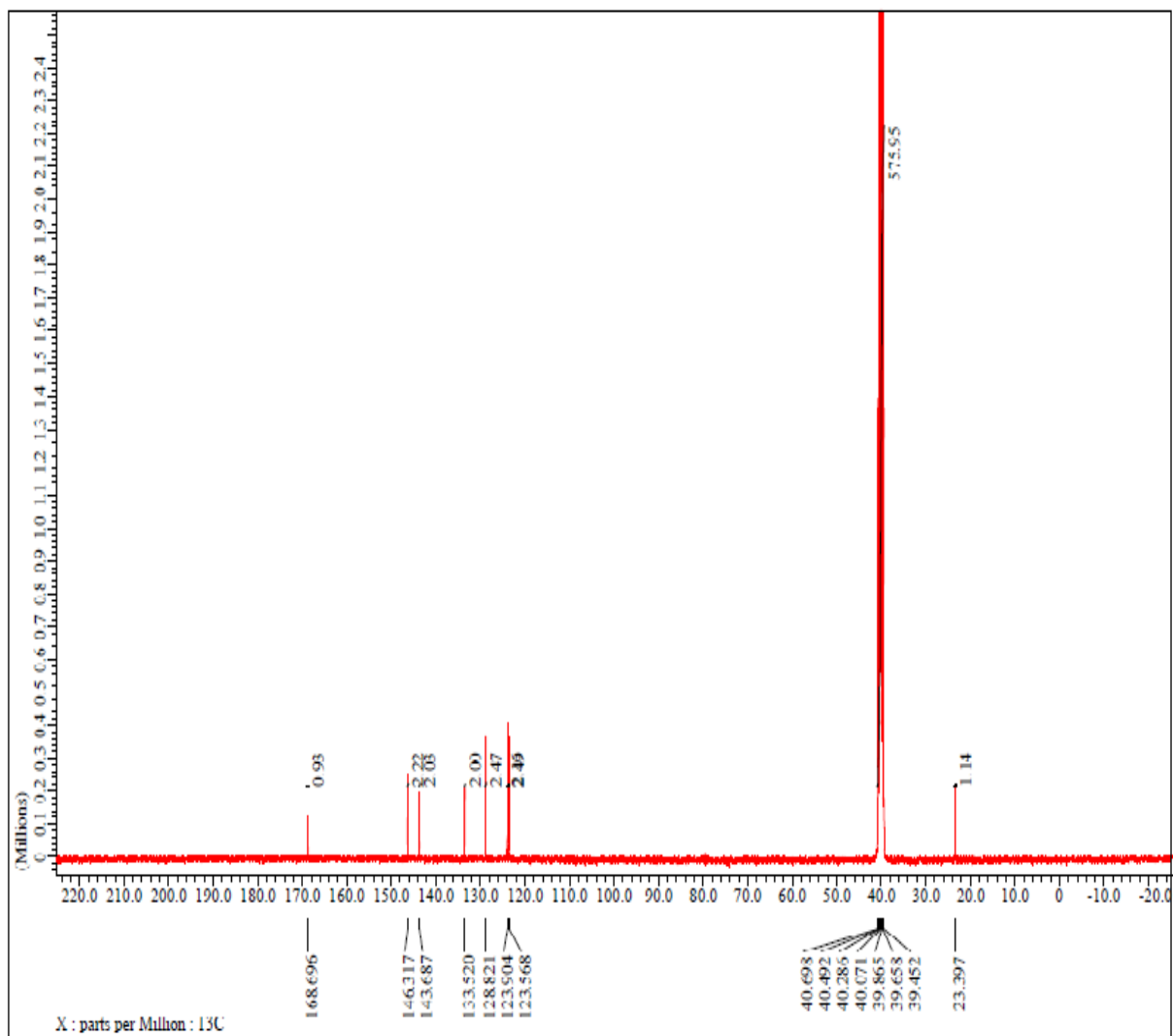
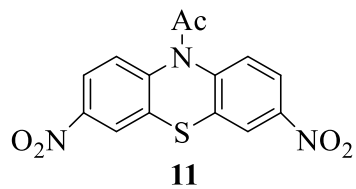
Appendix D1: ^1H NMR Spectrum for Compound **11** in DMSO- d_6



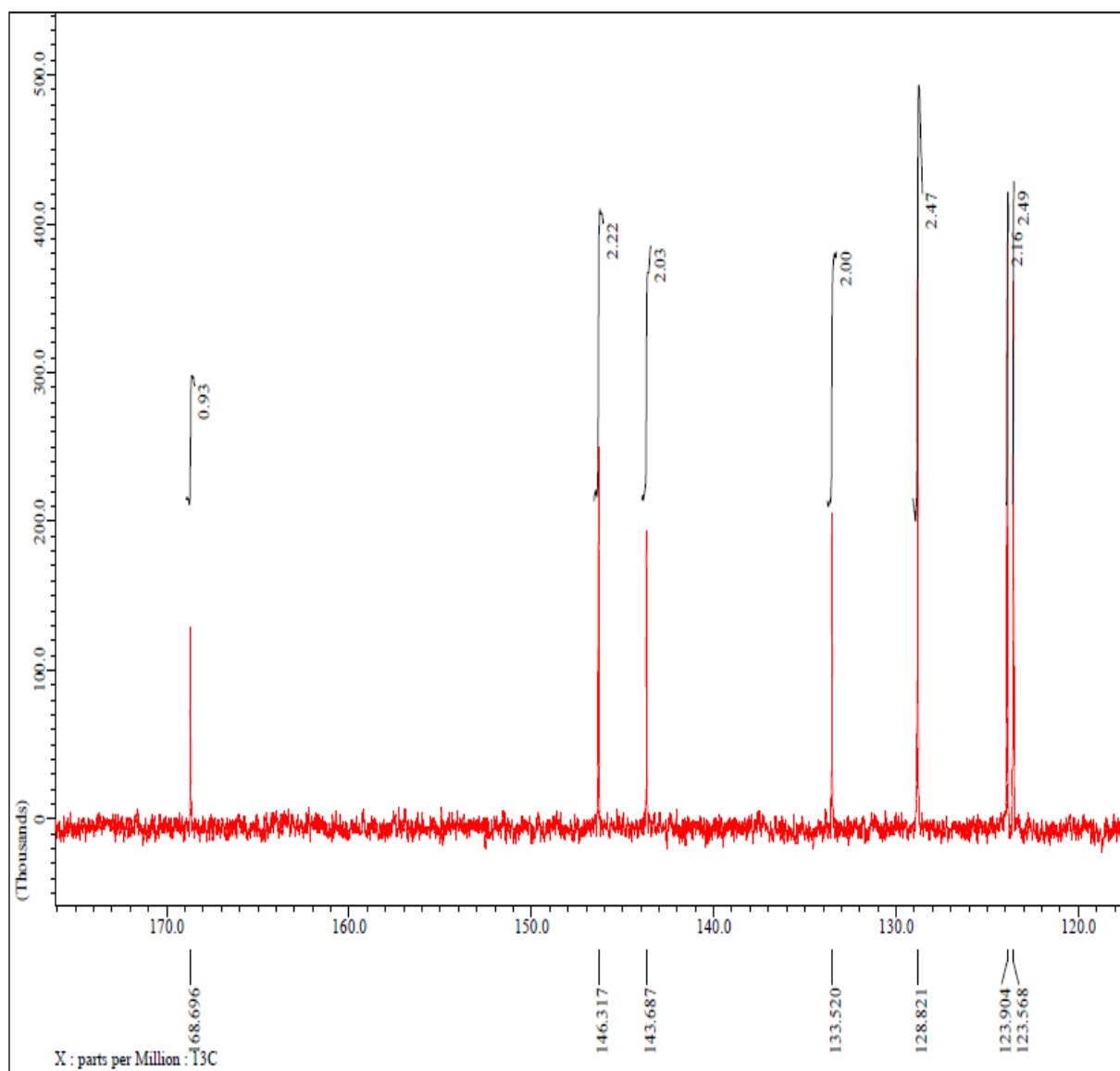
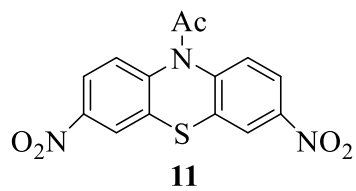
Appendix D2: ^1H NMR Spectrum for Compound **11** in DMSO- d_6



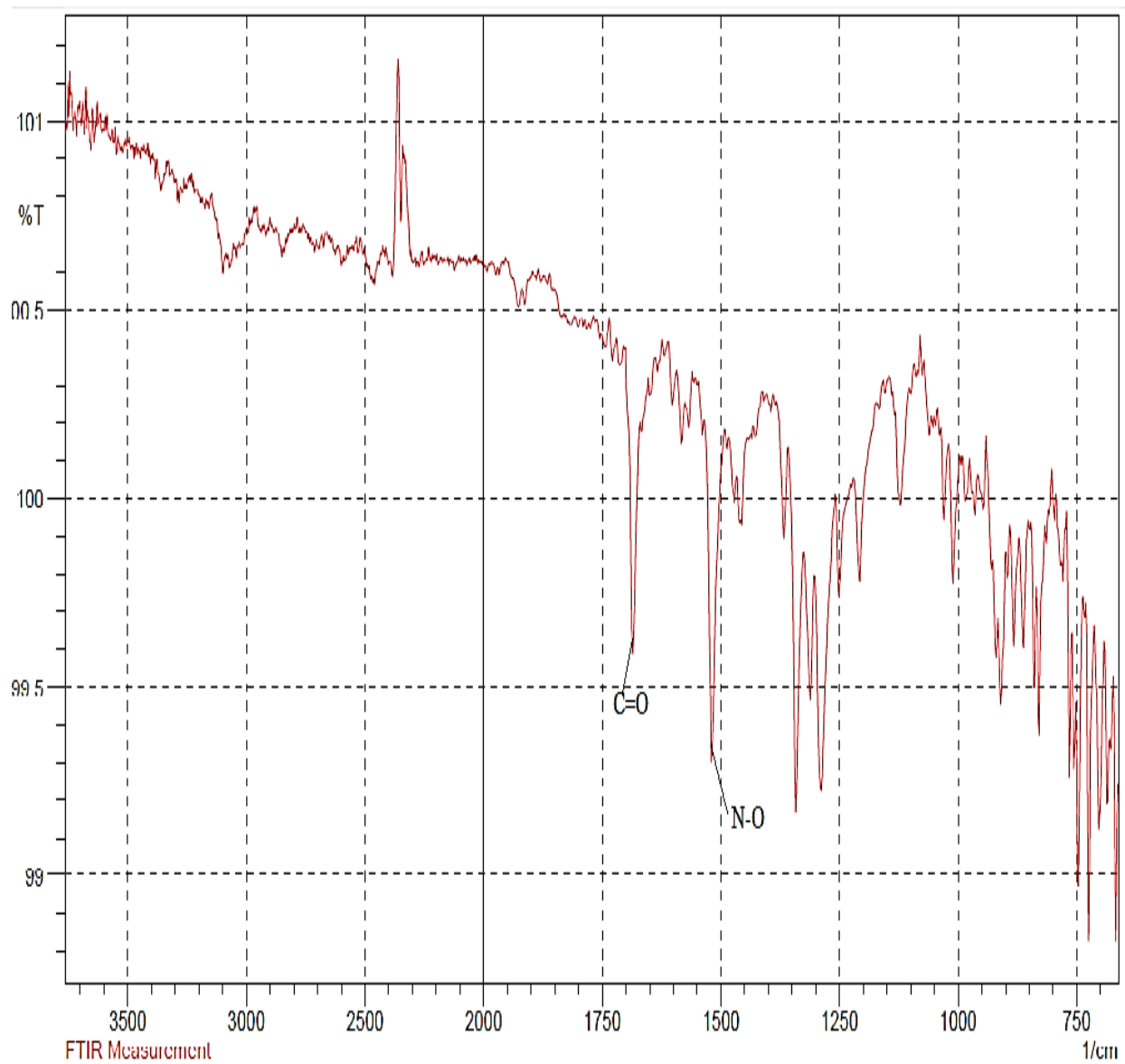
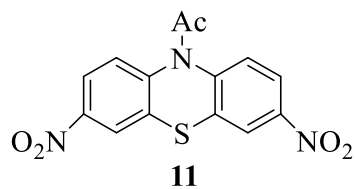
Appendix D3: ^{13}C NMR Spectrum for Compound **11** in DMSO-d₆



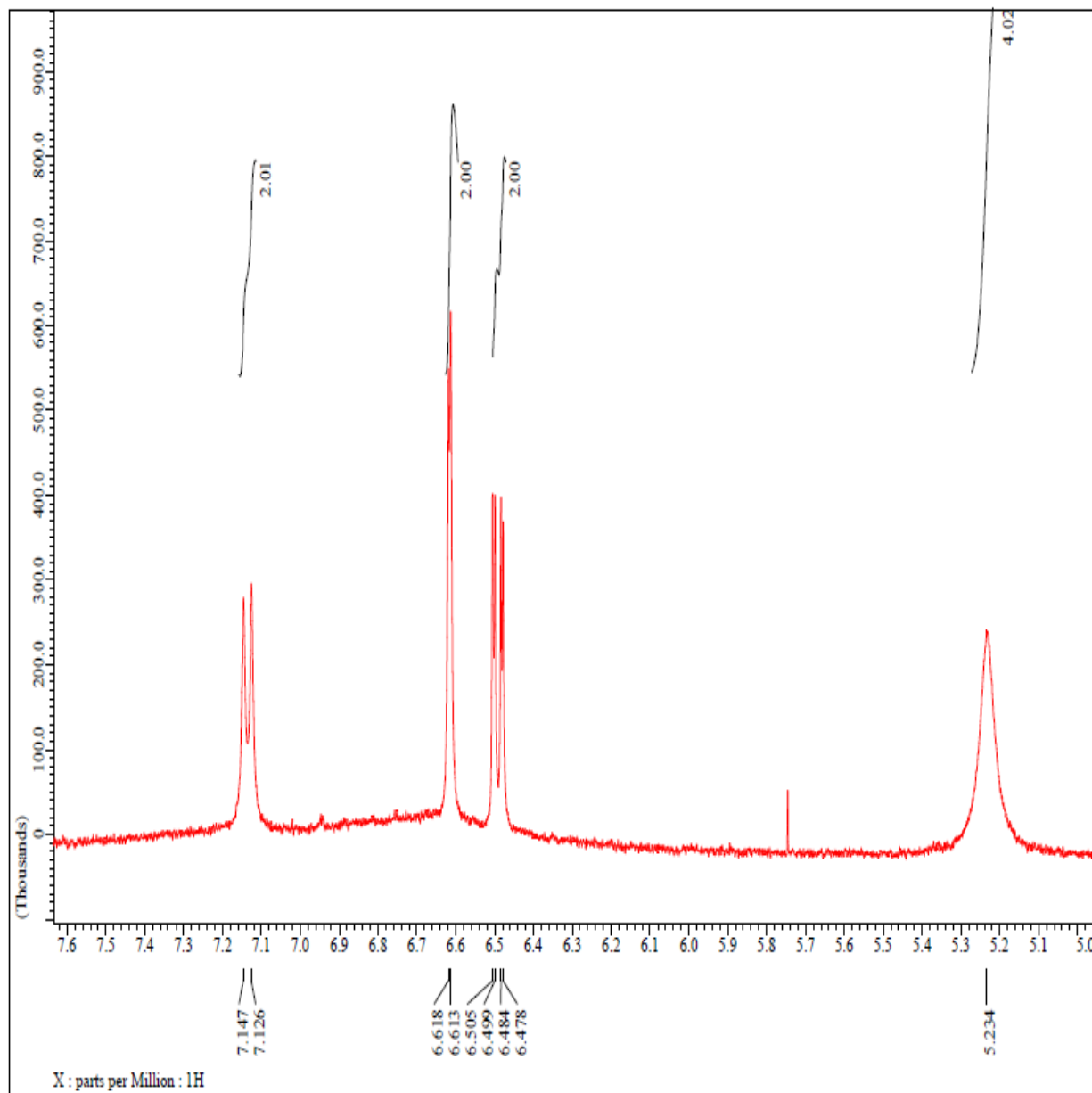
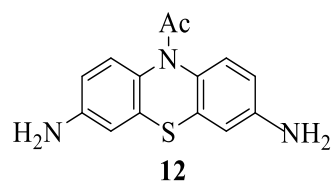
Appendix D4: ^{13}C NMR Spectrum for Compound **11** in DMSO-d₆



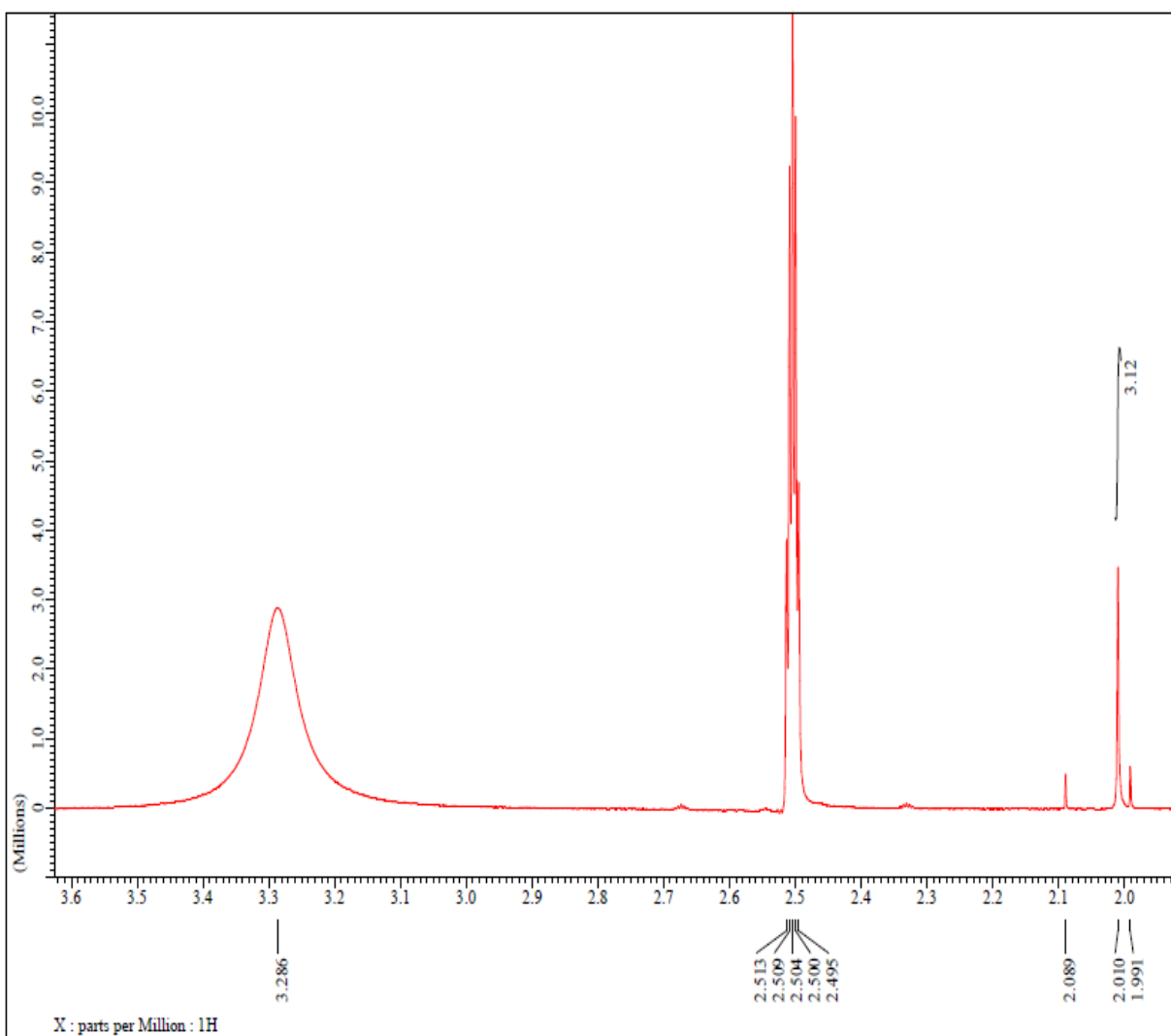
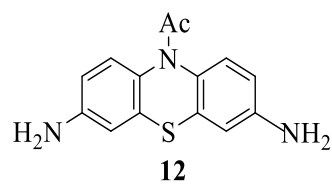
Appendix D5: IR Spectrum for Compound **11**



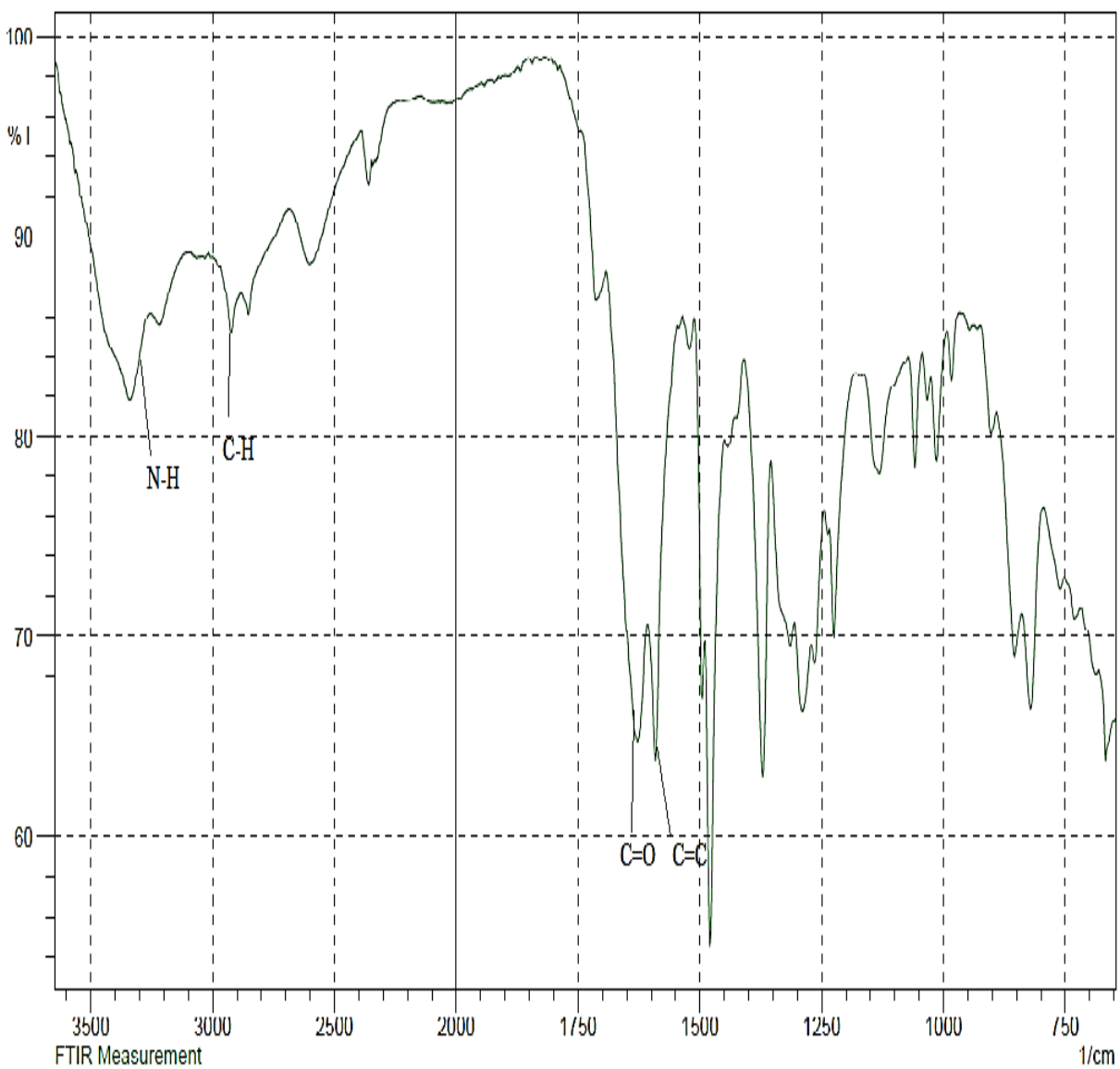
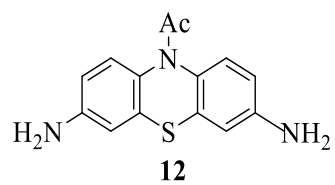
Appendix E1: ^1H NMR Spectrum for Compound **12** in DMSO- d_6



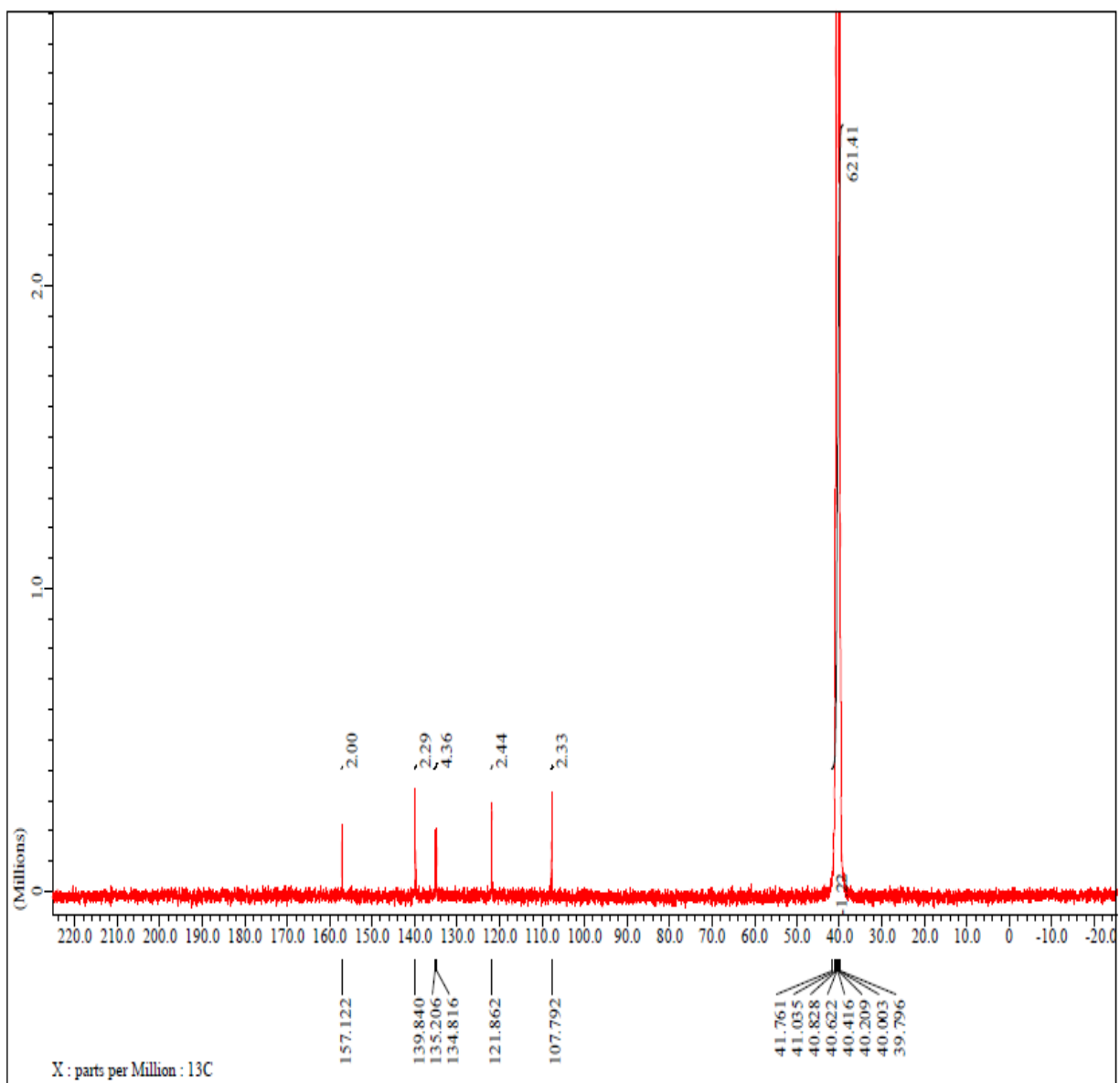
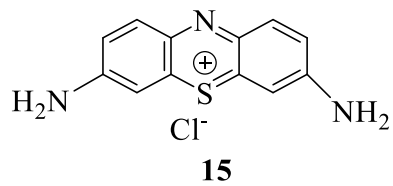
Appendix E2: ^1H NMR Spectrum for Compound **12** in DMSO- d_6



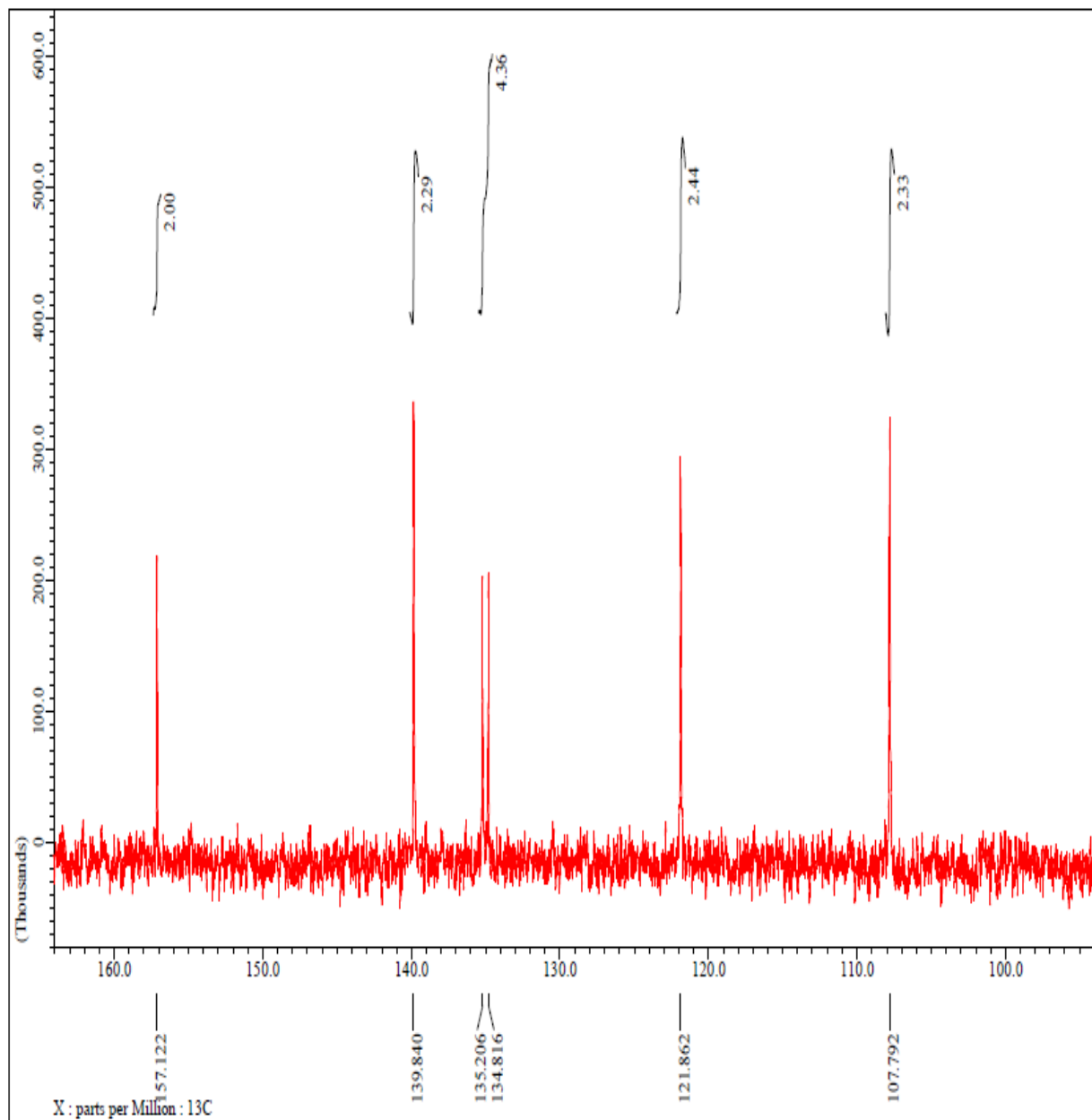
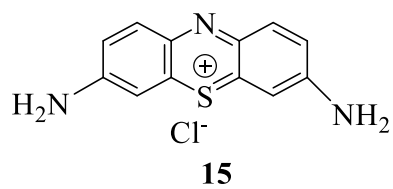
Appendix E3: IR Spectrum for Compound **12**



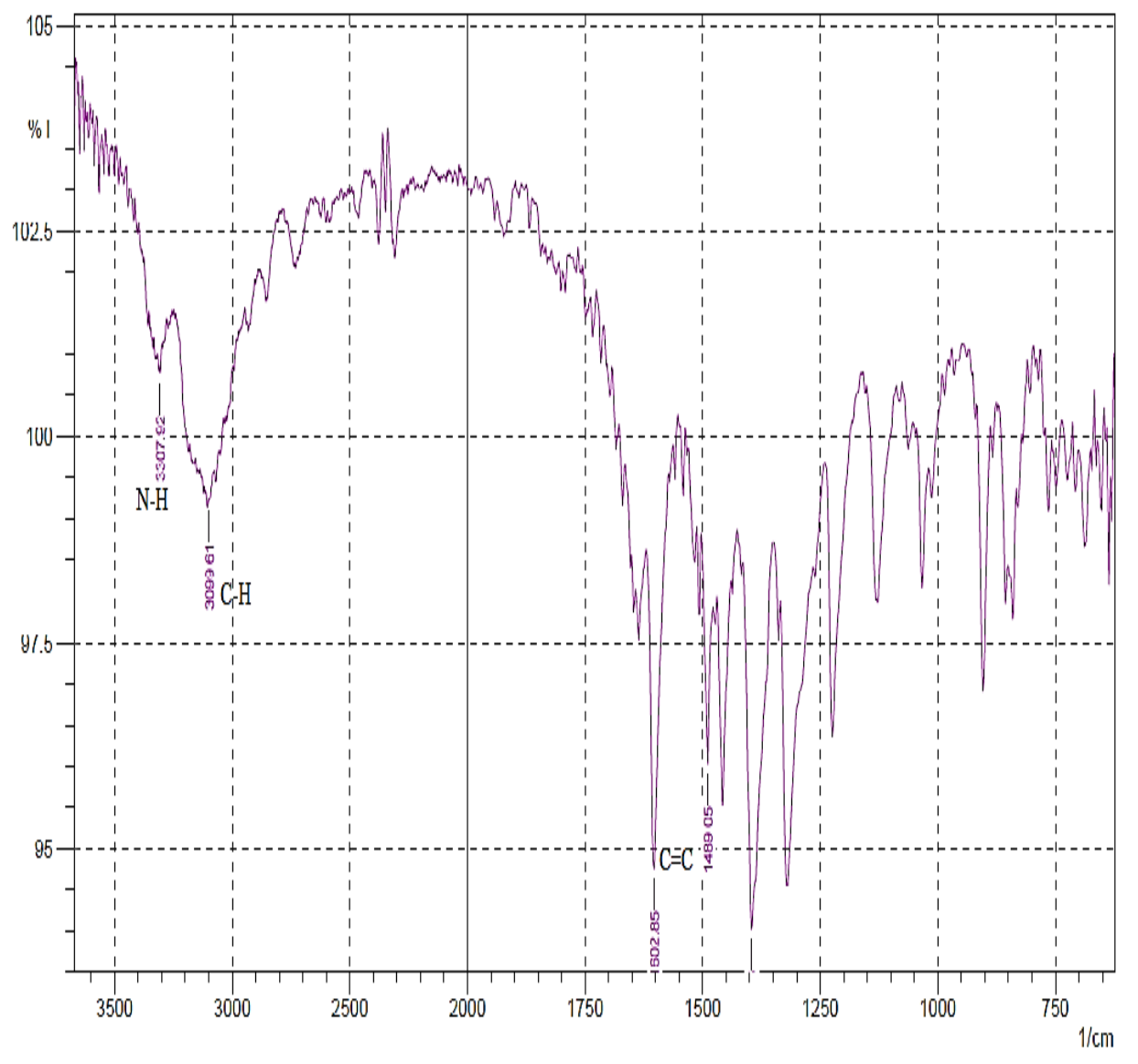
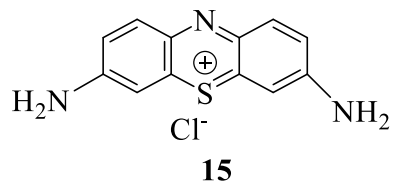
Appendix F1: ^{13}C NMR Spectrum for Compound **13** in DMSO-d₆



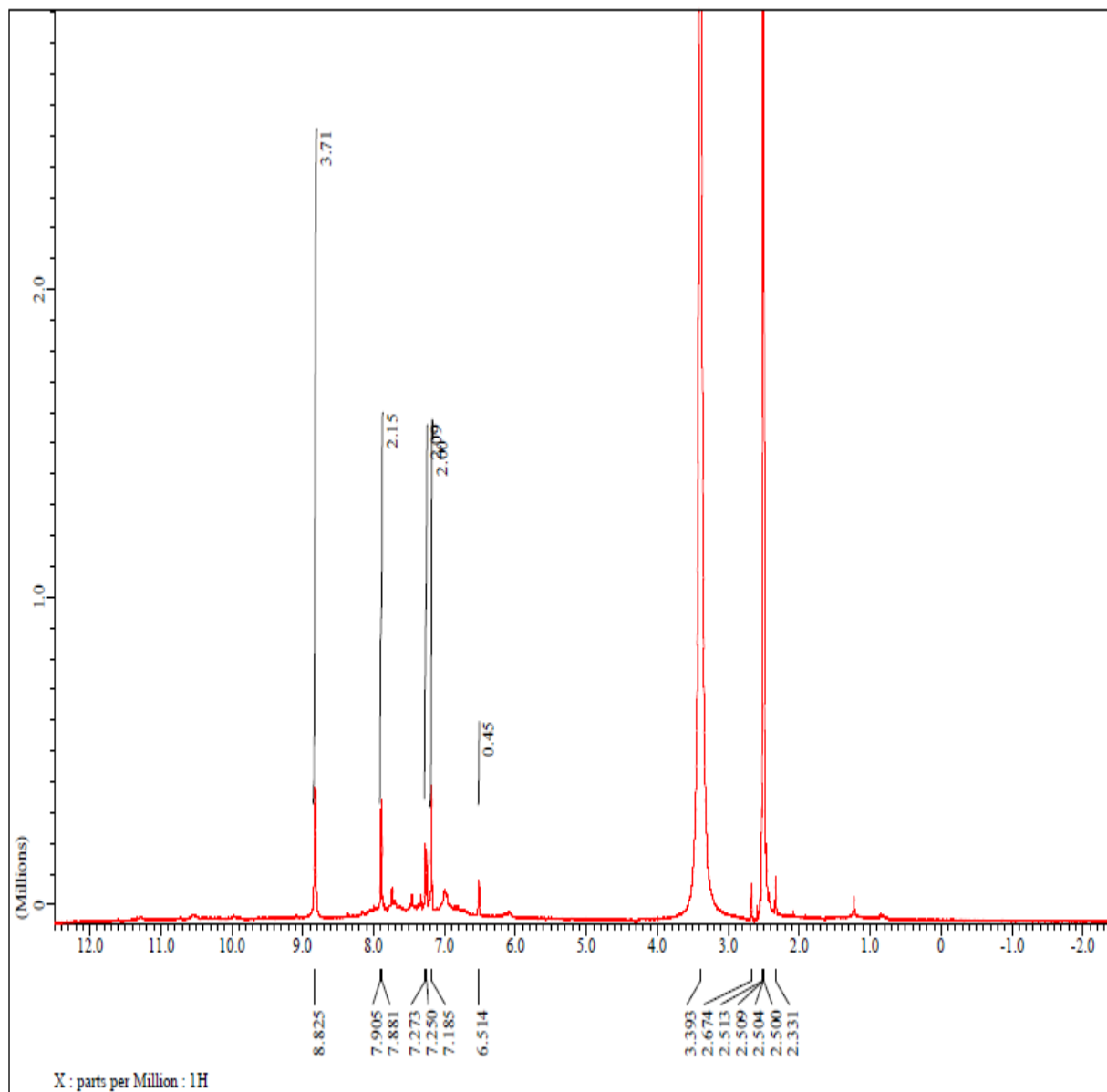
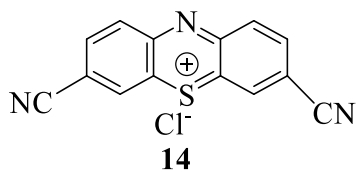
Appendix F2: ^{13}C NMR Spectrum for Compound **15** in DMSO-d₆



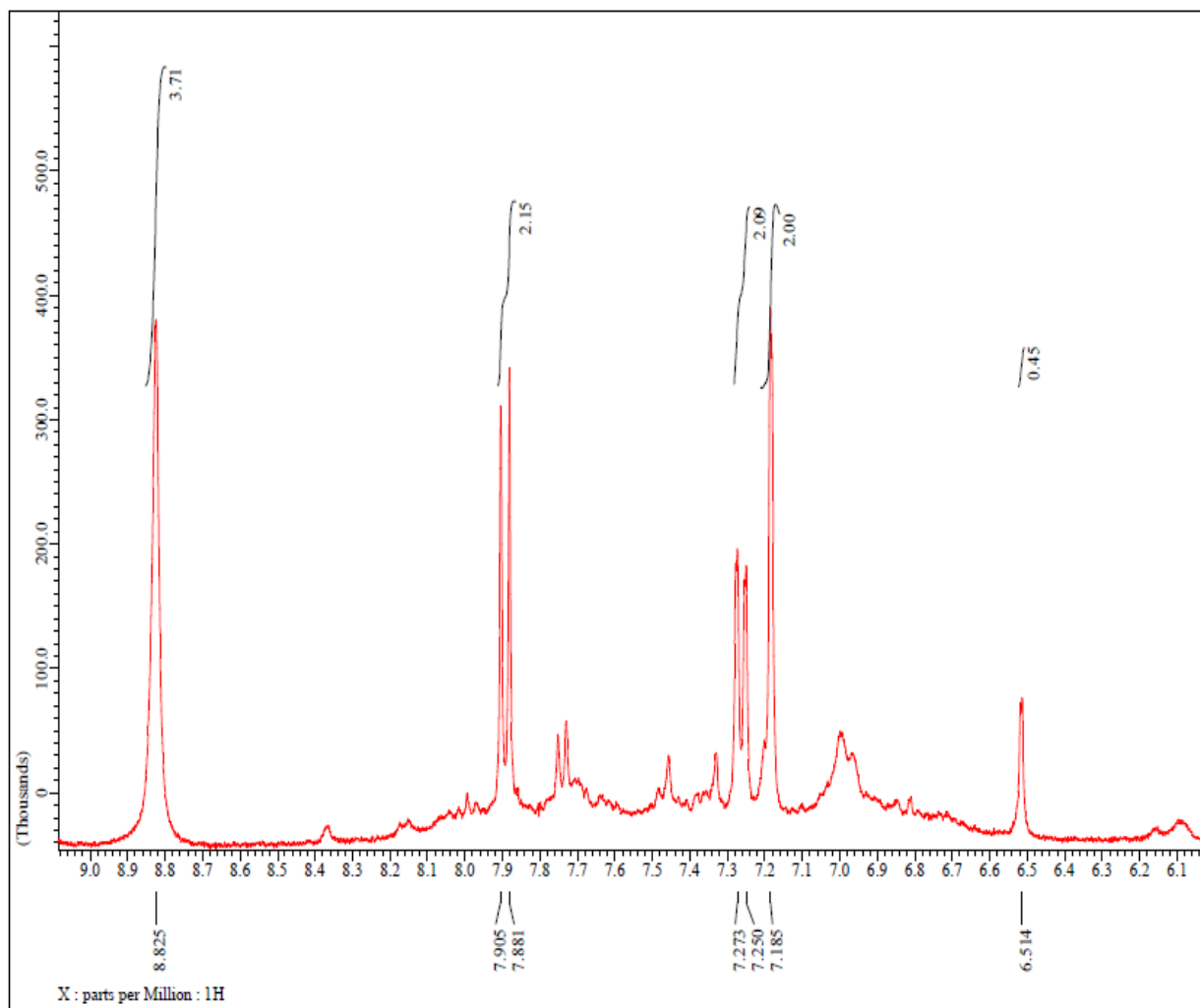
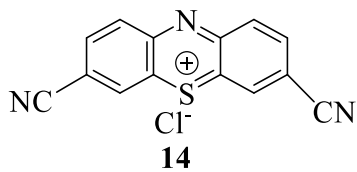
Appendix F3: IR Spectrum for Compound **13**



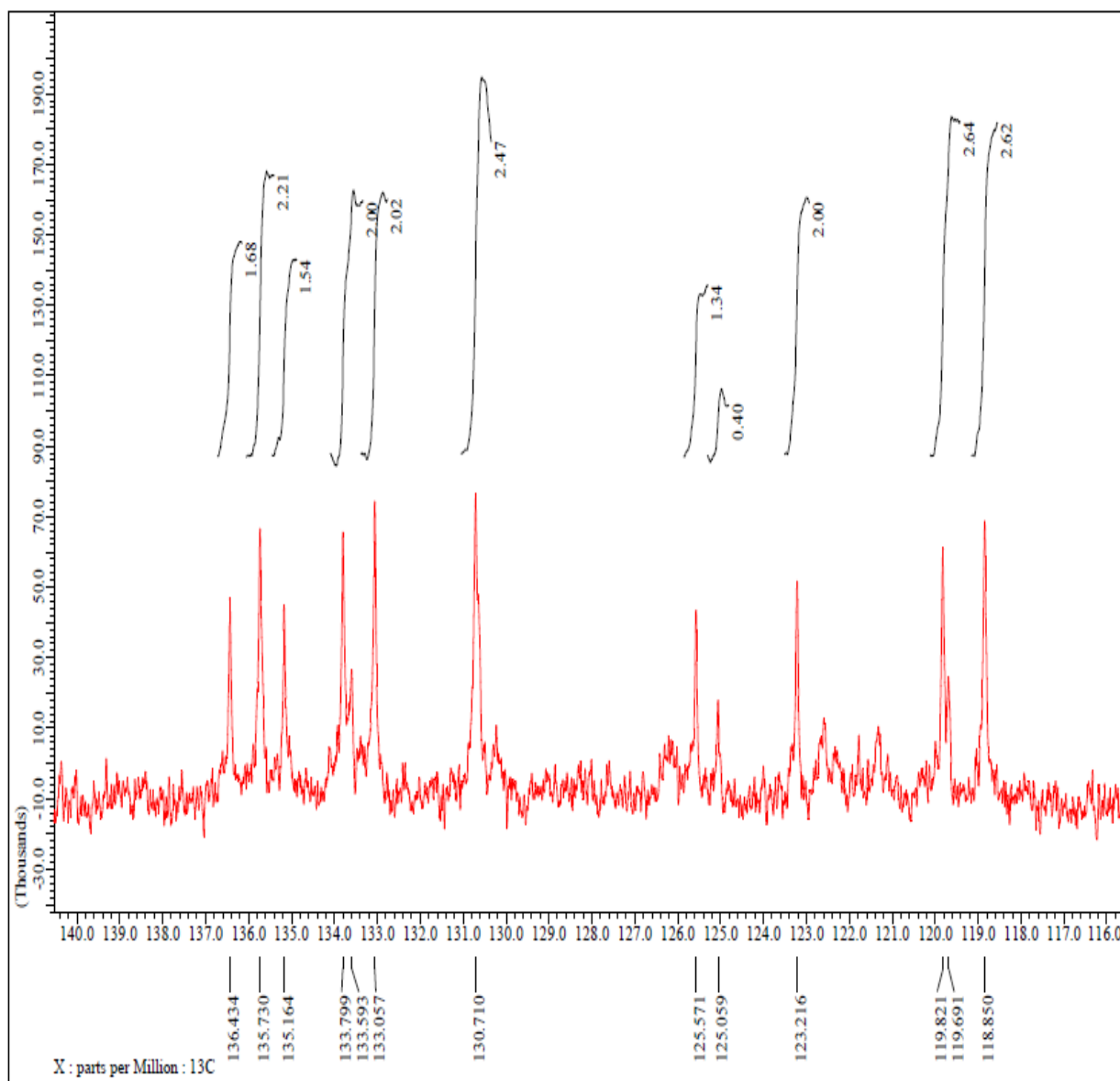
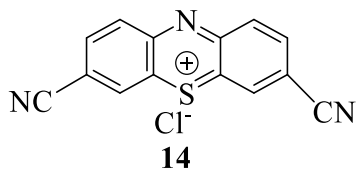
Appendix G1: ^1H NMR Spectrum for Compound **14** in DMSO- d_6



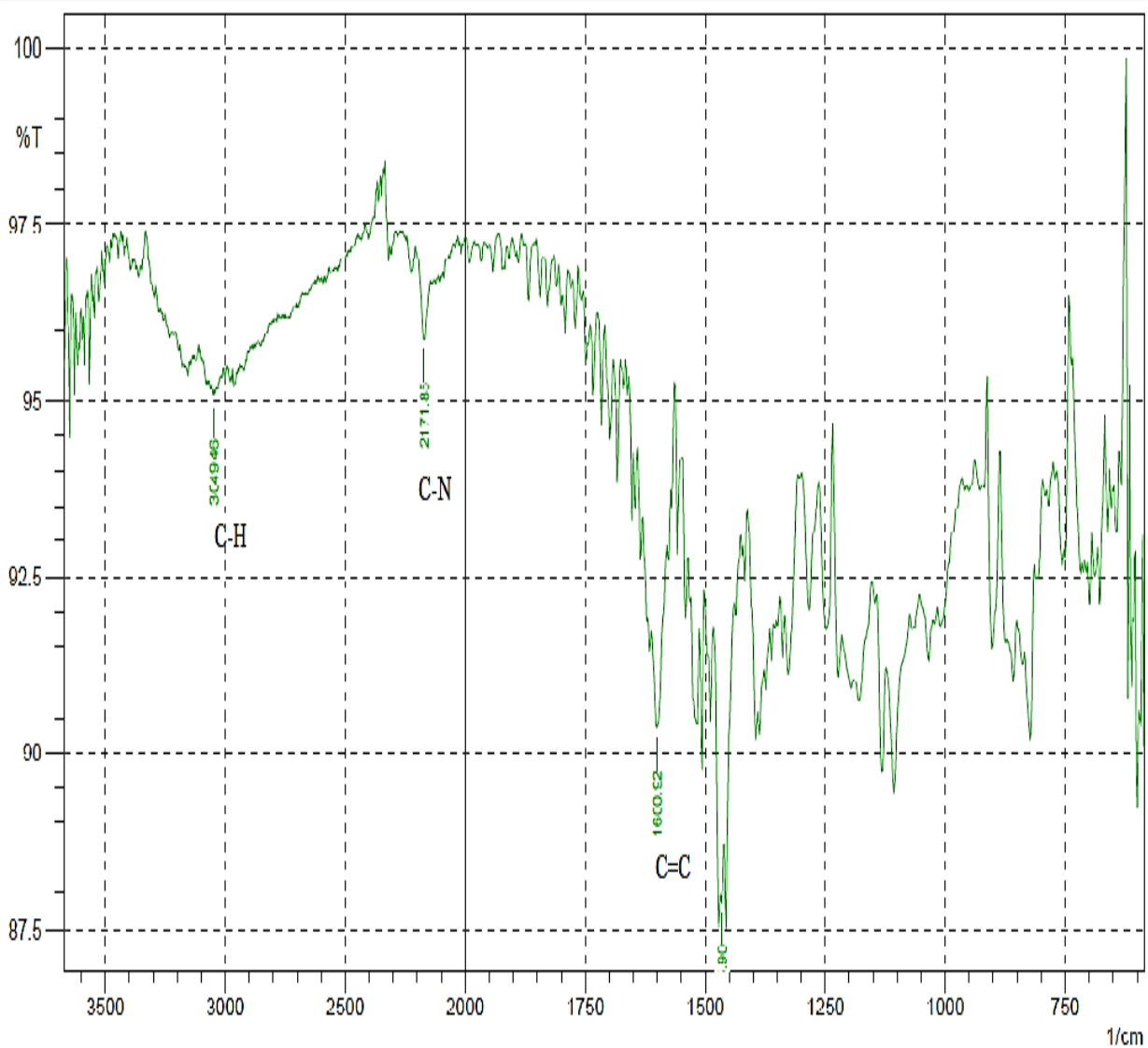
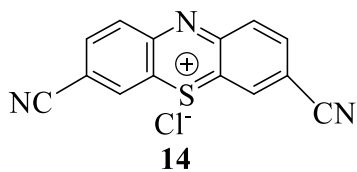
Appendix G2: ^1H NMR Spectrum for Compound **14** in DMSO- d_6



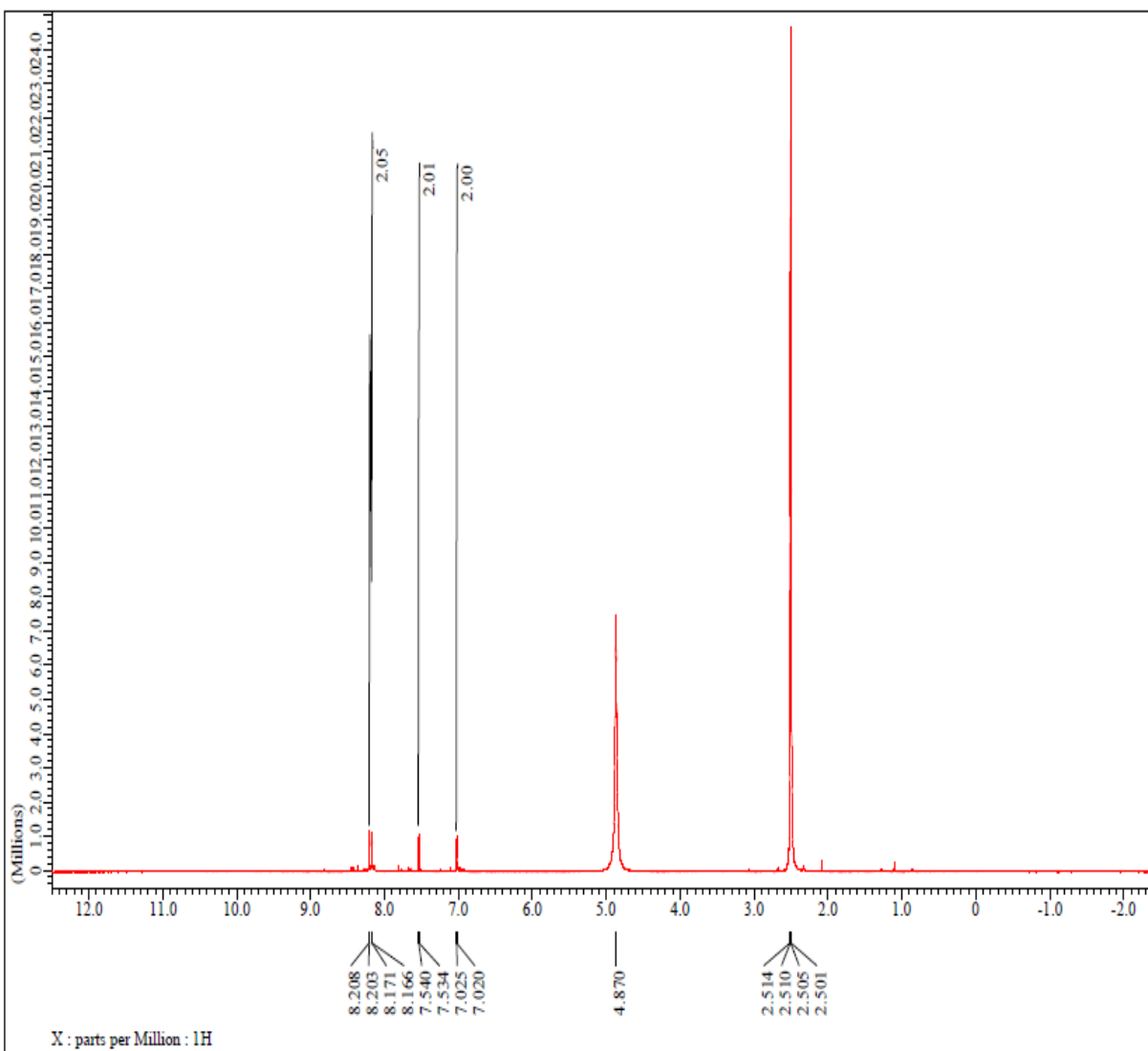
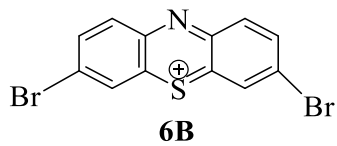
Appendix G4: ^{13}C NMR Spectrum for Compound **14** in DMSO- d_6



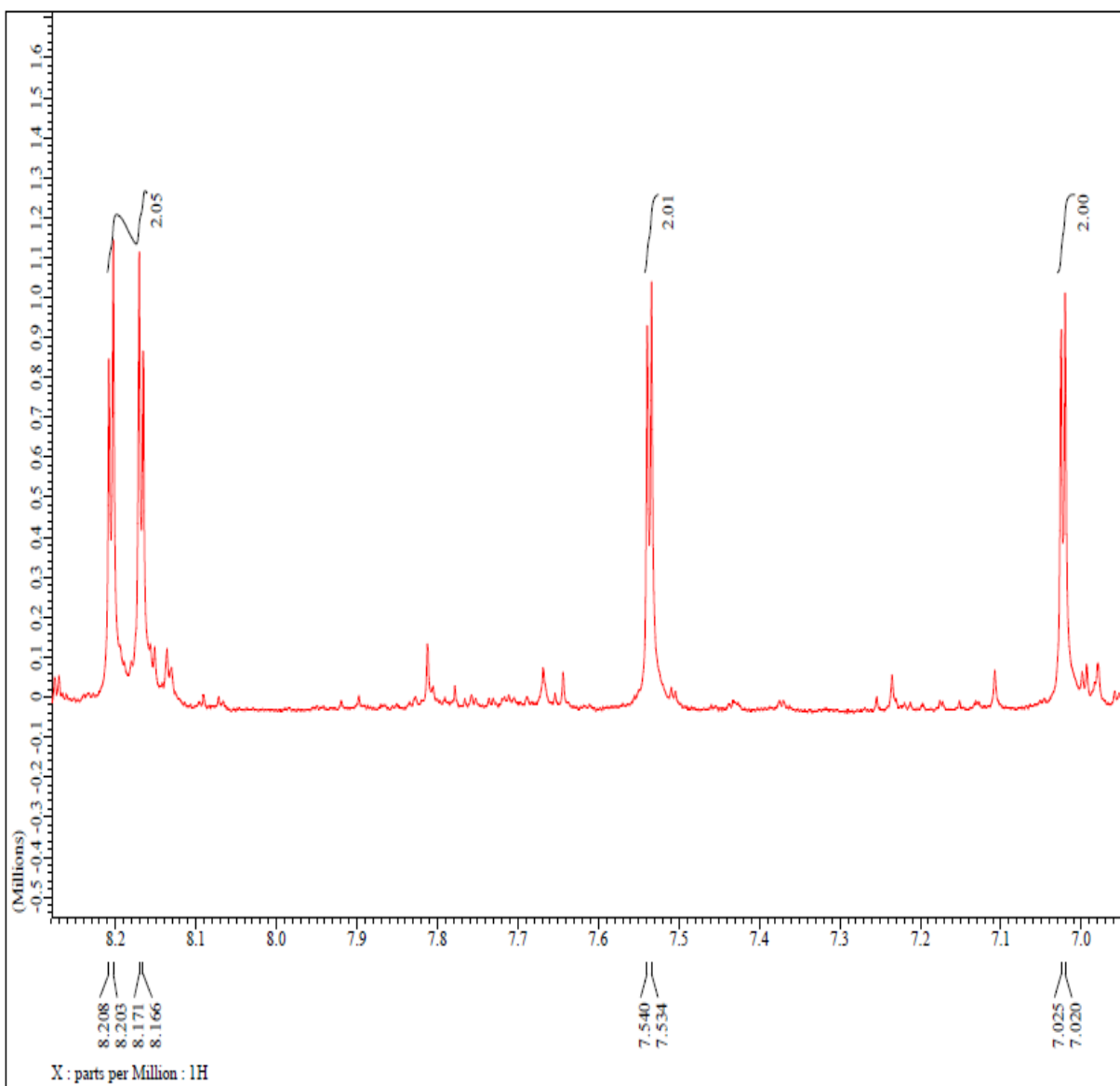
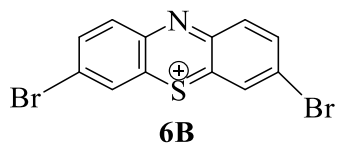
Appendix G5: IR Spectrum for Compound **14**



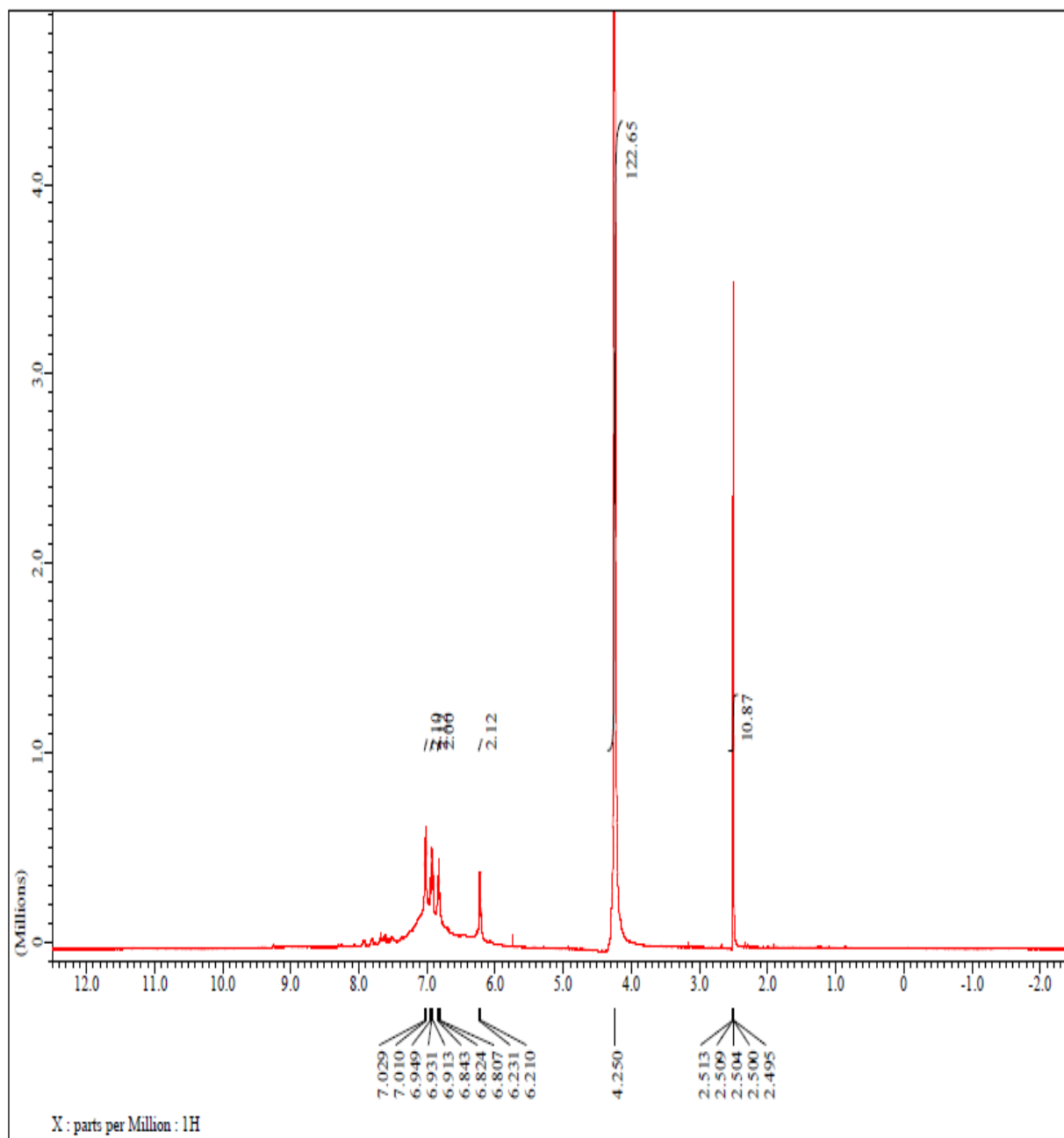
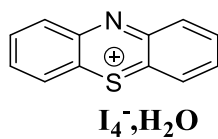
Appendix H1: ^1H NMR Spectrum for Compound **6B** in DMSO- d_6



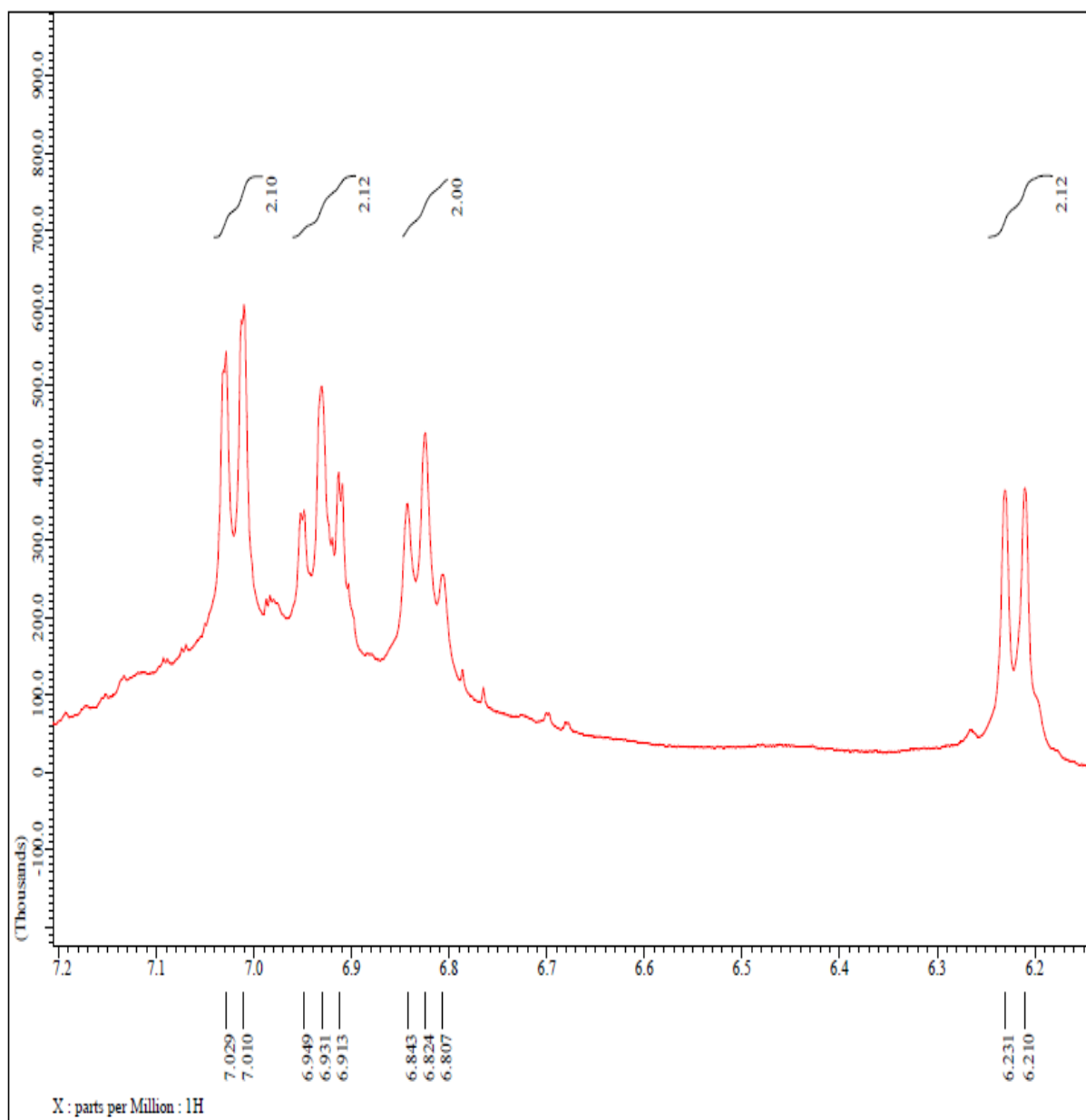
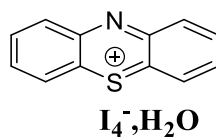
Appendix H2: ^1H NMR Spectrum for Compound **6B** in DMSO- d_6



Appendix I1: ^1H NMR Spectrum for **PTZN** in DMSO- d_6



Appendix I2: ^1H NMR Spectrum for **PTZN** in DMSO-d₆



VITA

SELORM J. FANAH

- Education: M.S. Chemistry, East Tennessee State University,
Johnson City, Tennessee, 2015
- B.Sc. Chemistry, University of Cape Coast, Cape Coast,
Ghana, 2012
- Professional Experience: Graduate Teaching Assistant, College of Arts and Sciences,
East Tennessee State University, 2013 – 2015
- Teaching Assistant, Department of Chemistry, University
of Cape Coast, Ghana, 2012-2013
- Lab Assistant, Anglo Gold Ashanti Ltd, Obuasi Mines,
Ghana, 2011
- Honors and Awards: Margaret Sells Endowment Award, Chemistry,
East Tennessee State University, Fall 2014